الجمهورية الجزائرية الديمقراطية الشعبية
République Algérienne Démocratique Et Populaire
وزارة التعليم العالي والبحث العلمي
Ministère de L'Enseignement Supérieur et de La Recherche Scientifique
جامعة فرحات عباس- سطيف1
Université Ferhat Abbas - Sétif 1

THÈSE

Présentée à l'Institut d'Optique et Mécanique de Précision pour l'obtention du Diplôme de

DOCTORAT 3ème Cycle LMD

Domaine : Sciences et Techniques
Filière : Optique et mécanique de Précision
Spécialité : Matériaux pour l'optique et pour l'optoélectronique

Par
AZIL KENZA

THÈME

Apport des capteurs optiques pour la détection et à l'analyse des polluants de l'eau.

Soutenue, le:…….

Devant le jury composé de:

Président du Jury	DEMAGH Nacereddine	Prof.	UFA Sétif1
Directeur de thèse	BOUZID Said	Prof.	UFA Sétif1
Co-directeur de thèse	ALTUNCU Ahmet	Prof	DPU, Turquie
Examinateur	BENCHEIKH Abdelhalim	Prof.	Univ BBA
Examinateur	BOUGUETTOUCHA Abdallah	Prof.	UFA Sétif1
Invité	FERRIA Kouider	Prof	UFA Sétif1

PEOPLE'S DEMOCRATIC REPUBLIC OF ALGERIA
MINISTRY OF HIGHER EDUCATIONAND SCIENTIFIC RESEARCH
FERHAT ABBAS UNIVERSITY – SETIF -1-

THESIS

Submitted to Institute of Optics and Precision Mechanics
For the degree
PhD
in: **Materials for optics and optoelectronics**
By
AZIL Kenza
Title

Optical methods for detection and analysis the pollutants in water

Defended on: …….. **In front of the composed committee of**

Chairman	**DEMAGH Nacereddine**	**Professor**	**F.A.U Setif -1**
Supervisor	**BOUZID Said**	**Professor**	**F.A.U Setif -1**
Co-supervisor	**ALTUNCU Ahmet**	**Professor**	**DPU, Turkey**
Examiner	**BENCHEIKH Abdel Halim**	**Professor**	**BBA University**
Examiner	**BOUGUETTOUCHA Abdallah**	**Professor**	**F.A.U Setif -1**
Invited	**FERRIA Kouider**	**Professor**	**F.A.U Setif -1**

ACKNOWLEDGEMENTS

I would also extremely express my thanks to my mentors & supervisors in applied optics laboratory, Prof. Pr: **FERRIA KOUIDER** & Pr: **BOUZID SAID** for their excellent assistance, support and guidance.

I would like also to thank my mentor & supervisor in photonics research laboratory, Prof. Pr: **ALTUNCU AHMET** for his excellent assistance, support and guidance.

I am extremely grateful to the Turkish laboratory members, who has been involved in this project.

I would like to thank committee members **DEMAGH Nacereddine**, **BENCHEIKH Abdelhalim** and **BOUGUETTOUCHA Abdallah** for including their contributions & accepting the examination of my thesis.

I would like to thank my **INSTITUTE OF OPTICS AND PRECISION MECHANICS** stuff for offering the opportunity to benefit from all the laboratories facilities during my studies since 10 years ago. Especially my previous and present working professors for providing to me a pleasant working environment.

In addition, I am thankful to technicians, engineers and special thanks to the current members (**PhDs Gen 2016, Soumia, and Djamila**) in the **APPLIED OPTICS LABORATORY**. As well **Nur Farhana** from Malaysia, besides; **Elif** and **Hazal** from Turkey.

I owe great thanks to my family members (my sisters & brothers) one by one accurately **my parents**, those who always supporting me, whether from the spirit side or the economical side.

My heartfelt thanks goes to my fiancé **HAID Slimane,** who motivated me and managed to make me smile even in difficult times

Lastly, I would like to thank everyone, who passed through my life, whether it was a lesson for me or a starting point to develop my personal career.

"The paradox between attempting to analyze "too much" information and still not having enough- although frustrating -, as well, this will lead to complex problems, and that problems do not have simple solutions. However, it should not be discouraging. No! It is for sure a step for **PROGRESS**".

For the domain of **WATER POLLUTION**, Chemistry without **OPTICS** is not complete, and vice versa. Accurately, pollution is complicated, exacting and dynamic, while chemistry compounded by a single source of pollution may at times be overwhelming. Thus, chemistry with multiple-variable pollutants involves extraordinary insight as well as foresight into placing the problems into perceptive." Therefore, certainly; the step of **MONITORING** precedes the treatment. In addition, this critical step requires innovative optical equipment to help solving this global issue.

I recommend reading this thesis carefully, it emerges such a coherent mixture between optic and chemistry.

Enjoy reading ☺

AZIL KENZA

ABSTRACT

Water pollution has become a huge problem in many countries all over the world. This small portion of freshwater is now under serious stress due to various reasons such as fast-developed population, this dominant trouble needs an innovative technology to control continuously and in situ the water quality. These optic methods are the response possible for our need; they open a developed manner of diagnosis. In this thesis the theory, design, fabrication and characterization was reported; to delve into the optical fiber sensor based on evanescent wave absorption, for testing methylene blue (MB) at the laboratory of applied optics (Algeria). The designed sensor represents a significant advancement to accurately monitor MB concentration changes in distilled water. This investigation was in good agreement with previously reported studies. In addition, a turbidity NaCl measurement system intended for water quality monitoring was carried out at the Photonics research laboratory (Turkey). Following to the theoretical investigation about the standard techniques to control the turbidity as well as, experimental results from turbidity system that was employed to control the water quality by using electro-optic components, based on a combined measurement of transmitted and forward scattered light using an optical CCD line sensor array was introduced. The experimental results have shown that trustable measurements of water turbidity in a wide turbidity range can be achieved with the proposed method.

Table of Contents

CHAPTER II: CLADLESS OPTICAL FIBER SENSOR BASED ON EVANESCENT WAVE ABSORPTION FOR MONITORING METHYLENE BLUE INDUCED WATER POLLUTION

CHAPTER III: TURBIDITY MEASUREMENT SYSTEM FOR PARTICLE ANALYSIS

List of figures

CHAPTER I: WATER POLLUTION OVERVIEW

CHAPTER II: CLADLESS OPTICAL FIBER SENSOR BASED ON EVANESCENT WAVE ABSORPTION FOR MONITORING METHYLENE BLUE INDUCED WATER POLLUTION

R_1. A decrease in colour intensity of ray R_1 represents the decreased power of the refractive ray.

Figure7: Theoretical investigation about the relationship between penetration depth (nm) and incident angle (θ_i).

Figure8: Different types of fiber probe design: (a).Tip probe; (b). Straight probe; (c). Tapered probe; (d). Biconical probe; (e). U-bent probe.

Figure 9: Clarified schematic representation depicts the global set up of the designed optical fiber sensor.

Figure10: The chemical pattern of MB.

Figure11. Emission spectrum response of the used LED.

Figure12: Absorption spectrum of methylene blue solution with C=5mg/l.

Figure 13: Used materials in solutions preparation.

Figure 14: Variation of the refractive index of the liquid [1-103.3] mg/L vs. The concentration of MB samples.

Figure 15: variation of acceptance angle according to the refractive indices**.**

Figure 16: Effect of the concentration of MB solutions on the numerical aperture (NA).

Figure 17: Output intensity vs. Wavelength for L=38cm for different concentration [1-103.3] mg/L.

Figure 18: Output intensity vs. Wavelength for L=28cm for different concentration [1-103.3] mg/L.

Figure 19: Output intensity vs. Wavelength for L=18cm for different concentration [1-103.3] mg/L.

Figure 20: Output intensity according to concentration [1-106] mg/L for the three lengths [18, 28, and 38] cm.

Figure 21: The output intensity according to concentration for exact wavelength [500,550,600, 650, and 700].

Figure 22: Penetration Depth and the output intensity analysis for an Evanescent Wave Absorption Sensor vs. the range of refractive indices (λ =664nm).

Figure23: Relationship between penetration depth (nm) and incident angle (θ_i) with Θ_c=69°.

CHAPTER III: TURBIDITY MEASUREMENT SYSTEM FOR PARTICLE ANALYSIS

Figure 1: the EPA method measures the amount of light scattered at a 90-degree angle from the transmitted light.

Figure 2: ISO 7027 design standards also rely on turbidity technology, within an infrared monochromatic light source.

Figure 3: GLI method as a turbidimeter that alternates light pulses from two light sources into two photodetectors.

Figure 4: the scattering processes of reflection, refraction and diffraction, and the attenuation process of light absorption due to particle suspended in water.

Figure 5: METTLAR TOLEDO conductivity and TDS measurement device.

Figure 6: Variation of TDS and TSS as a function of NaCl concentration for distilled and tap waters.

Figure 7: A micro TPI portable turbidity meter.

Figure 8: Turbidity (NTU) variation as a function of NaCl concentration in distilled water.

Figure 9: Turbidity (NTU) variations for the tap and distilled waters mixed with varying amount of NaCl concentration.

Figure 10: Experimental setup used for water turbidity characterization by transmitted and 90° -scattered light measurements.

Figure 11: The transmitted light measurement results obtained for a LD wavelength of 650 nm and as a function of NaCl concentration (g/l) in tap and distilled water samples. The distance between LD and PD1 was d=10cm.

Figure 12: The transmitted light measurement results obtained for a LD wavelength of 850 nm and as a function of NaCl concentration (g/l) in tap and distilled water samples. The distance between LD and PD1 was d=10cm.

Figure 13: The 90°-scattered light measurement results for the LD wavelength of 650 nm as a function of NaCl concentration (g/l).

Figure 14: The 90°-scattered light measurement results for the LD wavelength of 850 nm as a function of NaCl concentration (g/l).

Figure 15: The scattered light as a function of TSS for different distilled water-NaCl concentrations at 650nm LD wavelength. The distance between LD and PD is d=10cm and the scattered light angle is 90° and 10°.

Figure 16: The 90° and 10°-scattered light measured as a function TSS for tap water-NaCl sample at 650 nm wavelength. The distance between LD and PD1 is 10cm.

Figure 17: Turbidity (NTU1) measurements as a function of the 90° and 10°-scattered light for tap water-NaCl sample at 650 nm LD source. The distance between LD and PD1 is 10cm.

Figure 18: The ratio of 90 and 10°-scattered light/transmitted light = f (NTU) for 650nm for tap water.

Figure 19: The ratio of 90 and 10°-scattered light/transmitted light = f (NTU) for 650nm for distilled water.

Figure 20: CCD line sensor and (b) Schematic diagram of the water turbidity measurement setup with a LD-CCD line sensor system.

Figure 21: (0-10°) the forward scattered light measured as a function of TSS of tap and distilled water-NaCl sample using a 650nm LD source.

Figure 22: The transmitted light intensity measured as a function of TDS (g/l) in tap and distilled water. The wavelength of LD is 650nm.

Figure 23: The ratio of (0-10°) forward scattered/transmitted light measured as a function of turbidity (NTU) in tap and distilled water. The wavelength of LD is 650nm.

Figure 24: the comparison between the ratio of 90° and 10°-Scattered/transmitted light measured and the ratio of (0-10° degree) forward Scattered /transmitted light measured as a function of turbidity (NTU) of tap water, the wavelength of LD is 650nm.

Figure 25: the comparison between the ratio of-90°and 10° Scattered/transmitted light measured and the ratio of (0-10° degree) forward Scattered /transmitted light measured as a function of turbidity (NTU) of distilled water, the wavelength of LD is 650nm.

List of tables

CHAPTER I: WATER POLLUTION OVERVIEW

CHAPTER II: CLADLESS OPTICAL FIBER SENSOR BASED ON EVANESCENT WAVE ABSORPTION FOR MONITORING METHYLENE BLUE INDUCED WATER POLLUTION

Motivation, objectives, and organization of thesis

Water presents beyond 70% of the Earth's surface, and is a primordial resource for humanity and environment. Besides, it is well known that the water is a significant factor in our daily life. This important factor is intended for human consumption, especially drinking water of rivers, surfaces and lakes, which are often obtained by the most societies of the world. Albeit, it is always sensitive to contamination released from houses, farms, factories and hospitals. Consequently, it may contain polluting substances. Therefore, it effectively affects the human health and the natural environment. That is the main reason which makes the water needs purification, treatment and monitoring and it is necessary to protect the community before its consumption **[1, 2]**.

Water pollution has become a huge problem in many countries all over the world. It is known that water is a very significant factor in life, but if this water becomes contaminated, it will be very dangerous for the humanity and wildlife. Pollution is defined as ' to make fetid or unclear and dirty'.

Because of all these causes of water pollution, there are some unwanted effects. First of all, this type of pollution definitely influences the health of humanity, because many use large quantities of water for drinking or cooking. Thus, it is crucial to have pure water. Moreover, contaminated water can damage wildlife. The second effect of water pollution is the environmental influence such as the odour of water and the terrible sights on beaches or rivers. This leads to water scarcity because it limits its availability for humans and ecosystem **[3]**.

This small portion of freshwater is now under serious stress due to various reasons such as fast-developed population, urbanization and unsustainable use of water in agriculture and industries, **[4]**. Non-polluted water is a fundamental need of community and public health. On the event of World water day (2002), it had been highlighted that the significance of accessibility of high quality drinking water. According to this report- an estimated 1.1 billion people are unable to get safe water for drinking purpose, 2.5 billion people are not getting proper sanitation, and more than 5 million people lost their lives due to water borne as well as water-related diseases. So far, where sufficient or plentiful water supplies are available, they are growingly at risk from contamination and increasing demand. Accordingly, the two thirds of world's population is expected to live in countries with moderate or severe water crisis by 2025.

Contaminated water fundamentally bears different irresistible microbes (like microorganisms, infection and protozoa) such as cancer-causing natural anions and cations (NO_3, PO_4, SO_4, F, Ca^+ and Mg^+) and inorganic toxins (acids, salts, dyes and poisonous metals). At the point when

these substances surpass as far as possible can turn out to be perilous and can cause genuine ailments in people and other organisms of the ecosystem [5].

Natural activity like eruption will contribute a little a part of the sources of water pollutants however primarily the essential sources of water contaminants are anthropogenic like poorly treated or untreated municipal wastes, discharges from individual septic tanks, agricultural wastes like fertilizers, pesticides, industrial chemical wastes, spilled crude merchandise, mine evacuation, spent solvents, etc. [6]. Pollutants will be accessorial into water bodies (both surface and ground water) through numerous processes e.g., discharge processes, surface runoff, submerged infiltration, or atmosphere precipitation etc. Once the blending of pollutants with water bodies happens, they are forthwith carried into the water cycle during an international context. Consumption of impure water will cause numerous water borne diseases like channel sickness by pathogenic microbes and conjointly have an effect on liver, kidney, nervous system and immunity [7]. Such pollutants are acquainted to the society since long back termed as standard pollutants, as a result; of numerous researchers have reported their sources and the adverse effects on system as well.

This dominant trouble needs an innovative technology to control continuously and in situ the water quality. Several methods are used for monitoring water quality accurate the effluent pollutants optical process, overall, including spectroscopy process such as Fourier Transform Infrared (FTIR) spectroscopy [8], Laser-Induced Breakdown Spectroscopy (LIBS) [9], Nuclear Magnetic Resonance Spectroscopy [10], Raman spectroscopy [11] and chromatography process such as Liquid Chromatography Mass Spectrometry (LCMS) [12], High Performance Liquid Chromatography (HPLC) [13], enzymatic method [14], colorimetric method [15] and capillary electrophoresis [16]. These processes are extremely precise nevertheless, it has some disadvantages in the manner of complex offline procedures, additionally, and consuming long time in analysis and the operation with these expensive, bulky, cumbersome and complexed instrumentations produce issues, which is not appropriated with the basic requirement for the real-time monitoring [17].

These optic methods are the only response possible for our need, they open a developed manner of diagnosis [18] into various domains of structural health monitoring (strain, shape, temperature.etc,) [19], chemical-physical sensing [20, 21], environmental condition sensing (temperature and oxygen…) [22], future safety monitoring [23], fiber optic networks for remote sensing [24], and fiber optic biosensors [25]…etc. We can define an optical sensor as a device that it is able to react and detect continuously and reversibly the physical quantities wanted [26] whereas electrical sensors that it uses a fiber instead of copper wire and the electricity is

replaced by the light. The properties of light (intensity, phase, polarization, and wavelength) are modulated by this optical sensor [27].

In the first chapter, we will explain in details the water pollution problem including the origin of this phenomenon that needs a real time monitoring by different methods, this last, will be clarified in the chapter. We will provide a complete report about the general used methods for water pollution monitoring specifically the optical methods.

Next, the theory, design, fabrication and characterization was reported; to delve into the achieved methods including optical fiber sensor based on evanescent wave absorption, for testing specific pollutants (methylene blue) at the laboratory of applied optics (Algeria). The same chapter will present an experimental investigations conducted to explore the optical and the geometrical characteristic of the used fiber such as optical fiber type (single-mode or multi-mode), fiber core diameter, fiber probe geometry, fiber probe length, etc., are very important for a number of reasons. Because that optical fiber's users need the fiber characteristics to design the optical fiber systems. There is a great number of techniques, which have been reported for measuring the optical fiber sensor characteristics. This chapter presents an exhaustive study about the performance of fiber optic sensor characteristics, we will detail and discuss some typical experimental set ups which have been employed.

In addition, a turbidity NaCl measurement system intended for water quality monitoring was carried out at the Photonics research laboratory (Turkey). Following to the theoretical investigation about the standard techniques to control the turbidity as well as , we will introduce the experimental results from turbidity system that was employed to control the water quality by using electro-optic components, based on a combined measurement of transmitted and forward scattered light using an optical CCD line sensor array.

Finally, we conclude by the highlighted results; obtained from the different optical systems realized in this thesis; additionally, future prospects of the aforementioned work are also addressed.

Brief review about the water pollution problem in Algeria

Like other countries in the world, Algeria has not been spared the pollution crisis, which has been both a political and a social issue. The problem has been intensified by the distribution of waste and garbage in urban and rural areas, as well as in manufacturing facilities, posing significant threats to the environment and public health.

Contamination rates, which can mainly be due to toxic gases and smoke from factories, especially chemical ones, as well as CO2 pollution from cars, also continue to increase. Apart from the unregulated usage of fertilizers and chemicals, this has contributed to increased air emissions and agricultural toxicity for human use.

In this background, French researcher Jacques Moussafir, Chairman and Chief Executive Officer of the Qatar-based Aria Technology Company for the monitoring of environmental pollution, said in an interview with el-Massa newspaper on 5 February 2016 that Algeria has one of the highest levels of contamination in the world, requiring intervention by environmental protection authorities to devise mechanisms to reduce pollution.

According to a report by Harvard University in 2018, Algeria is among the countries at the greatest risk due to its strong dependence on food that loses nutrients as the concentration of CO2 in the air increases.' **[28]**.

This was the same conclusion reached by the World Bank and the Center for Health Measurements and Assessment, the academic institute concerned with accelerating health development. In the 2016 Joint Study on Air Quality Prices, the two organisations emphasized that Algeria is one of the most industrialized countries in the world, along with Mexico, China, India and the Middle East. The report also noted that the pollution-related mortality rate was 10% in 2013.

Pollution resulting from accumulated waste is among the most common forms of pollution. In this report, some witnesses working as responsible in Algiers province mentioned the highlighted pointed as follow:

- In an October 2018, interview with al-Nahar TV that waste has become a phenomenon common to all Algerian cities. He affirmed that citizens should assume responsibility for this problem since they are the primary cause of it, as a result of random dumping and disregard for waste collection times.
- A hotline was installed for citizens and allocated trucks and workers to remove private waste (from home renovations, defective electrical appliances etc.). However, these services have not provided the anticipated response and the continuation of dumping.
- The waste problem on three parties: citizens, the sanitation department and local authorities. Those three should cooperate to eliminate environmental pollution resulting

from indiscriminate dumping, which is threatening public health, endangering the environment and harming the beauty and splendour specially for the capital Algiers.

Water waste and food toxicity for human consumption are of special importance. The outbreak of cholera in October 2018 was caused by polluted water in Sidi Kabir, Tipaza, according to laboratory research. The Institute Pasteur (National Institute of Epidemiology in Algiers) warned Algerians against consuming fruit and vegetables without washing them properly or eating fruit and vegetables watered with polluted water, which may be the cause of the outbreak. Water and food are polluted with industrial residues, insecticides used in agriculture and as a result of dirty water being mixed with potable water **[29]**.

Algeria has been struggling for years to solve this issue by fining polluters. Several regulations for the conservation of the environment and natural resources have been enforced. The first of these was the Law on the Safety of the Environment, 1983. This was accompanied by a variety of other regulations and administrative rulings controlling different environmental factors and procedures, including penalties and other punishments imposed on polluters **[30]**.

How did the government deal with awareness?

Some of the events organized by the Ministry of Environment and Renewable Energy include the launch of national awareness campaigns to encourage the cleanliness of communities. These campaigns were directly supervised by the Minister for the Environment and Renewable Energy on 30 October 2018, when campaigns were initiated with the support of all related agencies as well as civil society organisations and associations.

According to the survey by Algeria 3 TV, an environmental culture should be developed among people who should have the most important role to play in reducing the amount of waste. In addition, the waste management process in cities should be the result of participation and collaboration between local authorities and all sectors of civil society.

Another important initiative aimed at protecting the environment and ensuring a high degree of cleanliness is the El-Harrach Valley, from which polluted water flows to the sea in Algiers. According to the report by el-Massa published on 23 September 2018, the process of removing and extending the valley could be completed by the summer of 2019. The project would build

500 hectares of recreation space, including playgrounds and bicycle paths, as well as rebuild the region that poses a serious threat to the capital.

Despite various environmental regulations and national plans to preserve and protect the environment, especially in major cities, pollution remains a major concern (50% of cases of bronchitis, asthma, lung cancer and others are caused by environmental pollution). This stresses the public treasury, which allocates hundreds of billions of dinars annually to treat these diseases and their economic and social consequences **[31]**.

References

[1] Vigil, K. M. (2003). Clean water. *As Introduction to Water Quality and Water Pollution Control*.

[2] Bartram, J., & Balance, R. (1996). A Practical Guide to the Design and Implementation of Freshwater, Quality Studies and Monitoring Programmes. *Water Quality Monitoring. E and FN Spon. London*.

[3] Yu, M. H., Tsunoda, H., & Tsunoda, M. (2011). *Environmental toxicology: biological and health effects of pollutants*. crc press.

[4] Ahamad, A., Madhav, S., Singh, P., Pandey, J., & Khan, A. H. (2018). Assessment of groundwater quality with special emphasis on nitrate contamination in parts of Varanasi City, Uttar Pradesh, India. Applied Water Science, 8(4), 115.

[5] Azizullah, A., Khattak, M. N. K., Richter, P., & Häder, D. P. (2011). Water pollution in Pakistan and its impact on public health—A review. Environment International, 37(2), 479– 497.

[6] Ahamad, A., Raju, N. J., Madhav, S., Gossel, W., & Wycisk, P. (2018). Impact of non-engineered Bhalswa landfill on groundwater from quaternary alluvium in Yamuna floodplain and potential human health risk, New Delhi, India. Quaternary International, 507, 352–369.

[7] Xagoraraki, I., & Kuo, D. (2008). Water pollution: Emerging contaminants associated with drinking water.

[8] Shirafuji, T., Hieda, J., Takai, O., Saito, N., Morita, T., Sakai, O., & Tachibana, K. (2010, November). FTIR study of methylene blue plasma degradation products through plasma treatment on water. In *TENCON 2010-2010 IEEE Region 10 Conference* (pp. 1938-1942). IEEE.

[9] Kasem, M. A., & Harith, M. A. (2015). Laser-induced breakdown spectroscopy in Africa. *Journal of Chemistry*, *2015*.

[10] Hooth, M. J. (Ed.). (2009). *Technical Report on Toxicology and Carcinogenesis Studies of Sodium Dichromate Dihydrate (CAS No. 7789-12-0) in F344/N Rats and B6C3F1 Mice (Drinking Water Studies)*. DIANE Publishing.

[11] Dashtbani Moghari, M. (2016). Optimised methylene-blue detection and quantification using conventional Raman spectroscopy.

[12] Khan, M. R., Khan, M. A., Alothman, Z. A., Alsohaimi, I. H., Naushad, M., & Al-Shaalan, N. H. (2014). Quantitative determination of methylene blue in environmental samples by solid-phase extraction and ultra-performance liquid chromatography-tandem mass spectrometry: a green approach. *RSC advances*, *4*(64), 34037-34044.

[13] Lefebvre, D., Gabriel, V., Vayssier, Y., & Fontagne-Faucher, C. (2002). Simultaneous HPLC determination of sugars, organic acids and ethanol in sourdough process. *LWT-Food Science and Technology*, *35*(5), 407-414.

[14] Greiner-Stoeffele, T., Grunow, M., & Hahn, U. (1996). A general ribonuclease assay using methylene blue. *Analytical biochemistry*, *240*(1), 24-28.

[15] Chitikela, S., Dentel, S. K., & Allen, H. E. (1995). Modified method for the analysis of anionic surfactants as methylene blue active substances. *Analyst*, *120*(7), 2001-2004.

[16] Borwitzky, H., Haefeli, W. E., & Burhenne, J. (2005). Analysis of methylene blue in human urine by capillary electrophoresis. *Journal of Chromatography B*, *826*(1-2), 244-251.

[17] Memon, S. F., Ali, M. M., Pembroke, J. T., Chowdhry, B. S., & Lewis, E. (2017). Measurement of ultralow level bioethanol concentration for production using evanescent wave based optical fiber sensor. *IEEE Transactions on Instrumentation and Measurement*, *67*(4), 780-788.

[18] Baranger, P. (2004). *Détection du kérosène par imagerie de fluorescence induite par laser, pour application sur foyer aéronautique* (Doctoral dissertation).

[19] López-Higuera, J. M., Cobo, L. R., Incera, A. Q., & Cobo, A. (2011). Fiber optic sensors in structural health monitoring. *Journal of lightwave technology*, *29*(4), 587-608.

[20] Wren, S. P., Nguyen, T. H., Gascoine, P., Lacey, R., Sun, T., & Grattan, K. T. (2014). Preparation of novel optical fibre-based Cocaine sensors using a molecular imprinted polymer approach. *Sensors and Actuators B: Chemical*, *193*, 35-41.

[21] Karimi, M., Fabian, M., Jaroszewicz, L. R., Schuster, K., Mergo, P., Sun, T., & Grattan, K. T. (2014). Lateral force sensing system based on different photonic crystal fibres. *Sensors and Actuators A: Physical*, *205*, 86-91.

[22] Chu, C. S., & Lin, C. A. (2014). Optical fiber sensor for dual sensing of temperature and oxygen based on PtTFPP/CF embedded in sol–gel matrix. *Sensors and Actuators B: Chemical*, *195*, 259-265.

[23] Li, X., Li, Q., Zhou, H., Hao, H., Wang, T., Zhao, S., ... & Huang, G. (2012). Rapid, on-site identification of explosives in nanoliter droplets using a UV reflected fiber optic sensor. *Analytica chimica acta*, *751*, 112-118.

[24] Fernandez-Vallejo, M., & Lopez-Amo, M. (2012). Optical fiber networks for remote fiber optic sensors. *Sensors*, *12*(4), 3929-3951.

[25] Bharadwaj, R., Sai, V. V. R., Thakare, K., Dhawangale, A., Kundu, T., Titus, S., ... & Mukherji, S. (2011). Evanescent wave absorbance based fiber optic biosensor for label-free detection of E. coli at 280 nm wavelength. *Biosensors and Bioelectronics*, *26*(7), 3367-3370.

[26] Aljaber, N. A., Mhdi, B. R., Ahmmad, S. K., Hamode, J. F., Azzawi, M. M., Kalad, A. H., & Ali, S. M. (2014). Design and Construction Fiber sensor detection system for water nitrite pollution. *IOSR J. Eng.*, *4*(2), 37-43.

[27] Gholamzadeh, B., & Nabovati, H. (2008). Fiber optic sensors. *World Academy of Science, Engineering and Technology*, *42*(3), 335-340.

[28] Fader, M., Shi, S., Bloh, W. V., Bondeau, A., & Cramer, W. (2016). Mediterranean irrigation under climate change: more efficient irrigation needed to compensate for increases in irrigation water requirements. *Hydrology and Earth System Sciences*, *20*(2), 953-973.

[29] Benhaddya, M. L., & Hadjel, M. (2014). Spatial distribution and contamination assessment of heavy metals in surface soils of Hassi Messaoud, Algeria. *Environmental Earth Sciences*, *71*(3), 1473-1486.].

[30] Shandra, J. M., Shor, E., & London, B. (2008). Debt, structural adjustment, and organic water pollution: a cross-national analysis. *Organization & Environment*, *21*(1), 38-55.

[31] Mustapha, H., Cherifa, H., Abdelkrim, H., Abdellah, G., & Abdelali, T. (2014). Assessment of water pollution in the semi-arid region: case watershed Wadi Saida (Northwest of Algeria). *Desalination and Water Treatment*, *52*(31-33), 5995-6008.

Chapter I

WATER POLLUTION OVERVIEW

I. Introduction

The center of life that allows us to survive is water and; the most vivacious that keeps us alive as well. Drinking clean and pure water is essential for all. Water is contaminated due to natural and anthropogenic causes, resulting in the production of multiple water pollutants. For the liveliness of humans, these water contaminants must be removed from the water as well; protected from different diseases.

Life is not practical without water. However, numerous poisonous, inorganic industrial chemicals have been polluted, resulting in many issues, such as unhealthy human consumption and irrigation operations. This contributes to water scarcity as it limits its usefulness to humans and the environment. Water contamination is the prime cause behind the water crisis. For irrigation use. At a certain threshold value, it should not be polluted. For use in irrigation and drinking water applications **[1]**.

II. Investigation about Water Pollution Origin

The origin of contaminants can be traced to their fundamental presence on earth, the creation by transformation of natural materials, and their synthesis produced by man. In particular, the particles may well emerge very naturally to become part of the biological context exposure levels. Many of them are excreted or detoxified by the animals. Nitrogen oxides and heavy metals are examples of certain contaminants that occur naturally and radioactive compounds and hydrocarbons **[2]**.

Most toxins can be produced by the concentration and transformation of naturally occurring compounds through their residential, agricultural or industrial use. Any important examples of contaminants that have resulted from this are the processing of sewage and wastewater containing agrochemicals, pesticides, petrochemicals, hydrocarbons, heavy metals, and radionuclides.

Many of the pollutants do not exist in nature and are completely manmade by the contamination they provoke. The synthesis of different pesticides, surfactants, plastics and petrochemicals, for instance, has created a huge number of environmental chemicals that have created serious environmental problems **[3]**.

Figure 1 illustrates how the release of toxic substances can be carried out and how polluted water influences humans and animals.

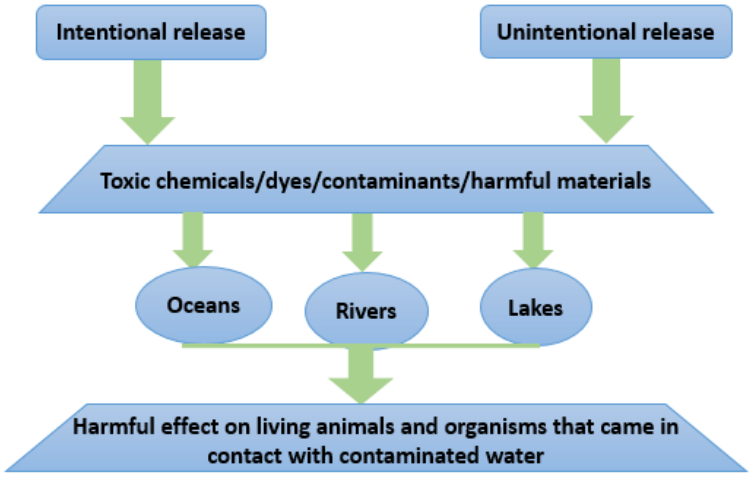

Figure1: Diagrammatic representation of release of toxic chemicals in various water bodies.

III. Types of existed pollutants

The primary sources of water pollution that result in degradation are direct and indirect ones. Direct contamination is caused by the discharge of fluids into the ocean, such as by a business expelling polluted ocean or radioactive solids into the sea or river immediately mixed with water.

This makes the water harmful to fish and other marine animals, sometimes resulting in death animals, however; still consume this water, which also results in ill health or premature death for them. It can influence human beings as well. People no longer rely on drinking water from a stream or river in developing countries. Many that swim in or engage in sports such as canoeing in dirty water are often at risk and some of them can cause sickness and even death [4].

Indirect water contamination is not caused by the incorporation directly into the water, nor by those that end up there. An example contains contaminants for fertilizers and pesticides that are slowly swept into the soil and make their way through groundwater and then into separate watercourses.

Furthermore, air pollution can cause acid rain that can be highly detrimental to ecosystems, including polluting lakes, streams and beaches, to collapse to the ground and make the water hazardous for any species that leave in and around it [4].

The various types of contaminants and their origins are shown in Table 1, mentioned above. Such contaminants and their associated impacts on humans have different components. Therefore, these contaminants need to be monitored.

Table1: Sources of water pollutants with their effects.

Sources	Components/pollutants and their effects
Agricultural run-offs and mill-waste	NO_3^- and PO_4^{-3} (in fertilizers) -Excess amount results to eutrophication
	Herbicide and **pesticide** residues -Accretion of pesticides and herbicides have lethal effects on organisms in the water and to the humans. -Level of pesticides start to build up as it passes over the food chain. -High dose of pesticides may collect in the tissues of ultimate consumers that are mostly carnivores.
Untreated sewage consisting mainly of human faeces and domestic waste	**Suspended solids** -Reduced penetration of light -If suspended solids are biodegradable, microorganisms can decompose them and their processes require a high oxygen requirement.
	NO_3^- and PO_4^{-3} -Results into eutrophication.
Domestic waste includes detergents and food waste	**Detergent** -'Hard' detergents create foam that reduces oxygen supply to water-borne organisms -Soft detergents are biodegradable but it may contain high phosphate levels that can sometimes give rise to eutrophication.
Animal waste from farm	Microorganisms such as bacteria and protozoa. -If water would be used to drink, perhaps it will cause waterborne diseases namely cholera to be properly treated
Effluents from industries	**Heavy metals** such as Cu, Hg, Zn and Cr

-Electronic and electroplating plants **-Food and beverage processing industry** **-Rubber product processing industry**	-Highly toxic accumulation through the food chain in the organism -Mercury can cause acute human nervous disorder -Waste water contains numerous contaminants, including sulphide of hydrogen.
Underground pipes	**Lead** -Lead is highly poisonous Heavy metals that could built up in living organisms tissues -Lead may affect children's mental capability.

IV. Water Pollutants category

There are various types of pollutants categorized; this taxonomy can classify the cited pollutants in the table 1 as follows [5]:

Figure2: A taxonomy presents the different categories of water pollutants.

V. Water quality parameters (WQ):

In this section, we will define common water quality parameters and their role in determining the status of water quality, this point plays an important position in clarification to understand the main tasks in this thesis. The commonly used parameters are briefly discussed below:

• **pH**: The water's pH determines how acidic or alkaline the water is. The acidic level is between 0 and 6, whereas it is between 8 and 14 in the alkaline range. The most appropriate pH range is 6.5-8.5. It is determined by pH electrodes and electrometry. Electrical conductivity, overall stiffness, sulphates and total suspended solids are strongly associated with **[6, 7]**.

• **Turbidity**: Water turbidity is the indicator in the water of non-filterable, dispersed solids. It can interfere with water treatment as well. It is measured in units of nephelometric turbidity (NTUs). It is measured by a turbidimeter or nephelometer. Total hardness, electrical conductivity, sulphates, total dissolved solids and demand for chemical oxygen are substantially associated with it **[7, 8]**.

• **Temperature**: One of the most important parameters is temperature, which has a considerable impact on marine life. It also influences the transport rates of gas and the amount of oxygen dissolved. It may alter the shape or concentration of some elements. In Celsius, it is often determined. The test is carried out using a thermistor or thermometry. It is strongly correlated with electrical conductivity and slightly with pH **[9, 10]**.

• **Chloride (Cl)**: It is normally present in water and although its amount is typically not harmful to humans, but if it rises more than 250 mg / l, consequently, it can be harmful to agricultural operations, so the taste of the water expands into the saltier zone. Total hardness, electrical conductivity, total dissolved solids, biological oxygen demand and chemical oxygen demand are highly correlated with this parameter **[11, 12]**.

• **Electrical Conductivity (EC)**: This implies the capacity of the water to conduct electric current. In terms of water efficiency, it is not explicitly beneficial. However, it helps most in terms of the ionic composition of liquids, which in consequence defines the hardness, alkalinity and any of the solids dissolved. The conductivity ranges from the source of water and is associated with the demand for pH, temperature, turbidity, chlorides, sulphates, dissolved oxygen, total dissolved solids and chemical oxygen. It is assessed using an electrometric method **[7, 12]**.

• **Dissolved Oxygen (DO)**: It indicates the solubility of oxygen in water. Water mostly absorbs or produces oxygen from the atmosphere by photosynthesis. For aquatic life, it would be very

important. It is often analyzed by the Winkler Titration or Electrometric Meter. It is strongly related to electrical conductivity, biological oxygen demand and sulphates [7, 12].

• **Total Hardness (TH)**: It is an important tool for determining the suitability of water for household and industrial use. That is mainly the amount of Calcium and Magnesium concentrations found in the water. Their mineral ratios contribute to a large degree of hardness in water. It is associated strongly with pH, turbidity, chloride, total dissolved solids, demand for biological oxygen and demand for chemical oxygen. It is measured in mg / l $CaCO_3$ [7, 8].

• **Total Solids (TS)**: That is the sum of solids in the water suspended and dissolved. It shows the remains of sulfur, arsenic, calcium, etc. in the water. It is measured in mg/l or by the Gravimetric process (Dried at specified temperature) [7, 9].

• **Total Suspended Solids (TSS)**: is the sum of residues suspended in the water of inorganic and organic solid matter. The increase in TSS makes the water sensitive to high light absorption, which raises the temperature of the water and in turn restricts the oxygen persistence potential of the water. It profoundly influences the aquatic life. It is weighed and measured in mg/l using the Gravimetric (Filtration, with drying at specified temperature) process. It is correlated significantly with pH and total dissolved solids [7, 8, 9].

• **Total Dissolved Solids (TDS)**: That is the sum of available inorganic and organic soluble solids in the water. It is directly associated with water salinity. It is highly correlated with turbidity, chlorides, electrical conductivity, total hardness, total suspended solids and demand for chemical oxygen. It is measured using the Gravimetric (Dried after filtration at the specified temperature) process and expressed in mg / l [7, 8].

• **Biological Oxygen Demand (BOD)**: It is the amount of consumed oxygen, especially by protozoa and bacteria during their biological activities in the water. If the amount of BOD is very high and surpass DO, so most species die due to a lack of oxygen. It is a very critical element showing the performance of water and is compatible significantly with chloride, dissolved oxygen and total hardness. It is determined by the Oxygen Meter or Winkler Process, by incubation technique with oxygen determinations and expressed in mg / l [7, 10, 11].

• **Chemical Oxygen Demand (COD)**: It is the amount of absorbed oxygen during organic material dissolution and current inorganic material oxidation. Like BOD, the water quality status is also an important factor, it is strongly correlated with turbidity, chlorides, electrical conductivity, total hardness, and total dissolved solids. It is expressed in mg / l [7, 11, 12].

Like other countries in the world, Algeria has relevant water quality parameters according to its available equipment, here in this section we will introduce some typical tests achieved in

the laboratory of water analysis (Tebessa, Algeria) on the natural mineral water type YOUKOUS:

Table2: Physico-chemical analysis bulletin type YOUKOUS non-gaseous natural mineral water.

ANALYSIS	RESULTS	NORMS	COD
organoleptic Factors			
Color	**00 PCU**	**Max 25 PCU**	**NA 745**
Odor	**Nope**	**Max 4**	**NA 6371**
Flavor (taste)	**Absence of declared anomalies**	**Max 4**	**NA 6346**
Turbidity	**0.00 NTU**	**Max 2 NTU**	**NA 746**
physico-chemical Factors			
Conductivity at 20°C	**397 µs/cm**	**Max 2800 µs/cm**	**NA 749**
Total hardness	**110 ppm =11°F = 2.20 m = 110 mg/l**	**from 100 to 500 mg/l NA**	**NA 752**
TDS	**210 ppm**	**/**	**/**
pH at 20°C	**7.84**	**from 6.5 to 8.5**	**NA 751**

Table3: Physico-chemical analysis bulletin type YOUKOUS non-gaseous natural mineral water (1.5 L).

ANALYSIS	RÉSULTS	NORMS	COD
Mineralization	**284.00 mg/L**	**-**	**-**
Real volume	**1500 ml**	**-**	**-**
Nitrites	**0.03 mg/L**	**Au Max 0.10 mg/l**	**NA 1657**
Nitrates	**5.90 mg/L**	**Au Max 50 mg/l**	**NA 1656**
Composition with mg/l			
Chlorides	**32.00 mg/L.**	**Max 500 mg/L**	**NA 6917**
Sulphates	**21.00 mg/L.**	**Max 400 mg/L**	**NA 6361**
Calcium	**81.00 mg/L.**	**Max 200 mg/l**	**NA 1655**
Magnesium	**19.00 mg/L.**	**Max 150 mg/L**	**NA 752**
Sodium	**7.50 mg/L.**	**Max 200 mg/L**	**NA 1652**
Potassium	**2.00 mg/L.**	**Max. 20 mg/L**	**NA 1652**
Bicarbonates	**226.00 mg/L.**	**/**	**-**


pH meter/ conductivity/TDS


Triturator for Magnesium


Titration for Calcium


Photometer with flame for k+, Na+

Reagent for Nitrite

Reagent for Nitrate


Reagent for Sulphate

Reagent for Bicarbonate

Figure3: Different equipment for water quality parameter achieved at the laboratory of water analysis (Tebessa, Algeria).

VI. Global techniques used for pollutant identification in wastewater:

In the beginning of this chapter, we started by explaining the origin of different pollutant. Following by detecting pollution timely and locating, the pollution source was of great importance in environmental protection. In addition, numerous water pollutants have been discovered. Having known about the various pollutants, we further discuss their original sources and their impact on the environment and human health. Up to now, we can establish the background that we require to understand the issue of the pollutant and their side effects on our day-to-day life, besides; conceived that efficient and selective sensors are required to monitor the exact quantity of these pollutants in the water. Thereby, we will discuss with details in the next section the methods available to monitor these pollutants.

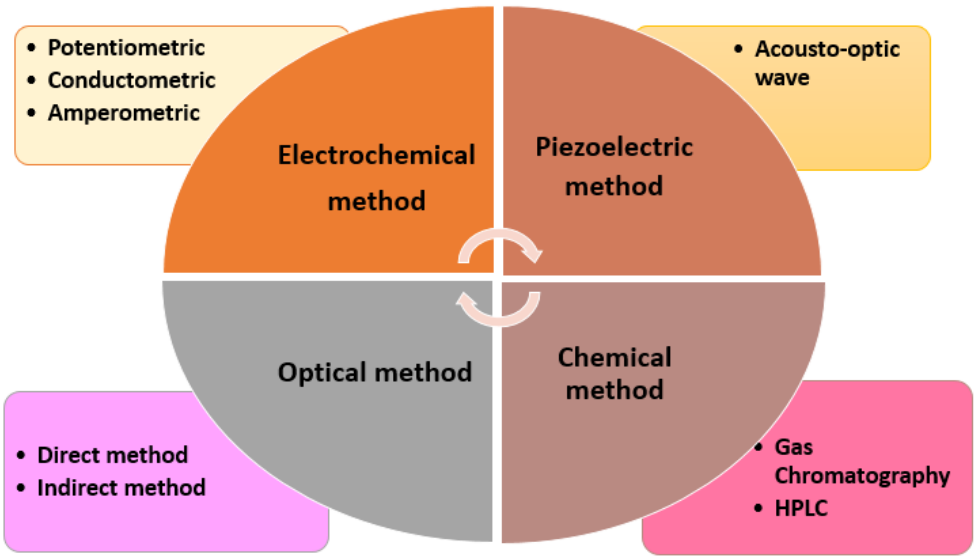

Figure 4: Four distinct classes and sub-classes of the available sensors.

VI.1. Electrochemical

Electrochemistry is a part of research that is concerned with the interdependency between electrical and material impacts, including the measurement of electrical quantities, such as flow, potential or charge, and their interaction with the parameters of compound.

In order to identify small sample sizes, fewer convergences of biological elements, and some of the reduced analytical gadgets **[13, 14]**, electrochemical biosensors have turned out to be useful instruments. In the manufacture and use of electrochemical biosensors for agro-food, biomedical and ecological tests **[15]**. Electrochemical-based poison identification procedures may be categorized as conductometric, coulometric or amperometric, voltammetric (fusing steps of pre-concentration and removal), and potentiometric.

Such biosensors that use electrodes enable organic signs to be changed into a discoverable yield flag. Using explicit natural elements, such as DNA, cells or enzymes, the affectability and selectivity of these signals can be obtained by improvement (Fig . 5).

Figure5: An electrochemical biosensor principle; the components of organic detection are connected to terminals into a reporting yield.

VI.2. Chromatography

Chromatography is a process that can be used to isolate the mixture to extract both qualitative and quantitative results. A consistent free phase, called a mobile phase, is practised by chromatographic divisions in a second sample-free phase, which maintains constant, called the stationary phase **[16, 17]**. When the sample passes through the mobile phase, it separates the segments into stationary and mobile phases.

It will take longer to complete the system for components whose delivery ratio supports the stationary phase, while those supporting the mobile phase will take a shorter time to complete. It is possible to separate solutes with a comparable distribution ratio, given sufficient time and stationary and mobile phases. For example, many analytical chemistry devices, high-performance liquid chromatography (HPLC) and gas chromatography (GC) are used in chromatography.

VI.2.1 Gas Chromatography (GC)

Gas chromatography (GC) is an analytical tool that is used to isolate and then detect the chemical components of a sample mixture to determine their presence or absence and/or how much is present. These chemical elements are typically compounds or gases that are biological. These components need to be volatile for GC to be effective in their study, typically with a molecular weight below 1250 Da, and thermally stable so that they do not degrade in the GC system **[16]**.

GC is a method commonly used in most industries: for quality monitoring in the manufacture of many goods, from vehicles to chemicals to pharmaceuticals; for scientific purposes, from

meteorite detection to natural products; and for environmental, nutritional and forensic protection. To allow the detection of chemical components, gas chromatographs are frequently hyphenated into mass spectrometers (GC-MS) [18].

VI.2.2 High-Performance Liquid Chromatography (HPLC)

It is a tool used to isolate, classify, and measure each component in a mixture in analytical chemistry. It depends on pumps to move through a column filled with a solid adsorbent substance through a pressurized liquid solvent comprising the sample mixture. Each component in the sample interacts with the adsorbent material somewhat differently, allowing the various components to have differing flow rates and contributing to the isolation of the components as they migrate out of the column.

HPLC was used for industrial uses (e.g. during the manufacturing phase of pharmaceutical and biological products), legal (e.g. identification of performance enhancing drugs in urine), analysis (e.g. isolation of components from each other of a complex biological sample or related synthetic chemicals) and medical (e.g. identification of blood serum vitamin D levels) [16].

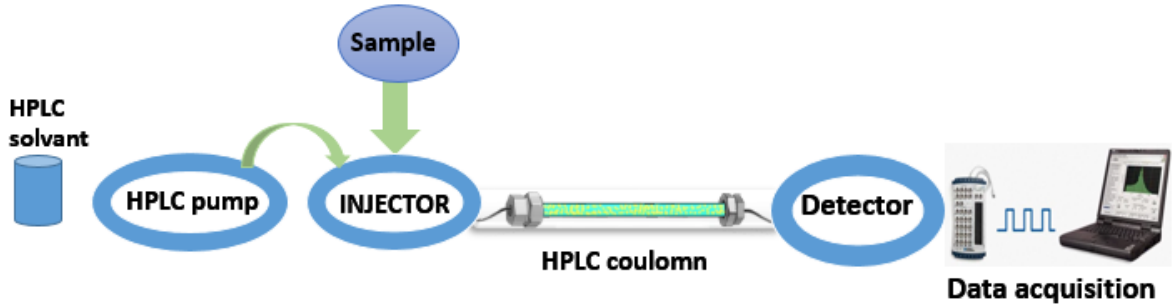

Figure6: Schematic diagram of HPLC process [16].

VI.3.Piezo-electrical techniques

These techniques strongly introduced by the acousto-optic method, due to their relationship in operation principle, in this section, the acousto-optic is used for water pollution monitoring. Basically, this approach is based on the use of the light beam diffraction effect owing to its contact with the ultrasonic wave in dirty water, which acts as an interaction medium (figure 7). The basic principle is to use the direction of the diffraction orders as a sensor, which is responsive to any change in the acoustic velocity due to a difference in the fluid interaction of the pollutant. On the other hand, the light intensity of these diffracted orders can be used as an additional sensor, sensitive to some variation of the refractive index of the medium, the density or the photoelastic constant [19].

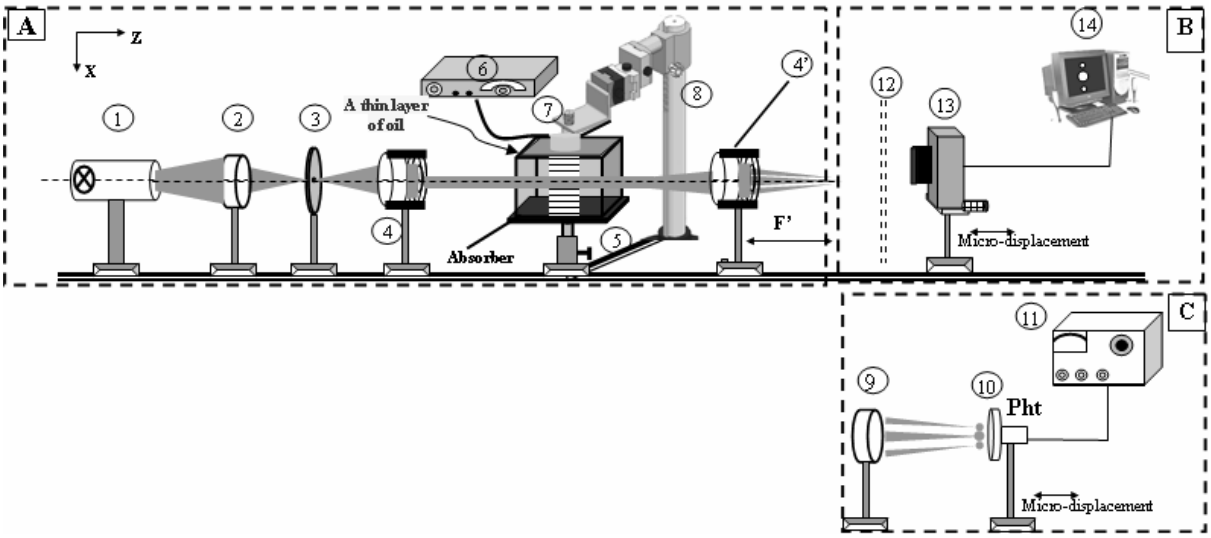

Figure 7: Acousto-optic configuration for water pollution monitoring. It consists 1- He-Ne Laser source (output power 30 mW at l=632.8nm), 2- microscope objective (focal length = 8mm) , 3- spatial filter (diameter = 20 µm) used as a beam cleaner, 4 and 4' refers to photographic objectives (focal length =210mm), 5- acousto-optic cell, 6-frequency generator, 7- piezoelectric transducer, 8- piezoelectric transducer holder 9- microscope objective (focal length =5mm) used to magnify the diffraction pattern , 10-photodiode (BPW21) , 11- photodiode Amplifier (Edmund optics, the order of sensitivity is close to Nano-Ampère), 12- light attenuator : used to prevent camera saturation, 13-CCD camera (resolution 644x484 pixel with pixel size: 8.4x8.4µm), 14-computer **[19]**.

VI.4.Optical techniques

Optical methods are optical-based methods used to record the capture of receptor target analytes. An overview of optical techniques that have been used in literature is depicted in Figure 8. It can be broadly categorized, according to the optical technique used, as direct and indirect sensors. Based on their inherent optical properties, the first detects analytes, whereas the second one requires an intermediate reagent that indicates the analyte's existence **[20]**.

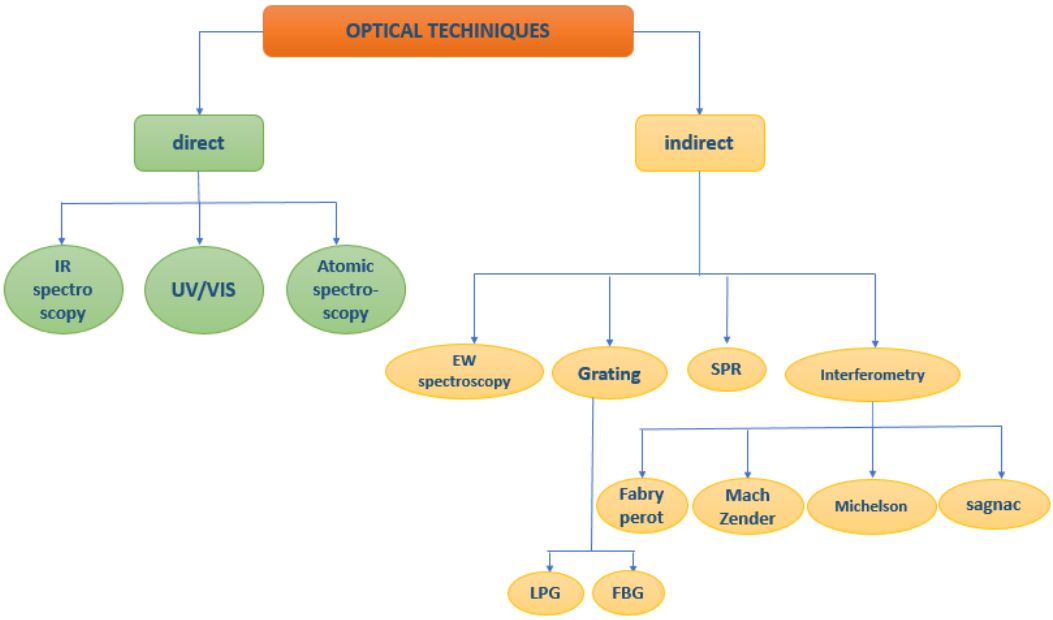

Figure8: A taxonomy for the general optical techniques [20].

VI.4.1. Direct optical techniques

Direct optical sensors measure the intrinsic properties of the analyte, such as IR absorption, UV-Vis absorption or atomic spectroscopy.

VI.4.1.1. IR spectroscopy

IR spectroscopy is the analysis of the interaction of infrared radiation with matter. It is used to analyze and classify solid, liquid or gaseous types of chemical compounds or functional groups. The infrared spectroscopy process or technique is carried out using an instrument called an infrared spectrometer (or spectrophotometer) that creates an infrared spectrum [21, 22]. In a graph of infrared light absorption (or transmittance) vs. frequency or wavelength, an IR spectrum can be visualized [23].

VI.4.1.2. UV-Vis Spectroscopy

UV/Vis spectroscopy is an important analytical method used to assess several water constituents. Molecules with π-electrons or non-bonding electrons can absorb electromagnetic energy in the visible ultraviolet spectrum to excite these electrons to higher molecular orbitals and can thus, be independently verified by UV-Vis spectroscopy [24].

VI.4.1.3. Atomic Spectroscopy

Every single analytical method that utilizes the emission and absorption of electromagnetic radiation by individual atoms is introduced into atomic spectroscopy. It is an exemplary tool for evaluating the trace amounts of certain elements in the periodic table [16, 25]. The element is known by the unique wavelength of the radiation (emitted or absorbed), while the amplitude of the transmitted (or absorbed) radiation is proportional to the measure of the present element

[26] (Fig. 9). Examples of these techniques include inductively coupled plasma and spectroscopy of atomic absorption.

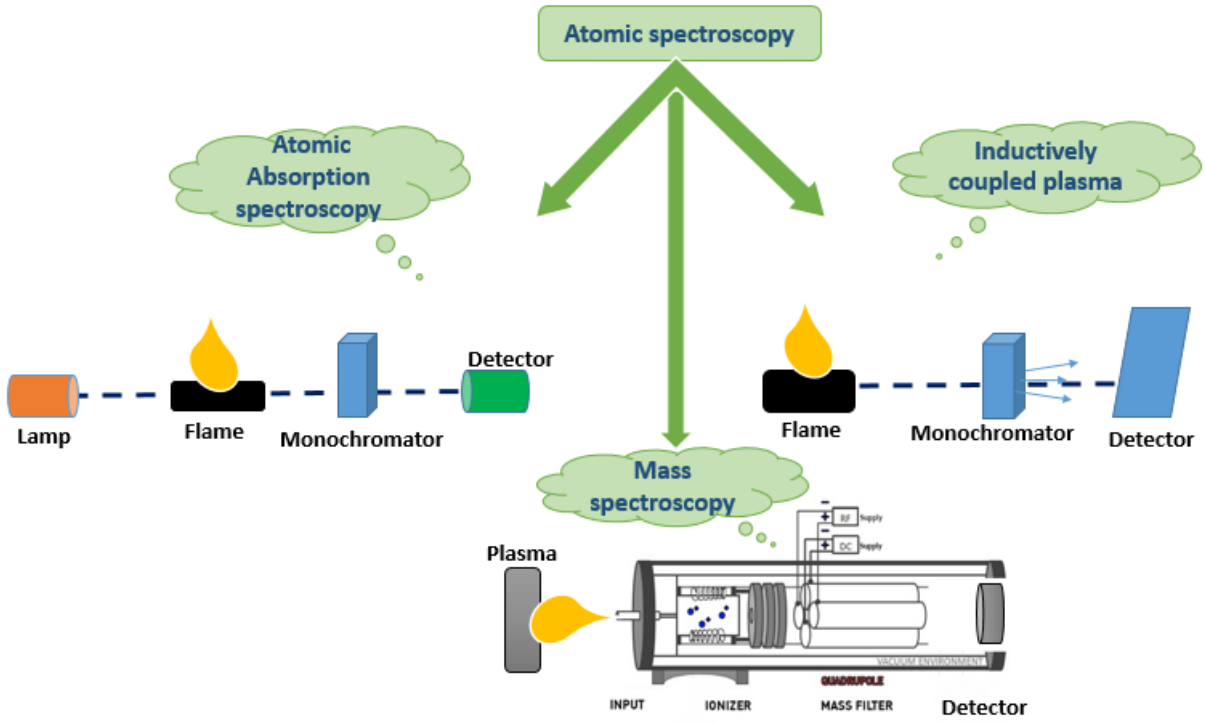

Figure9: Types of atomic spectroscopy.

VI.4.1.3.1. Atomic Absorption Spectroscopy (AAS)

By exciting the atoms of the ground state to higher energy values, atomic absorption spectroscopy estimates the discrete radiation absorbed by the absorption of an energy photon. Using the Beer-Lambert equation with the absorption coefficient of the ground-state atoms, the radiant power of the absorbed radiation is defined. Selectivity is provided by atomic absorption. When using flame atomization, the analysis time is fast, using a fully automated device with a test throughput of 250-350 findings every hour by using this method, however, it involves a broad sample preparation process [16].

VI.4.1.3.2. Inductively Coupled Plasma (ICP)

ICP is a spectroscopic technique for atomic emission that uses plasma for the atomization process. Plasma has an impressive percentage of electrons and positive ions that cancel and neutralize molecules. The plasmas consist of very energizing and ionized gases formed in argon-like inert gases.

They are useful for atom dissociation as well as for atomic and ionic emissions from excitation and ionization. ICP offers lower detection limits compared to ICP with AAS, but requires a highly qualified operator. The biggest downside of all atomic spectroscopic techniques is that

they do not have any data on the element's oxidation state or its speciation. In addition, like AAS, this technique involves a highly qualified operator and large training of examples [27].

VI.4.1.4. Fluorescence-Based Detection of Water Pollutants

The fluorescence-based technique has been used for the monitoring of water quality for many years, and it is still the primary technique for the consistent calculation of organic matter dissolved in water, such as chlorophyll and algae [28]. At a lower limit than the UV-Visible spectrum, it detects organic matter, and it also provides more detail. This technique requires fewer samples and detects the sample without processing; thus, the sample structure is not damaged; Strong reproducibility and high sensitivity are highly selective.

The method of identification of water pollution is based on the absorption under UV-vision of contaminants. The Fluorescence-Based Detection System is used to identify water pollutants through detecting light released by the chemicals at a separate wavelength (lower wavelength) after absorption [29].

VI.4.2. Indirect optical techniques

Most indirect optical methods require the presence of an analyte to be identified by an intermediate reagent. These intermediates are also, in most cases, receptors that undergo an analyte-dependent change in the optical properties of the transducer, mainly fluorescence, absorption, color change or refractive index [20].

VI.4.2.1. Evanescent wave spectroscopy

Evanescent wave spectroscopy is the overwhelming majority of the optical methods used. The core mode can excite an evanescent field; it is directed to the photodetector by the fiber (this technique will be further clarified in the next chapter) and absorbed by the surrounding medium, resulting in an overall decrease in the detector's light intensity (the techniques are often referred to as attenuated total reflection, ATR).

For indirect optical techniques using the evanescent field, Ref [30] offers a study of typical optical fiber setups, whereby the fiber cladding is normally stripped; or changed geometrically by an intermediate reagent. To improve evanescent field contact with reagent, tapering [31] and bending [32] of fibers were also mentioned.

VI.4.2.2. Fiber Bragg grating

Fiber Bragg gratings (FBG) are fiber-based gratings such as long duration gratings (LPG) that have also been used in Fiber Optic sensor. A FBG is an optical fiber with a periodic modulation of refractive index that has been inscribed into its core. As the FBG is illuminated with a

broadband light source that follows Bragg's law, this periodic modulation represents a series of beams.

For measurements of physical parameters such as temperature, strain and pressure, FBGs have long been documented. The duration of the core index modulation varies with some changes to these parameters, thereby varying the Bragg wavelength. More recently, for chemical sensing, FBGs have also been investigated [33].

VI.4.2.2.1. Long period grating

LPG also has a periodic refractive index, identical to FBG, included in its center. Since cladding modes are strongly attenuated, the LPG transmission range displays the transmission minimum of each reflecting coupling to a given cladding mode.

Because of their sensitivity to the refractive index in the surrounding area, LPGs have been used for chemical sensing. The improvement in refractive index modifies the coupling between the modes of core and cladding, leading to a phase transition in the minima transmission wavelength [34].

VI.4.2.3. Surface plasmon resonance (SPR)

The potential of SPRs for chemical process control was identified in the late 1970s [35], leading to the successful demonstration in 1982 of gas sensing and biosensing [36]. Since then, with the development and reports of new SPR configurations and applications, SPR sensing has attracted a lot of interest from the scientific community. Most of this interest is due to its ability, without the use of labeled molecules, for real-time monitoring of chemical / biochemical interactions.

In SPR fiber optics sensors, the evanescent field has propagation for the excitation of surface plasmon wave within metal films coated onto the thinned (or removed) cladding fiber, constant along the core-cladding interface is used. This excitation of the surface Plasmon transfers energy inside the fiber away from guided light, decreasing the transmitted light intensity. Hence, for a given light frequency and metal dielectric constant. Change in the dielectric environment affects the conditions of the resonance, leading to a shift in the wavelength of the resonance in the emitted light. This is the fundamental concept of the SPR fiber optic sensors [37].

VI.4.2.3.1. Localized surface plasmon resonance (LSPR)

The localized surface plasmon resonance is a closely related technique to SPR. (LSPR) involving noble nanoparticles of metal. Oscillations in the mutual charge. In addition to the

incidence of resonant frequency radiation, the nanostructure contributes to high dispersion and absorption within the UV-vis band [38].

The LSPR of an isolated nanosphere depends on the material, its size and its dielectric environment. For a group of nanoparticles or nanoparticles existing as a colloid, the LSPR often relies on inter particle spacing, resulting in two key mechanisms for the transduction of chemical events, namely a transition in the refractive index [39] or nanoparticles aggregation [40].

VI.4.2.4. Interferometry

Fiber interferometry is a relatively recent type of fiber optic methods used for chemical sensing. It uses light interference that has passed through various optical paths in the fiber, one of which changes the optical path difference through the presence of an analyte, resulting in a phase change in the interferogram. Fiber interferometers can provide extremely sensitive, precise, broad dynamic range readings. Moreover, measurements can be quantified using a few methods, including wavelength shift, phase, intensity, frequency or bandwidth [41]. Various fiber interferometers such as Fabry Perot, Mach Zehnder, Michelson and Sagnac are reviewed in Ref [42] (see figure 10).

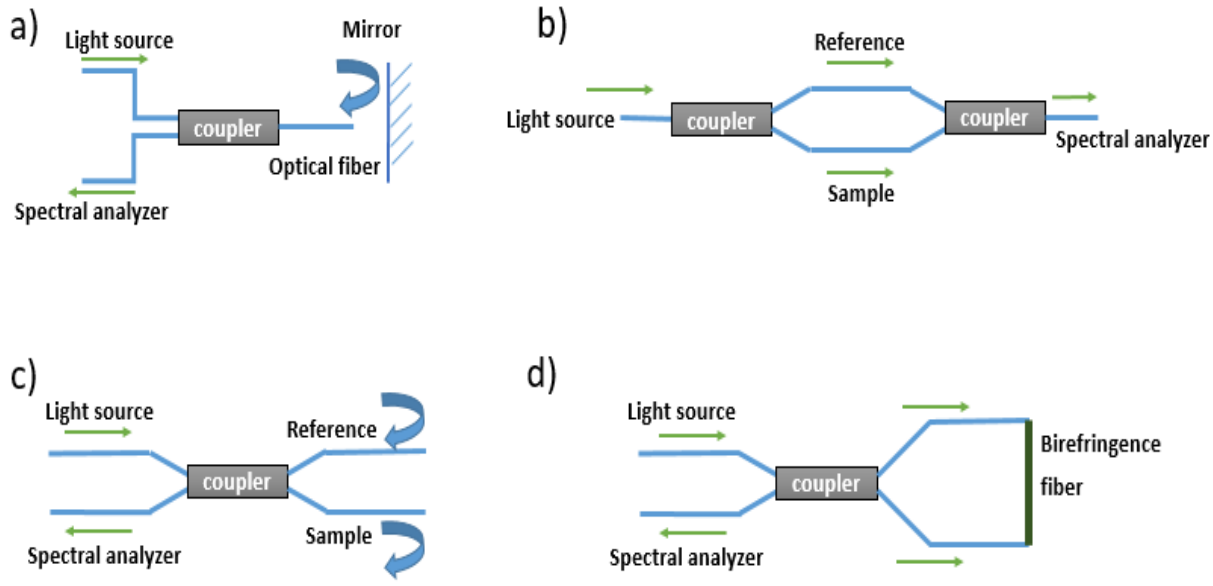

Figure10: Illustration of the a) Fabry Perot, (b) Mach Zehnder, (c) Michelson, (d) Sagnac fiber.

Conclusion

Water quality is defined as a measure of the physical, chemical, biological, and microbiological characteristics of water. Monitoring water quality in the 21st century is a growing challenge because of the large number of pollutants used in our everyday lives and in commerce that can make their way into our waters. General Methods of water analysis and knowledge of contaminants toxicity were reviewed in the background of this thesis. Therefore, development of simple and sensitive, low cost, portable sensors capable of direct measurement of environmental pollution are of considerable interest in this context.

Water pollution has become a huge problem in many countries all over the world. It is known that water is a very significant factor in life, but if this water becomes contaminated, it will be very dangerous for the humanity and wildlife. Pollution is defined as ' to make fetid or unclear and dirty'.

Because of all these causes of water pollution, there are some unwanted effects. First of all, this type of pollution definitely influences the health of humanity, because many use large quantities of water for drinking or cooking. Thus, it is crucial to have pure water. Moreover, contaminated water can damage wildlife. The second effect of water pollution is the environmental influence such as the odour of water and the terrible sights on beaches or rivers. This leads to water scarcity because it limits its availability for humans and ecosystem.

In the first chapter, we have explained in details the water pollution problem including the origin of this phenomenon that needs a real time monitoring by different methods, this last, was clarified in this chapter. We provided a complete report about the general used methods for water pollution monitoring specifically the optical methods.

References

[1] Dwivedi, A. K. (2017). Researches in water pollution: A review. International Research Journal of Natural and Applied Sciences, 4, 118–142.
[2] Bonavigo, L., Zucchetti, M., & Mankolli, H. (2009). Water radioactive pollution and related environmental aspects. Journal of International Environmental Application & Science, 4, 357–363.
[3] Tóth, J. (2009). Origin, distribution, formation, and effects. Groundwater-Volume I, 27.

[4] Barbera, A. J., & Mcconnell, V. D. (1990). The impact of environmental regulations on industry productivity: Direct and indirect effects. Journal of environmental economics and management, 18, 50–65.
[5] Pooja, D., Kumar, P., Singh, P., & Patil, S. (Eds.). (2020). *Sensors in Water Pollutants Monitoring: Role of Material*. Springer.
[6] Ahmed, U., Mumtaz, R., Anwar, H., Mumtaz, S., & Qamar, A. M. (2020). Water quality monitoring: from conventional to emerging technologies. *Water Supply*, *20*(1), 28-45.
[7] Environmental Protection Agency 2001 Parameters of Water Quality, Interpretation and Standards. Available from: https://www.epa.ie/pubs/advice/water/quality/ Water_Quality.pdf (accessed 19 November 2018).
[8] Bhandari, N. S., & Nayal, K. (2008). Correlation study on physico-chemical parameters and quality assessment of Kosi river water, Uttarakhand. *Journal of Chemistry*, *5*(2), 342-346.
[9] Verma, A. K., & Singh, T. N. (2013). Prediction of water quality from simple field parameters. *Environmental earth sciences*, *69*(3), 821-829.
[10] Ali, M., & Qamar, A. M. (2013, September). Data analysis, quality indexing and prediction of water quality for the management of rawal watershed in Pakistan. In *Eighth International Conference on Digital Information Management (ICDIM 2013)* (pp. 108-113). IEEE.
[11] Khatoon, N., Khan, A. H., Rehman, M., & Pathak, V. (2013). Correlation study for the assessment of water quality and its parameters of Ganga River, Kanpur, Uttar Pradesh, India. *IOSR Journal of Applied Chemistry*, *5*(3), 80-90.
[12] Patel, J. Y., & Vaghani, M. V. (2015). Correlation study for assessment of water quality and its parameters of par river Valsad, Gujarat, India. *IJIERE*, *2*, 150-156.
[13] Arduini, F., Cinti, S., Scognamiglio, V., Moscone, D., & Palleschi, G. (2017). How cutting-edge technologies impact the design of electrochemical (bio) sensors for environmental analysis. A review. Analytica Chimica Acta, 959, 15–42.
[14] El Harrad, L., Bourais, I., Mohammadi, H., & Amine, A. (2018). Recent advances in electrochemical biosensors based on enzyme inhibition for clinical and pharmaceutical applications. *Sensors*, *18*(1), 164.
[15] Hughes, G., Westmacott, K., Honeychurch, K. C., Crew, A., Pemberton, R. M., & Hart, J. P. (2016). Recent advances in the fabrication and application of screen-printed electrochemical (bio) sensors based on carbon materials for biomedical, agri-food and environmental analyses. *Biosensors*, *6*(4), 50.
[16] Harvey, D. (2000). *Modern analytical chemistry* (Vol. 1). New York: McGraw-Hill.

[17] Moini, M. (1998). GC/MS: A practical user's guide by Christopher McMaster and Marvin McMaster (University of Missouri, St. Louis). Wiley: New York. 1998, ISBN 0-471-24826-6. Journal of the American Chemical Society, 121, 4931.

[18] Beilby, A. L. (1977). In R. L. Pecsok, L. D. Shields, T. Cairns, I. G. McWilliam (Eds.), Modern methods of chemical analysis (2nd ed.). Journal of Chemical Education, 54, A463.

[19] Ferria, K., Griani, L., & Laouar, N. (2012, May). Acousto-optic method used to control water pollution by miscible liquids. In *AIP Conference Proceedings* (Vol. 1433, No. 1, pp. 76-83). American Institute of Physics.
[20] Tou, Z. Q. (2015). *Fiber optics chemical sensors based on responsive polymers* (Doctoral dissertation).

[21] Wang, H., Q. Wang, et al. (2008). "Measurement technique for methane concentration by wavelength scanning of a distributed-feedback laser." Laser Physics **18**(4): 491-494.

[22] Wu, X.-j., P. Wang, et al. (2009). "Methane Optic Fiber Sensor Network Based on Infrared Spectrum Absorption in Coal Mine." Spectroscopy and Spectral Analysis **29**(9): 2365-2369.
[23] Cubillas, A. M., J. M. Lazaro, et al. (2009). "Gas Sensor Based on Photonic Crystal Fibres in the 2 nu(3) and nu(2)+2 nu(3) Vibrational Bands of Methane." Sensors **9**(8): 6261-6272.
[24] Tao, S. Q. and T. V. S. Sarma (2006). "Evanescent-wave optical CrVI sensor with a flexible fused-silica capillary as a transducer." Optics Letters **31**(10) : 1423- 1425.
[25] De Levie, R. (1997). Principles of quantitative chemical analysis. New York: McGraw-Hill.

[26] Patnaik, P. (2004). Dean's analytical chemistry handbook (Vol. 1143). New York: McGraw-Hill.
[27] Khopkar, S. M. (2009). Basic concepts of analytical chemistry. New Delhi: New Age International (P) Limited Publishers.
[28] Foley, J., Batstone, D., & Keller, J. (2019). The R & D challenges of water recycling-technical and environmental horizons. In Advanced wastewater management centre.
[29] Yu, H. B., Wang, Y. Y., & Song, C. Y. (2011). Study of three-dimensional fluorescence spectra for measuring chlorobenzene in water. Guang Pu Xue Yu Guang Pu Fen Xi, 31(7), 1823–1827.
[30] McDonagh, C., C. S. Burke, et al. (2008). "Optical chemical sensors." Chemical Reviews **108**(2): 400-422.
[31] Leung, A., P. M. Shankar, et al. (2007). "A review of fiber-optic biosensors." Sensors and Actuators B-Chemical **125**(2): 688-703.
[32] Khijwania, S. K. and B. D. Gupta (2000). "Maximum achievable sensitivity of the fiber optic evanescent field absorption sensor based on the U-shaped probe." Optics Communications **175**(1-3): 135-137.
[33] Rao, Y. J. (1997). "In-fibre Bragg grating sensors." Measurement Science & Technology **8**(4): 355-375.
[34] James, S. W. and R. P. Tatam (2003). "Optical fibre long-period grating sensors: Characteristics and application." Measurement Science & Technology **14**(5): R49-R61.
[35] Gordon, J. G. and S. Ernst (1980). "Surface-Plasmons as a Probe of the Electrochemical Interface." Surface Science **101**(1-3): 499-506.
[36] Liedberg, B., C. Nylander, et al. (1983). "Surface-Plasmon Resonance for Gas-Detection and Biosensing." Sensors and Actuators **4**(2): 299-304.
[37] Sharma, A. K., R. Jha, et al. (2007). "Fiber-optic sensors based on surface plasmon resonance: A comprehensive review." IEEE Sensors Journal **7**(7-8):1118-1129.
[38] Haes, A. J. and R. P. Van Duyne (2002). "A nanoscale optical blosensor: Sensitivity and selectivity of an approach based on the localized surface plasmon resonance spectroscopy of triangular silver nanoparticles." Journal of the American Chemical Society **124**(35): 10596-10604.
[39] Storhoff, J. J., A. A. Lazarides, et al. (2000). "What controls the optical properties of DNA-linked gold nanoparticle assemblies?" Journal of the American Chemical Society **122**(19): 4640-4650.
[40] Sepulveda, B., P. C. Angelome, et al. (2009). "LSPR-based nanobiosensors." Nano Today **4**(3): 244-251.

[41] Grattan, K. T. V. (1995). Sources for optical fiber sensors. In *Optical Fiber Sensor Technology* (pp. 45-74). Springer, Dordrecht.
[42] Lee, B. H., Y. H. Kim, et al. (2012). "Interferometric Fiber Optic Sensors." Sensors **12**(3): 2467-2486.

Chapter II

CLADLESS OPTICAL FIBER SENSOR BASED ON EVANESCENT WAVE ABSORPTION FOR MONITORING METHYLENE BLUE INDUCED WATER POLLUTION

I. Introduction

This chapter describes the necessary theoretical background, design, fabrication and characterization of unclad evanescent wave fiber optic sensors (EWFS) and their application for trace detection and measurement of certain pollutants in water especially the effluents steamed from industrial rejects such as ammonia. Methylene blue, Congo red ….etc.

The superior performance of these sensors is established by comparing their performance in terms of lower detection limit, dynamic range etc., with that of the conventional spectrophotometric method. Efforts are made to reduce the size and cost of the sensors by using various light emitting diodes (LED) as sources.

In particular, a prevalent, low cost, and effective technology for real time detection of methylene blue in distilled water is discussed in this chapter.

II. Optical Fibre Sensor systems

Basically, except that the fiber optic sensors (FOS) uses a glass fiber instead of copper wire and light instead of electricity, FOS work as most electrical sensors. It modulates light characteristics, including intensity, phase, polarization, or change in wavelength **[1]**.

Most of the instrumentation changes in this specific application have been recorded to date. In order to manipulate the incident radiation, various sensor implementations involve different types of transducers (optical fibres). Therefore, optical fibre sensor instrumentation needs an overview **[2]**.

II.1.Fibre Sensor System Configuration

Basically, an optical fibre-sensing device consists of a light source, an optical fibre, a transducer or sensing component, and a detector. Table 1 provides brief explanations of the fiber optic sensor (FOS) elements. The simple optical fibre structure consists of a core surrounded by a lower refractive index of any cladding material and both are transparent, cylindrical, and dielectric.

The FOS specification is to have low optical and mechanical attenuation without output loss under all planned operating conditions **[3]**. It is possible to divide FOS into two groups: intrinsic and extrinsic **[4]**.

The simple construction of extrinsic FOS and intrinsic FOS, respectively, which can be seen in figures 1 (a and b). So-called intrinsic devices rely on a light beam that propagates through the fibre, and the environmental effect within the optical fibre itself are interactive. Extrinsic fibre optic systems are used to couple light via the optical fibre. The light beam transmits the revealed ambient effect from the fibre and passes it out.

The light then doubles out again to the fibre. The light beam to and from the fiber area is also influenced by the measurement [5].

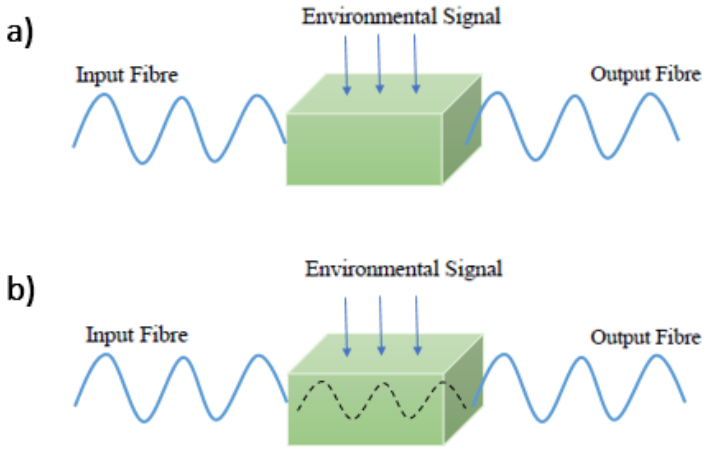

Figure1: Schematic representation for a) extrinsic FOS, b) intrinsic FOS [1].

Table1: The basic optical sensor topologies are built up with light source, fibre, and detector.

Item	Types	Key words	Reference
Optical fiber	Single mode fiber	(a) core diameter : 9µm (b) cladding diameter:125µm	[6]
	Multimode fiber	(a) step index fibers which is uniform refractive index medium (i) core diameter: 50 to 85 µm (ii) cladding diameter: 125 µm (b) Gradient index fibers, which core transverse refractive index variation nearly parabolic. (i) core diameter: 50 to 85 µm (ii) cladding diameter: 125 µm (c) It can couple large amount of light and is easy to handle both arising from its large size.	[6]
	Silica fiber	(a) A resonant optical cavity allows a beam of light to circulate in a closed path	[7]
	Hollow fiber	(a) Structure comprises an extern layer, porous support layer and fiber bore.	[8]
	Plastic fiber	(a) Fiber made from polymer materials such as PMMA.	[6]

		(i) core diameter: 1mm (ii) cladding diameter: /μm	
Light source	Light emitting diode (LED)	(a) Low coherence length, broad spectral width, low sensitivity to back reflect light and high reliability.	[9]
	Laser diode (LD)	(a) Exhibits high coherence, narrow line width and high optical output power, and more expensive.	[9]
	Super radiant diode	(a) operating properties between LED and LD and exhibit high power, low coherence device	[9]
	He-Ne laser	(a) relatively low cost and ease of operation compared to other visible lasers producing beams of similar quality in terms of spatial coherence	[6]
detectors	Semiconductor photodiode	(a) Good for visible and near IR wavelengths. (b) There is no bandwidth limitation due to the detector.	[6]
	Avalanche photodiode	(a) Sense low light levels due to the inherent gain because of avalanche multiplication, but need large supply voltage (100V).	[6]

In order to facilitate distributed sensing, optical fibers take advantage of their specific characteristics, which are susceptible to linear and non-linear environmental effects. Therefore, a comprehensive system design that fits the system to the environment is important to achieve optimal efficiency for a given measurement [5].

Majority of FOS have the propensity to operate in the way that is depicted in Figures 3(a–c). Figure 3(a) depicts a sensor tip sensitized to respond to the measured parameter, which then detects the amount of light reflected at the tip. The sensor element can provide an extended sensing response with a long length of fibre [9].

This sensitivity can be increased by covering the fiber in a compact shape to serve as a transducer head. Other interesting sensing possibilities can also be provided by fibre optic sensing practices, including the ability to distinguish spatially at various locations over an identical fibre length, as seen in Figure 3(b). FOS is small and lightweight, thereby allowing the possibility of sensing geometries being distributed or quasi-distributed [10].

This means that FOS can be multiplexed and can be measured over a continuous region or in a region (multi-channel) with a large number of discrete sensing geometry points, as shown in Figure 3(c). Otherwise, it would be expensive to consume or intricate to use traditional sensors. Using FOS, several external parameters such as pressure [11], acoustics [12], strain [13], pH [14], temperature [15], and heavy metal [16] can be determined with greater accuracy and velocity.

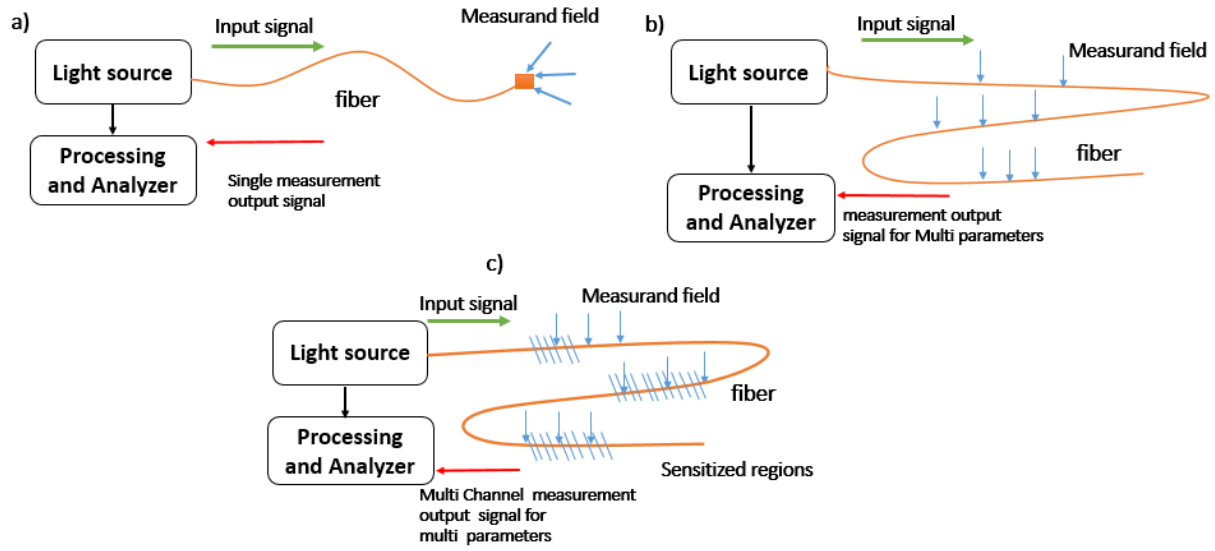

Figure2: Basic fiber optic sensor system configuration [1].

II.2. Characteristics of FOS development

FOS has many advantages over conventional devices, largely due to the properties of the optical fiber itself. FOS can be very small in size, resistant to harsh (chemical) environments and resistant to electromagnetic interference. They can be located in remote locations that overcome challenging measurement conditions. Devices are thus inherently secured by low optical strength and lack of electrical current at the sensing stage [6].

Absorption and fluorescence based observations are also related to the target analyte, which is due to either the atom, ion or molecule with its unique characteristic reference to electromagnetic radiation. The optical sensor study is therefore an analysis of colors, quantities, sensitivity and selectivity that leads to the assessment of the chemical species and is specifically designed to meet the requirements of many specific conditions [3].

Design of extrinsic and intrinsic sensor types with various fibre optic based on optical Sensors transduction mechanisms can be further classified as shown in Figure 3, and as discussed below. They include direct spectroscopy, evanescent wave, fibre grating and interferometric sensors.

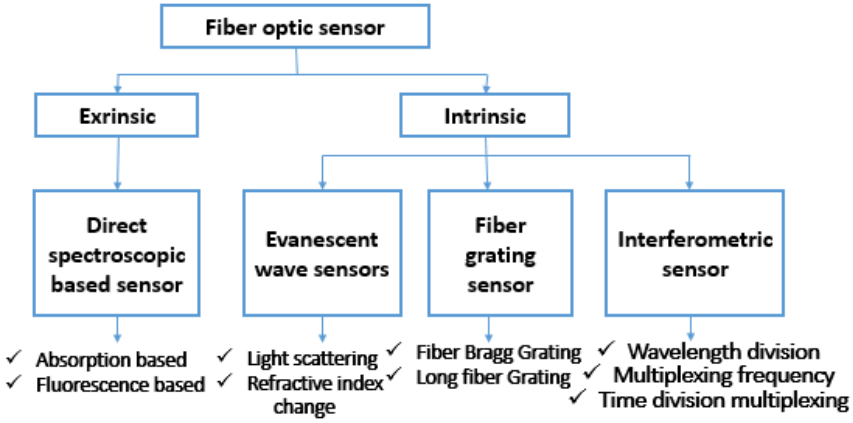

Figure3: Design of fiber optic sensor categories [1].

This chapter details the design and construction of EWA-based fiber optic sensors for bio sensing applications, starting with the theoretical background of the EWA-based fiber optic sensor. A debate on the different geometries used to improve the sensitivity of the EWA-based fiber optic sensor is also included.

II.3.Theory of Evanescent Wave Absorption Based Fiber-Optic Sensor

Evanescent wave absorption dependent sensing phenomena is determined by the leakage / loss of electromagnetic energy at the center and cladding medium interface during the total internal reflection (TIR) occurrence. This section would discuss the physics involved and the parameters that control the activity of such sensors.

II.3.1. Important Parameters in Optical Fiber

The optical signals are directed by total internal reflection through waveguides/fibers. Consequently, the amount of light guided is modulated by the refractive indices of the different media (i.e. core and cladding) and can be expressed in terms of the critical angle (θ_c) and the numerical aperture (NA) (Eq. (II.1) and (II.2)).

$$\theta_c = \sin^{-1}\left(\frac{n_{clad}}{n_{core}}\right) \quad \text{(II.1)}$$

$$NA = \sqrt{n_{core}^2 - n_{clad}^2} \quad \text{(II.2)}$$

The number of modes supported (M) depends on the NA, the fiber radius (r) and the wavelength of the light signal. The relationship may be as follows:

$$M = \frac{4V^2}{\Pi^2} = \frac{V^2}{2.5} \quad \text{(II.3)}$$

Where: $$V = \frac{2\Pi r}{\lambda} NA \quad \text{(II.4)}$$

V is referred to as the V-number (or normalized frequency) for the fiber, which helps in determining the operations of the fiber i.e. single mode or multimode **[17]**.

II.3.2. Evanescent Wave (EW)

Usually, the ray tracing technique is used to describe total internal reflection (TIR) of multimode optical fibres. This method can be useful if the measurements of the fiber are wide relative to the wavelength of the light. It is helpful to clarify terms such as numerical aperture and to illustrate the laws of refraction.

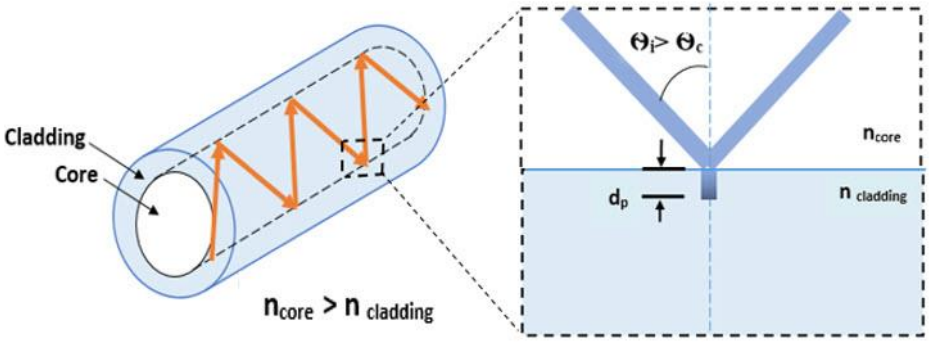

Figure4: Ray-tracing approach describes the evanescent wave phenomenon.

When the incident angle (θ_i) of the propagating ray is greater than the critical angle (θ_c), the ray is reflected back from the core-cladding interface due to the TIR. At each TIR case, a small portion of the guided wave energy penetrates the cladding medium and produces an electromagnetic field referred to as the "evanescent wave" (Fig . 4).

Wave theory provides in-depth understanding of the phase changes and the evanescent area that surround the TIR phenomena. A detailed derivation can be found in ref. **[18]**. According to wave theory, energy outside the core is essential for the application of a biosensor based on EWA in the case of $\theta_i > \theta_c$ (Fig. 4). The wave equation transmitted may be given as follows:

$$E_T = \tau E_0 e^{-k_0 z n_{core}\sqrt{(n_{core}^2/n_{clad}^2)\sin^2\theta_i - 1}} e^{jk_0 n_{clad}\sin\theta_i y} \quad \text{(II.5)}$$

Out of the Eq. (II.5). It is obvious that the amplitude of the evanescent wave decays exponentially as the energy moves away from the z-direction interface. It can also be shown that the evanescent wave is very sensitive to RI shifts at the core- the cladding interface. These facts have been used to create evanescent wave absorption sensors.

II.3.2.1. Evanescent Wave Parameters

Various physical, optical and geometric parameters of all optical fibers influence the evanescent wave. Penetration depth and evanescent power (or fractional cladding power) are the two essential parameters for assessing the operation of EWA-based sensors.

- **Penetration depth (dp)**

The penetration depth (dp) of the evanescent field , i.e. the distance at which the amplitude of the electrical field decreases to 1 / e of its magnitude at the interface, increases with a decrease in the refractive index contrast at the core cladding interface. It is also a function of the wavelength of the light and of the angle of incidence (Eq. II.6).

$$dp = \frac{\lambda}{2\pi\sqrt{n_{core}^2 \sin(\theta_i) - n_{cladding}^2}} \qquad \text{(II.6)}$$

Theoretically, the evanescent wave will interact with all molecules up to an infinite distance, though at a reduced degree of interaction. From the point of view of laboratory activities, dp is the distance to which molecules may have a discernible influence.

- **Evanescent power (Fractional power in cladding)**

Evanescent power can be approximated by calculating the amount of fractional power present in the cladding of a multimode fiber and given as **[19]**:

$$\frac{P_{clad}}{P} = \frac{4}{3\sqrt{M}} = \frac{4\sqrt{2}}{3V} \qquad \text{(II.7)}$$

From eq. (II.7):

$$\frac{P_{clad}}{P} = \frac{4\sqrt{2}}{3} \frac{\lambda}{2\Pi\sqrt{n_{core}^2 - n_{clad}^2}} \qquad \text{(II.8)}$$

Where, P_{clad} = optical power in cladding, P = total optical power in core and cladding together. From Eq. (II.7), it is observed that increase in V-number will reduce fractional power in the cladding **[20]**. Therefore, selection of V-number is very important in determining evanescent power of the fiber-optic sensor.

II.3.2.2 Evanescent wave absorbance (EWA)

The evanescent wave at the surface of the core is eligible for contact with the surrounding medium, but restricted by its depth of penetration. If any absorbing molecule is present within the depth of interaction of the evanescent field, it will absorb the evanescent field and result in attenuation of the amplitude of the propagating wave (guided in the core of the fiber). The transmittance of power at the end of the unclad zone shall be effected by:

$$P_L = P_0 \times e^{-\gamma \bullet L} \tag{II.9}$$

Where, P_L = optical power transmitted across length (L), P_0 = initial optical power launched in optical fiber, γ = evanescent wave absorption coefficient of the molecule and L = length of unclad fiber probe.

Evanescent wave absorption coefficient is proportional to fractional power in cladding (or medium surrounding the fiber core in case of unclad fiber), concentration (C) and absorption coefficient (α) of the molecule. (Eq. (II.10)):

$$\gamma = \frac{P_{clad}}{P} \alpha \bullet C \tag{II.10}$$

From Eq. (II.9) and (II.10), we get the equation for evanescent wave absorbance, given by pseudo Beer-Lambert Law **[21]**:

$$A = \frac{P_{clad}}{P} \frac{\alpha CL}{\ln(10)} \tag{II.11}$$

Combining both Eq. (II.8) and (II.11), we get the equation for evanescent wave absorbance (A).

$$A = \frac{4\sqrt{2}}{3} \frac{\lambda}{2\pi r \sqrt{n_{core}^2 - n_{clad}^2}} \frac{\alpha CL}{\ln(10)} \tag{II.12}$$

Thus, the evanescent wave absorbance is inversely proportional to the RI contrast (between core and cladding) and the optical fiber radius. It is strictly proportional to the absorption coefficient, the concentration of the molecule, the wavelength of the light and the length of the stripped fiber. These considerations are very critical for designing sensors focused on evanescent wave absorption (or attenuated total reflection sensors).

II.3.3. Loss Due to V-Number Mismatch

As light moves from one fiber to another with different V-numbers (due to variations in cladding / core material or core radius), there is a lack of signal (Fig. 5). Owing to the low V-number in the receiving fiber, the higher-order modes of the transmitting fiber are not assisted by the receiving fiber and the signal carried by higher-order modes is lost.

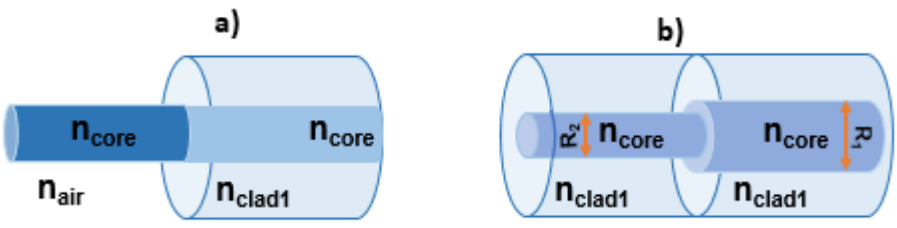

Figure5: Schematic representation of V-number mismatching (a). Due to different cladding material (NA mismatch) and (b). Differences in core radius (R_1<R_2).

II.3.3.1. NA Mismatch

As the light propagates from the high-numeric aperture fiber (NA_1) to the low-numeric aperture fiber (NA_2), the effect is a loss of rays (Fig. 5(a)). This loss (P_L) can be determined by the basis of NA mismatch as follows [22]:

$$P_L = -10\log(\frac{NA_2}{NA_1})^2 \quad \text{(II.13)}$$

II.3.4. Working of EWA Based Fiber-Optic Sensor

In the design of the fiber optic sensor, all the parameters and losses listed in the preceding sections, we discovered that the penetration depth of the evanescent wave is very small and can only impact the weak cladding modes of the fiber while the core modes remain unaffected. In order to increase the sensitivity, the sensing area of the fiber is usually unclad thus that the evanescent field of the core modes will communicate directly with the fiber.

II.3.4.1 Refractive Loss

In the unclad fiber optic probe, the increase in refractive index (RI) in the field around the unclad region (i.e. sensing region) reduces the local numerical aperture and results in light attenuation due to loss of refraction. Fig. 6 explains the loss of refractive in the fiber optic sensor. As the unclad fiber is held in the RI medium (n_2), certain rays (R_1 and R_2) are guided by the critical angle. If the surrounding RI is modified from n_2 to n_3 ($n_3 > n_2$), the critical angle increases.

This current critical angle (θ_c ') is greater than the existing R_1-ray incidence angle, resulting in the R_1-ray being refracted and ultimately lost (Fig. 4(b)). Depending on the Fresnel reflection coefficient, a certain proportion of the incident light will be reflected in the fiber and will continue to propagate with decreasing power for any interaction with the core surface.

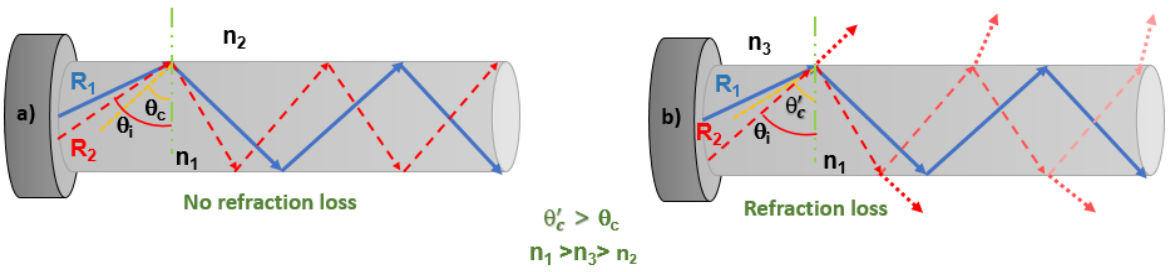

Figure6: Schematic representation of refraction loss in optical fiber sensor due to change in surrounding RI; (a). No refraction loss occurs because $\theta_i > \theta_c$ for both the rays; (b). Change in RI from

n_2 to n_3 ($n_3 > n_2$) increases the critical angle to (θ_c ') and causes the refractive loss of ray R_1. A decrease in colour intensity of ray R_1 represents the decreased power of the refractive ray **[23]**.

Refractive loss is due to an increase in the effective refractive index in the sensing region and can be determined from Eq. (14). In the case of a sensor, the refractive loss equations can be updated as follows:

$$P_{RL} = -10\log\left(\frac{NA_a}{NA_r}\right)^2 \quad \text{(II.14)}$$

Where, P_{RL} is the refractive loss (dB), NA_a is the numerical aperture of the sensing region in the presence of the analyte, NA_r is the numerical aperture of the sensing region in presence of reference medium. This refractive loss is an instantaneous response of the fiber due to change in bulk RI.

II.3.4.2. EW Absorbance

If the analyte molecule is adjacent to the surface (due to its affinity to surface groups or due to physical adsorption), it joins the interface area of the evanescent field and may also be attached to the receptors on the surface of the fiber. Each molecule interacts with the evanescent wave, based on its size and optical parameters, such as the refractive index (n) and the extinction coefficient (k).

The relationship between the absorption coefficient and the extinction coefficient shall be calculated by:

$$\alpha = 4\pi k / \lambda \quad \text{(II.15)}$$

The evanescent wave absorbance given by eq. (II.11) may be modified to:

$$A = \frac{4\sqrt{2}}{3} \frac{\lambda}{2\pi r \sqrt{n_{core}^2 - n_{analyte}^2}} \frac{\alpha CL}{\ln(10)} \quad \text{(II.16)}$$

This absorption may be directly related to the concentration of the analyte, if other parameters are known. Refractive loss can be insignificant at extremely low concentrations due to a very small RI difference between the analyte solution and the reference solution. Therefore, EWA dominates the sensor response at a lower concentration. In the other hand, at a high concentration, there will first be a refractive loss due to a large variation in bulk RI relative to the reference medium.

However, owing to the binding of a large number of molecules, the effective RI of cladding varies significantly, adding to the refractive loss. The sensor reaction is therefore a cumulative

consequence of both the refractive loss and the EWA, which varies with the concentration of the analyte and/or its density (after binding) on the sensor surface.

II.3.4.3. V-Number Mismatch

Usually, the unclad sensing area of the EWA sensor is accompanied by the cladded optical fiber. It induces mismatch in the V-number between the sensing area and the receiving component (Fig. 3(a)). This results in a lack of signal when moving from the sensing area back to the passive cladding fiber end leading to a loss of higher order modes that can not be coupled. This decreases the signal-to - noise level.

One of the practical solutions is to reduce the fiber core radius at the output end to meet the V-number. Criteria for minimizing the V-number mismatch are given by **[24]**:

$$r_a \leq r_{clad}\left(\frac{n_{core}^2 - n_{clad}^2}{n_{core}^2 - n_{analyte}^2}\right)^{\frac{1}{2}} \quad \text{(II.17)}$$

Where, r_a is the radius of the core at the end of the sensing region, r_{clad} is the radius of the cladding, n_{core} is the RI of the core, n_{clad} is the RI of the cladding and n analyte is the effective RI due to presence of analyte in sensing region.

The sensor response of the evanescent wave absorbance dependent fiber optic sensor is therefore a cumulative result of refractive loss, evanescent wave absorbance and loss due to V-number mismatch. In the next section, we can see various parameters that have been explored to enhance the sensitivity of EWA-based fiber optic sensors.

II.3.5. Sensitivity enhancement of EWA based fiber-optic sensor

The sensitivity of the EWA-fiber-optical sensor is limited by penetration depth and fractional power. As we have noted, all of these parameters are depending on different variables. The following is a list of variables that can be changed to enhance sensitivity:

II.3.5.1. Incident Angle

From Eq. (6), it is obvious that the penetration depth depends on the incident angle. The closest the incident angle to the critical angle, the greater the degree of penetration (Fig. 7).

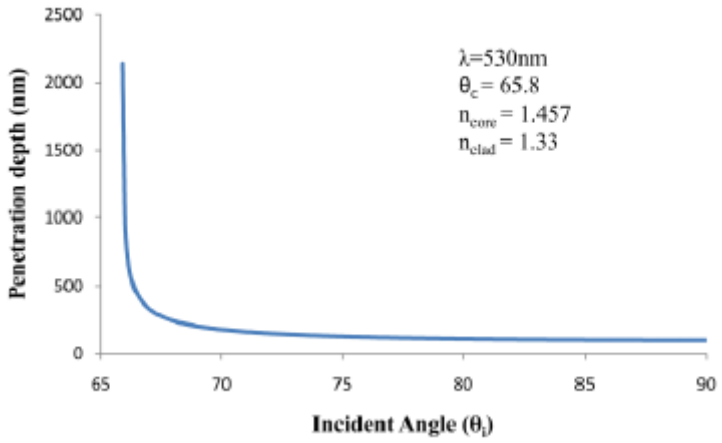

Figure7: Theoretical investigation about the relationship between penetration depth (nm) and incident angle (θ_i).

Some groups have attempted to adjust the launch angle so that the incident angle is similar to the critical angle of the fiber optic sensor probe, thereby increasing the sensitivity of the sensor [25]. It requires a complicated configuration to match the source with the fiber optic probe.

II.3.5.2. Input wavelength

Evanescent wave parameters are proportional to the wavelength of the incident light. The higher the wavelength, the deeper the penetration depth. As a result, IR wavelengths would have greater penetration depths. The difficulty here is that biological molecules are typically transparent in IR, so there are no peaks of absorption. There is also a high water absorption peak in IR, which can interfere with the assessment.

II.3.5.3. Geometry

The geometry of the fiber optic probe has a crucial impact on the performance of the sensor. For biosensor applications, optical fibers are commonly used in two configurations. In the first case, analyte is observed at the distal end of the immobilized fiber bioreceptor probe (Fig.8 (a)). The absorption/reflection of light input or luminescence resulting from biomolecular interactions is controlled in distal end configurations [26]. In the second case, sensing is conducted on the bio receptor immobilized core of the fiber.

The earliest and most typical configuration is the straight probe as seen in Fig. (b) 8. The critical problem with the configuration of the straight probe is poor penetration depth and hence mediocre sensitivity. It is clear from Eq. (II.15) the sensitivity can be improved by increasing the length of the sensing area and decreasing the effective contrast between NA and the fiber radius. If the length of the unclad section is raised, the structure will become more fragile and difficult to handle.

Complex coupling systems, along with an improvement in the fragility and cost of the complete sensor, would also have to be introduced by decreasing the core fiber diameter. By taking into account, the limitations set out above; researchers have built a range of geometric designs to increase the sensitivity of these fiber optic sensors. These different designs showed enhanced fractional power (P_{clad} / P) and penetration depth (d_p) due to the conversion mode phenomenon and increased the number of TIR events in short length **[27]**. Some of the usual geometric patterns are tapered fiber **[28, 29]**, biconical fiber **[30, 31]** and bent fiber **[32]** (Fig.8(c), 8(d) and 8(e)).

These probes have been used for numerous chemical and biochemical sensing applications **[33–41]**. Among the various geometric designs, bent and tapered probes have shown an enormous potential for bio sensing applications due to the high penetration depth, the conversion of lower order modes into higher order and its effect on sensor performance. We can see in depth the benefits of these two designs in improving the efficiency of a fiber optic sensor based on evanescent wave absorption.

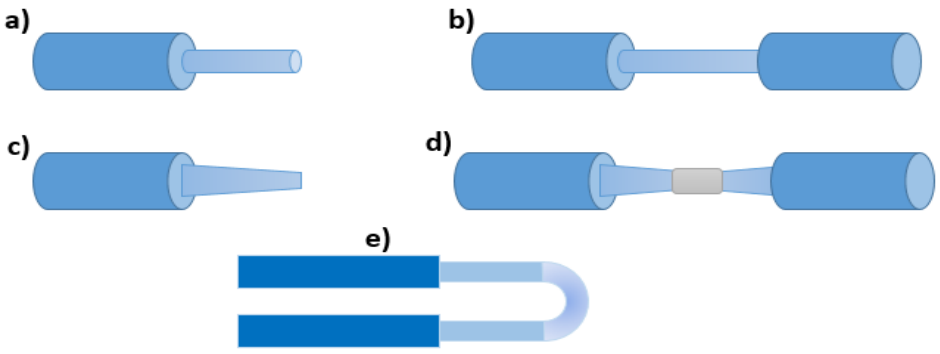

Figure8: Different types of fiber probe design: (a).Tip probe; (b). Straight probe; (c). Tapered probe; (d). Biconical probe; (e). U-bent probe.

III. Role of Evanescent wave Fiber Optic Sensors (EWFOS) in water pollution monitoring:

The optical waveguide sensors for chemical and biological organisms dependent on these evanescent wave (EW) interactions have drawn significant attention from researchers. Compared to other sensing methods, the evanescent wave sensing technique offers a number of advantages, especially in chemical sensing applications.

1. As the interrogating light remains directed, no coupling optics are needed in the sensor region and all fiber approach is feasible. Considerable miniaturization with EW interaction is commonly available in integrated optics.

2. Surface and bulk effects can be discriminated by using proper launch optics and thereby reducing the EW field to a short distance from the guiding interface.

3. The fiber optic EW sensors are perfectly suited for accurate absorption measurements on highly absorbing and highly scattering media due to their short effective path length.

4. If the optical fiber is designed to be sensitive to EW interactions along its length or in distinct areas, then full or quasi-distributed sensing is possible which enables the measurement of the spatial profile of the analyte concentration over considerable distances.

5. In comparison to traditional approaches, the EW approach allows the sensor designer control over interaction parameters such as volume sensing and response time.

6. By inventing light emitting diodes (LEDs) and highly sensitive photodetectors, EWFOS offers significant economic benefits **[42, 43, 44]**.

IV. Materials and methods

In this chapter, polluted water with methylene blue is monitored by an optical method based on an optical fiber sensor without cladding. The liquid to be analyzed (considered as a liquid cladding) interact directly with the fiber core.

Experimental investigation relevant to fiber's characterization including (fiber diameter, numerical aperture, refractive index profile, V-number) have been carried out.

The following data in table 2 indicates the obtained results from specific experimental set ups:

Table 2: Optical fiber characteristics and their importance in the system performance.

Parameter characterized	**Obtained results from experimental investigation**	**importance in system performance, sensitivity**
Diameter and refraction index of fibre core.	Φ=259.2 μm , n_{core} =1.425.	Enhance the sensitivity of optical fiber sensor.
Numerical aperture	NA=0.529 for ($n_{cladding}$ =1.3333,n_{core} =1.425).	It indicates the light accepting efficiency of an optical fiber.
Refractive index profile	step index fiber	Optical fiber behaviour.
V-number (normalized frequency)	V> 2.405 ,multimode fiber	Depends on the characteristics of the core-cladding combination.
The profile height parameter	Δ=1.59 (for n_{core}=1.425 and $n_{cladding}$=1.3333)	Describes the dispersion between modes. Higher the profile height parameter, the more will be the dispersion phenomena.

The selection of the microscopic objective is based on the overfilled launch condition **[45]**; the main principle is that the launched spot of the microscopic objective has a numerical aperture

NA, greater than the fiber NA. Consequently, the spot size of microscopic objective is greater than the core diameter.

Preventions must be considered while coupling light from the fiber end-face to the detector, thus, one should take care that the light emerging from the fiber illuminates about 70% of the detector area around the center. This would take care of any non- uniformities presents in the detector surface and would reduce the intensity level on the detector, thus reducing problems of saturation. While performing measurements on multimode fibers, if the detector area happens to be smaller than the illuminated spot, then one may have problems of modal noise **[45]**.

NB: you can find more details about these characterizations in the [appendix 1] at the end of this thesis.

IV.1.Global experimental set up:

IV.1.1. Principle Operation:

An optical de-cladded fiber sensor has typical components including illumination source, optical de-cladded fiber probe, and modulator/modulant under investigation, besides it requires a light detector for gathering and focusing light and finally electronics materials utilized for treatment and acquisition of the obtained signal as reported by Mason **[17]**

The phenomenon of Light propagation in the core is generally explained when the Total Internal Reflection (TIR) takes place.

Total Internal Reflection (TIR) happens firstly when the incident ray verify the critical angle due to the difference between the two refractive indices of core and cladding mediums (where $n_{core} > n_{cladding}$) then, accordingly; it bounces off the outer walls of the waveguide and reflected back into the same medium in successive way. Thus, at each (TIR), the confinement of the guided energy in the core medium is ensured. Therefore, a small portion of energy is escaped into the cladding medium.

An electromagnetic field is generated by this leaky energy in the cladding medium as an 'Evanescent Wave'. Then, it rapidly attenuates as identified by ref **[46, 47]**. A lot of experimental investigation was conducted to explore the evanescent wave absorption based sensor for various applications.

This section critically examines the evanescent wave absorption (EWA) based sensor for water pollution monitoring. The main reason of the EWA is that the surrounding medium can absorb the evanescent field and consequently it produces a loss in the output energy. The findings of this study will help to confirm this hypothesis and to accomplish this aim. Further, to respond to a recent call for research about water pollution quality measurement.

The following figure below represents a clarified schematic representation of our experimental set up (figure9):

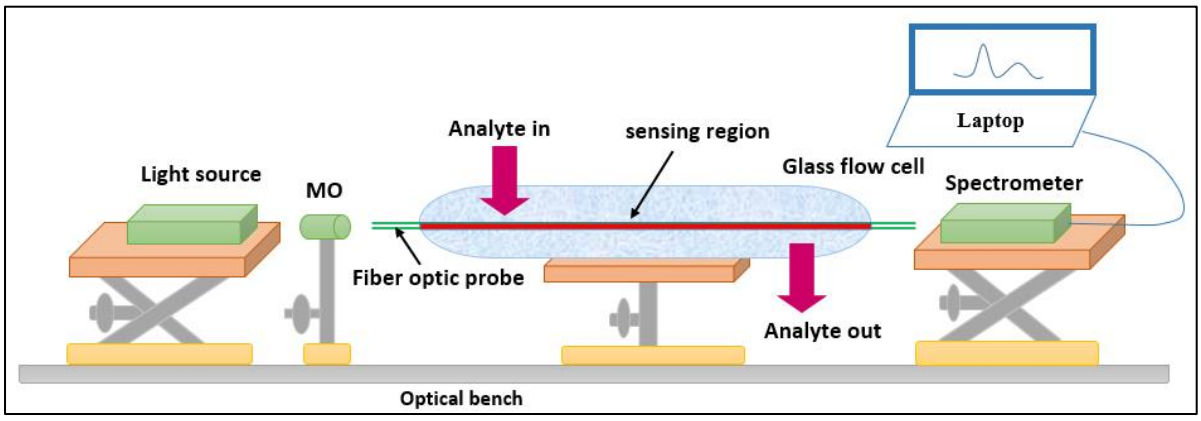

Figure 9: Clarified schematic representation depicts the global set up of the designed optical fiber sensor.

The experimental set-up consists of an illumination source, which emits in the visible range [400-800] nm, it is served to illuminate the fiber end face and we assume that the core cross-section is covered by the focused light using a microscope objective (MO) (40X, 0.65). Besides, we consider that the maximum portion of emitted rays are guided.

The multimode fiber core with a well-known diameter reaches the value 259 µm. A sensor cell of 38 cm length is well designed to hold the methylene blue-water samples. It is made of a cylindrical glass tube with a known diameter of 1.5 cm with inlet and outlet stands.

The light propagating through the fiber interacts with the surrounding liquid. This interaction induces an intensity loss in the propagating light along the sensing region. The light emerging from the output end of the optical fiber was detected and analyzed using an optical fiber spectrophotometer (Spectrovio C5210), which is connected to a laptop to display the spectral response of the polluted liquid.

IV.1.2.Identification of the pollutant:

The Methylene Blue (MB) is a colored effluent cationic and an organic pollutant, the figure 10 below shows its chemical structure:

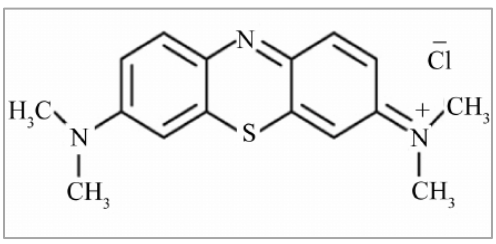

Figure10: The chemical structure of MB.

In this essay, methylene blue is chosen as a model pollutant due to a lot of explanation. Next, the widespread colored effluent in the waste industry has dangerous harmful effects on humans and the environment. In addition, the visible spectrum of the excited source is sufficient since the absorption peaks in this domain are seen in Figure 11 below. The methylene blue-water solution was tested by a spectrophotometer (UV-VIS) of type SHIMADZU, at the organic chemistry laboratory, University Ferhat Abbas Setif1:

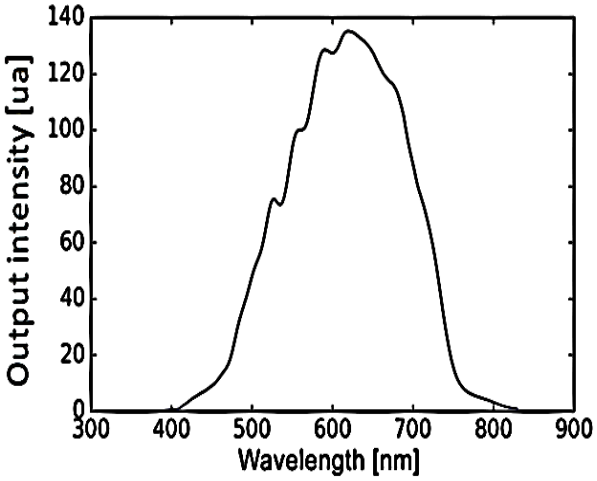

Figure11. Emission spectrum response of tungsten halogen lamp

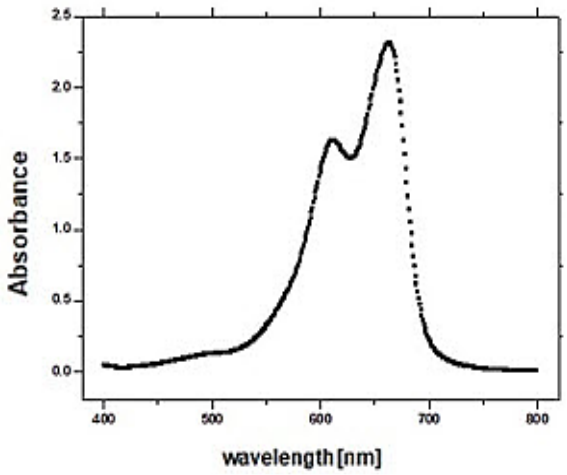

Figure12: Absorption spectrum of methylene blue solution with C=5mg/L

Figure 12 indicates the absorbance of methylene blue solution vs. wavelength (nm). It can be clear that the pollutant examined has a high degree of absorption in the visible spectrum, which is valid for λ=614 nm and λ=664 nm.

IV.1.3. Preparation of solutions

Methylene blue-water samples are prepared by dissolving the measured amount of MB powder in the liquid water (mg /L).

Materials used:

-Electronic balance for the weight of the MB powder (mg).

-Magnetic stirrer for homogenization of the MB-water solution. (1 hour).

-Flasks: in order to keep solutions for different doses.

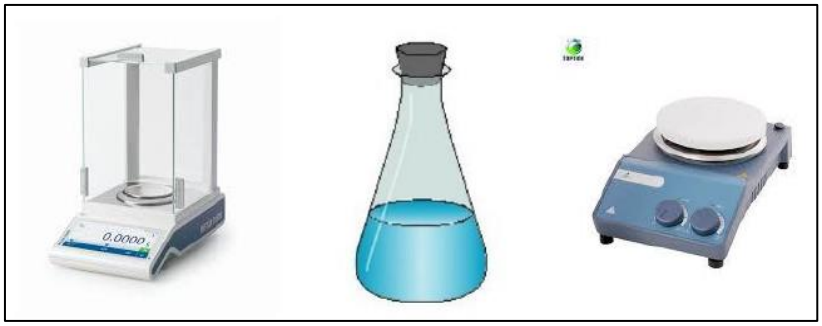

Figure 13: Used materials in solutions preparation.

-In order to prepare a solution with 1mg / L, the following procedure must be followed:

-First of all, tare the electronic scales

-Use a clean spatula to put the necessary MB powder on an electronic scale and save the exact value of the powder mass (m=1 mg).

-After that, the weighted MB mass is placed in a flask with 1⁄4 L of distilled water.

-Put the flask on the magnetic stirrer for 1 hour until the MB powder is dissolved.

-Complete the whole volume with distilled water (e.g. 1L).

-Close the flask and stir again until the homogeneity of the MB-water solutions is complete.

-The same protocol shall be used for the preparation of other concentrations of MB-distilled water solutions.

-Abbe Refractometer accomplishes the measurement of the refractive index.

V. Results and discussion

V.1. Variation of MB samples concentration according to refractive index

The following figure (14) shows the variation of MB samples concentration as a function of the refractive index measured by Abbe refractometer:

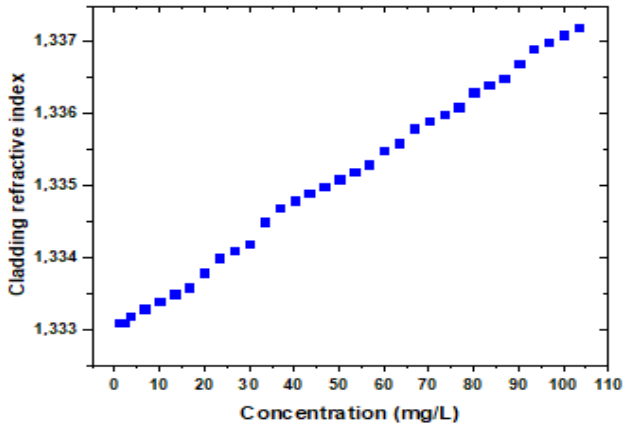

Figure 14: Variation of the refractive index of the liquid [1-103.3] mg/L vs. The concentration of MB samples.

It is clear that the refractive index measured is increasing with the rise of the MB sample concentration.

- **Refractive Index Contrast (Δn) (RIC):**

Refractive index contrast is defined as the difference between the refractive indices core and cladding i.e.

$$\Delta n = \sqrt{n_{core}^2 - n_{cladding}^2} \qquad \text{(II.18)}$$

Generally, in unclad optical fiber sensor, an increase of refractive index contrast at the sensing region decreases automatically the numerical aperture and induces an attenuation of light due to the refraction loss.

V.2. Effect of the pollutant refractive index on the acceptance angle of the fiber (refraction loss)

In order to delve into the internal conditions of our experiment, unclad fiber can be immersed in MB-water solutions. Consequently, certain difference in the concentration of the solution induces a change in its refractive index, which often contributes to variation in the numerical aperture of the unclad fiber at its angle of acceptance.

The following figure shows the variation of the acceptance angle of the unclad fiber with the variation of the absorbing medium (MB-water solutions).

In order to predict this phenomenon, a program [Appendix 2] has been created. Figure 15 below shows the variation of the acceptance angle as a function of the refractive index of the liquid cladding:

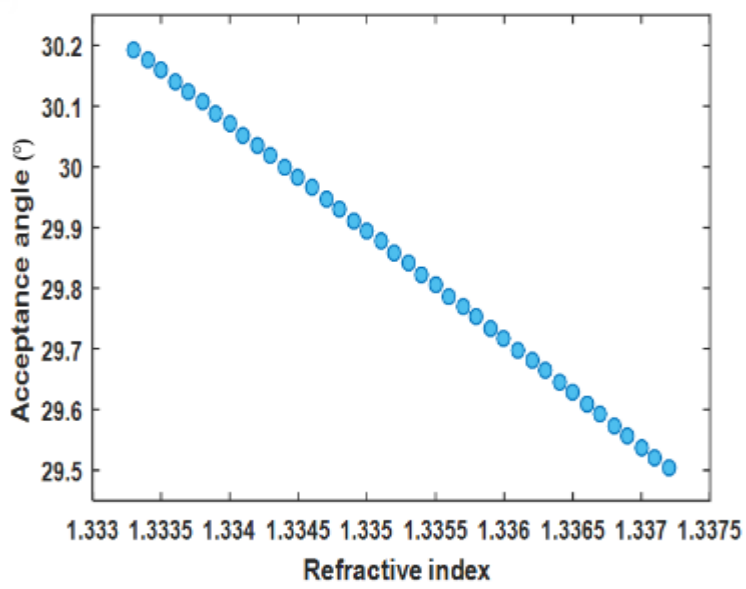

Figure 15: Variation of acceptance angle vs. the refractive indices.

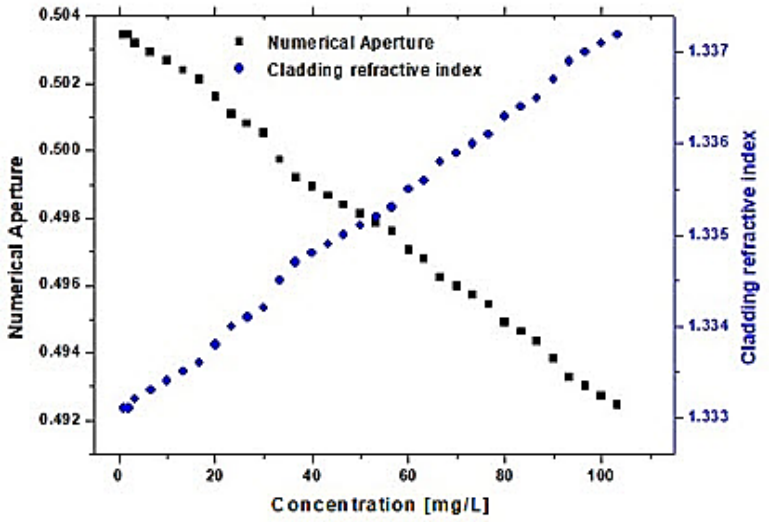

Figure 16: Effect of the concentration of MB solutions on the numerical aperture (NA).

From the above figures, it emerges from the obtained curves that the refractive index increases linearly from 1.333 to 1.337 according to the variation of MB concentration from 0 to 100 mg/L. This behavior slightly affects the NA, which varies from 0.492 to 0.504. This means that the acceptance angle undergoes a maximum variation of less than 1°.

We noticed that the acceptance angle decreases with the increase of the refractive index of the cladding. Consequently, the numerical aperture also decreases during the increase of the methylene blue-water solutions concentration, which is proportional to the refractive index where it was afore-mentioned. The main reason for this decrease is the refraction rays loss.

V.3. Transmitted intensity vs. concentration for three sensitive probe lengths [18, 28, and 38] cm:

In this special part, we applied three sensitive probe lengths [38cm, 28cm, 18cm], after that we measured the output transmitted intensity; then, we verified that the length of sensing region is an important parameter which affects on the sensitivity of the method.

The following figures (17, 18, and 19) depict the effect of sensitive probe lengths (L) [18cm, 28cm, and 38cm] for different concentrations [10-33.3] mg/L:

For L=38cm:

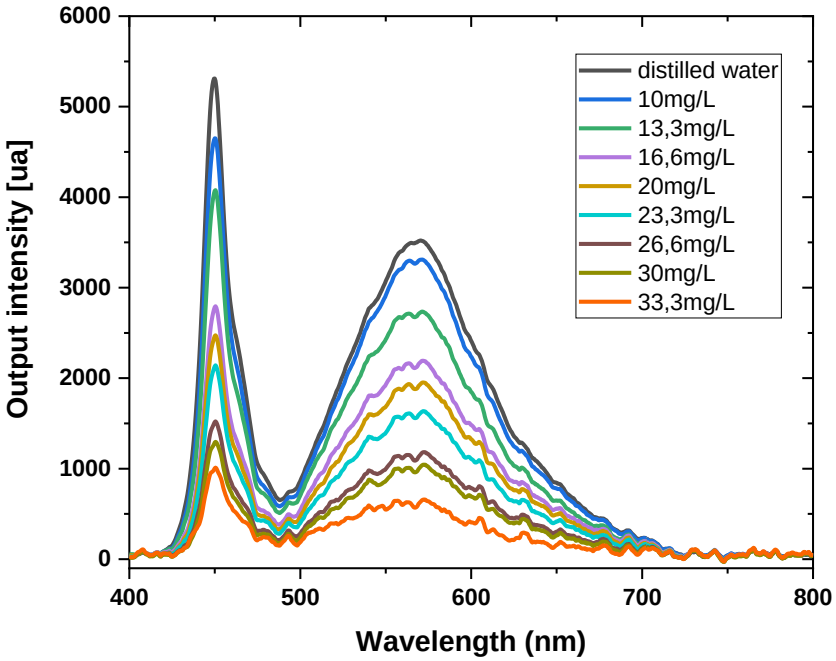

Figure 17: Output intensity vs. Wavelength for L=38cm for different concentration [10-33.3] mg/L.

For L=28cm:

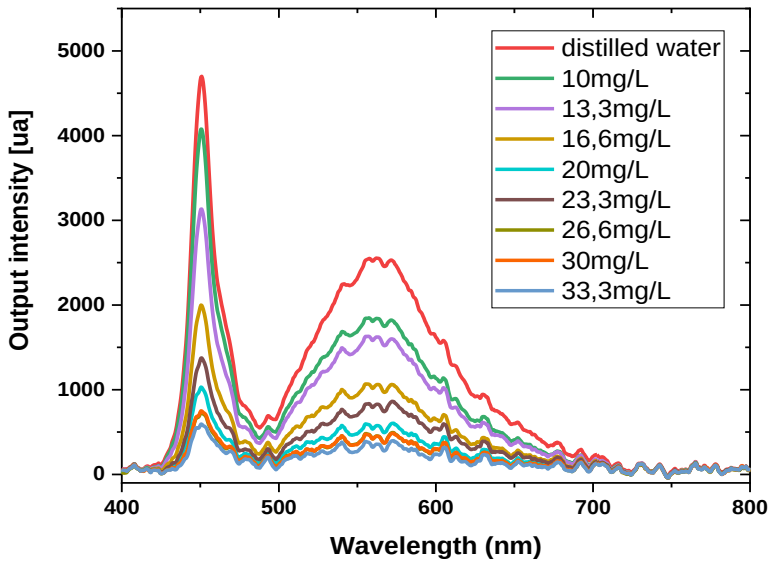

Figure 18: Output intensity vs. Wavelength for L=28cm for different concentration [10-33.3] mg/L.

For L=18cm:

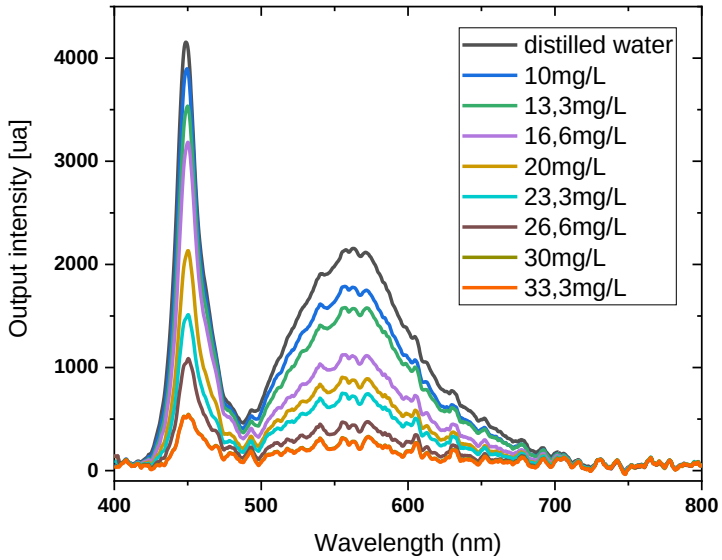

Figure 19: Output intensity vs. Wavelength for L=18cm for different concentration [10-33.3] mg/L.

From the afore-plotted figures, it is clear that the output intensity decreases with the increase of the concentration of the surrounding medium, it is clearly explained by the phenomena of evanescent wave absorption by the liquid cladding; besides, it is obvious in the three probe lengths that they have the same behaviour; the longer sensing region has the more transmitted length as well as the more evanescent wave absorbed by the surrounding medium (MB solution): as the theory mentioned that the phenomenon of EWA is dictated by an exponentially loss of the electromagnetic field at the core-cladding interface; induced by total internal reflection. Additionally, it can also be noticed, that the evanescent wave is very sensitive to any variation in refractive index (RI) of the cladding medium at the core-cladding interface. Thus, for that reason evanescent wave absorption have been exploited to develop sensors based on this phenomenon.

Furthermore, to provide a clear & deep idea about the output power; we have plotted the output intensity according to the range of concentration [1-103.3] mg/L for the three sensitive probe lengths at λ=664nm (see figure 20):

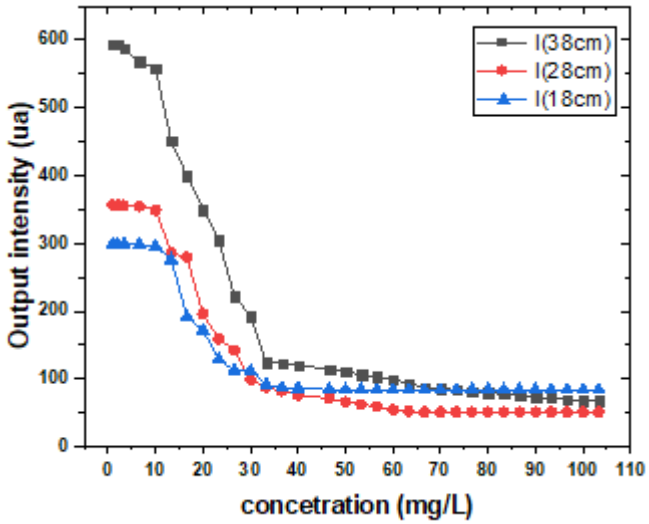

Figure 20: Output intensity according to concentration [1-103.3] mg/L for the three lengths [18, 28, and 38] cm, for λ=664nm.

Thus, in every manner, the evanescent field absorption is caused by the absorbing analyte such as the methylene blue in our case. This medium has an absorption sensitivity in the visible range. In addition, it has been shown that the evanescent field absorption increases according to the sensitive probe length; this is also related to the number of reflection at the core-cladding interface. Thus, whenever the number of TIR events increase the absorption of the evanescent field will be appreciable.

To get an idea about the responsivity of the designed sensor as a function of the wavelength. We have plotted the curves that present the variation of output intensity according to the concentration for exact wavelength [500,550,600,650,700] for L=38cm (see figure 21).

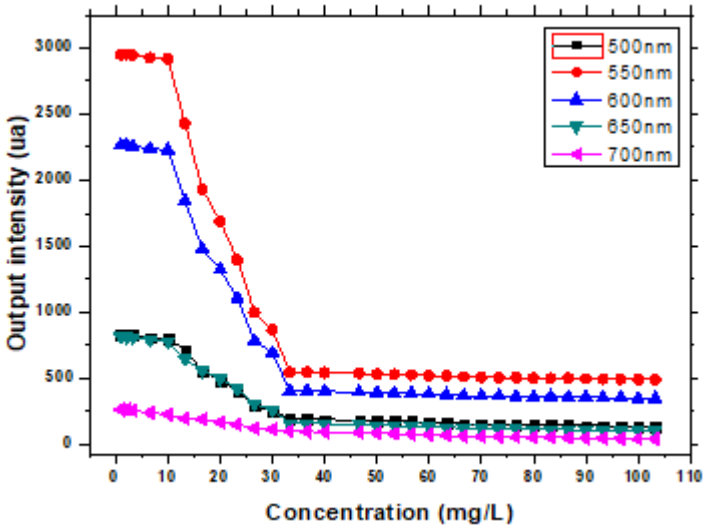

Figure 21: The output intensity according to concentration for exact wavelength [500,550,600, 650, and 700] nm, for L=38cm.

It can be stated that the optical fiber sensor is more sensitive in the range of wavelength [500-600] nm, this sensitivity is due to the high absorption domain of our pollutant: the methylene blue.

V.4. Investigation of the effect of the penetration depth on the responsivity of the fabricated sensor

As we described in the previous chapter the parameters that affects the EW (optical, physical and geometrical …etc.), we will focus accurately on the penetration depth (d_p) (see equation 6).

Penetration Depth and the output intensity analysis for Evanescent Wave Absorption Sensor vs the range of refractive indices are presented in the following figure (22):

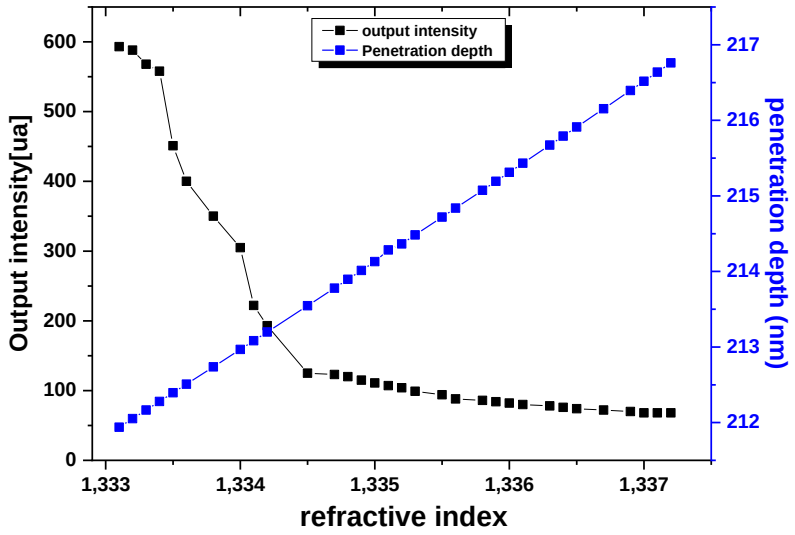

Figure 22: Penetration Depth and the output intensity analysis for an Evanescent Wave Absorption Sensor vs. the range of refractive indices (λ =664nm).

It can be seen from figure that with the increasing refractive index of water-methylene blue solutions, the evanescent power (penetration depth) increases and hence it adds to the increased interaction of light with the surrounding medium. We have also observed; that there is an attenuation of output intensity at the detector due to the evanescent field absorption as we explained before.

Thus, from the point of view of experimental practice, d_p is such a distance where the molecules may have a detectable effect.

V.5. Investigation about the sensitivity of EWA based fiber optic sensor

The sensitivity of the EWA optical fiber sensor is limited by the penetration depth and fraction power in the cladding. As we mentioned before, the both of these parameters are dependent on various factors.

The list of the main factors that can affects the optical fiber sensor's sensitivity and performance are incident angle, input wavelength and the geometry of the probe.

We will focus in this section on the incident angle effect:

V.5.1. Incident angle (Θ_i):

In this part, we are interested with the influence of the incidence angle on the penetration depth (figure23), by using the equation (II.6):

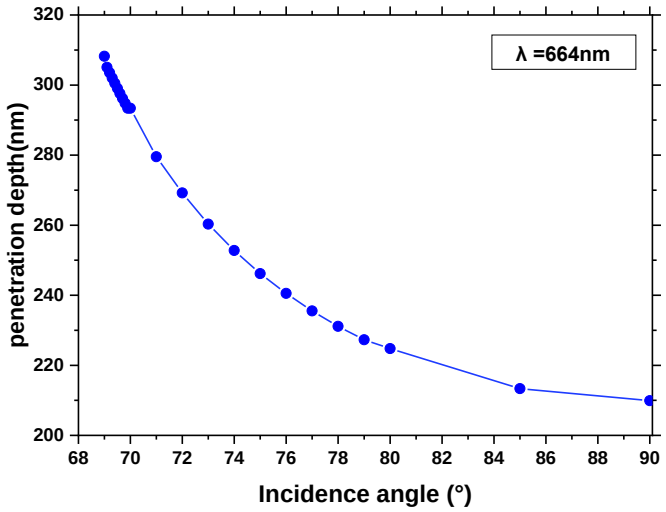

Figure23: Relationship between penetration depth (nm) and incident angle (θ_i) with Θ_c=69°.

From the figure above, which represents the guided part. It is clear that the penetration depth depends on the incident angle θ_i with the normal at the core-cladding interface. In the case, the incident angle approximates the critical angle; it consequently generates an increase in the penetration depth.

NB: all the measurement is obtained at laboratory temperature 22°C measured by a thermometer.

Conclusion

In this chapter, the theory, design, fabrication and characterization was reported; to delve into the achieved methods including optical fiber sensor based on evanescent wave absorption, for testing specific pollutants (methylene blue) at the laboratory of applied optics (Algeria). The same chapter will present an experimental investigations conducted to explore the optical and the geometrical characteristic of the used fiber such as optical fiber type (single-mode or multi-mode), fiber core diameter, fiber probe geometry, fiber probe length, etc., are very important for a number of reasons. Because that optical fiber's users need the fiber characteristics to design the optical fiber systems. There is a great number of techniques, which have been reported for measuring the optical fiber sensor characteristics. This chapter presents an exhaustive study about the performance of fiber optic sensor characteristics, we will detail and discuss some typical experimental set ups which have been employed.

In the framework of this thesis, we were interested about the optical methods; accurately in the laboratory of applied optics, we selected the field of fiber optic sensor based on evanescent wave absorption, due to; that field of optical fiber technology offers several advantages for chemical sensing over conventional methods and hence, it is worthwhile to investigate the feasibility of this method to the above problem of pollution monitoring. The present thesis gives a detailed account on the design, fabrication and characterizations; likewise, the implementation of various sensitive and low cost fiber optic sensors for the detection of certain environmental pollutants such as dissolved methylene blue (MB). The designed sensor represents a significant advancement to accurately monitor MB concentration changes in distilled water. This investigation was in good agreement with previously reported studies, on other pollutants by different authors.

Accordingly, we achieved the expected objectives; a simple low-cost real-time response optical fiber sensor system was theoretically and experimentally carried out; to monitor various concentrations of water-MB solutions. The basic idea involved using a polymer optical fiber without cladding immersed in a polluted solution. The sensing operation depends primarily on the evanescent wave penetration depth in the surrounding medium. A high penetration depth results a higher evanescent wave absorption, and the sensor becomes more effective. Any variation in the liquid refractive index and thus, the MB concentration, can be effectively monitored by detecting the fiber output intensity. The proposed sensor is sensitive to a wide range of MB concentrations (for a light wavelength of =664 nm and different sensitive regions

lengths (18, 28, and 38) cm). Further, we observed that the sensitivity of the proposed sensor is fundamentally modulated by the emission spectrum of the LED source.

References

[1] Chong, S. S., Aziz, A. R., & Harun, S. W. (2013). Fibre optic sensors for selected wastewater characteristics. *Sensors*, *13*(7), 8640-8668.

[2] Weber, A. Meeting the Fiber Optics Challenge. *Assembly*, 1 January 2001.

[3] Ahmad, A. B. H. (1994). Development of a Portable Optical Fibre Chemica Sensor Measuring Instrument. *Department of Instrumentation and Analytical Science. University of Manchester: United Kingdom*, *187*.

[4] Udd, E. (1995). An overview of fiber-optic sensors. *Review of scientific instruments*, *66*(8), 4015-4030.

[5] Grattan, K. T. V., & Sun, T. (2000). Fiber optic sensor technology: an overview. *Sensors and Actuators A: Physical*, *82*(1-3), 40-61.

[6] Thyagarajan, K. S., & Ghatak, A. (2007). *Fiber optic essentials* (Vol. 10). John Wiley & Sons.

[7] Vahala, K. J. (2003). Optical microcavities. *nature*, *424*(6950), 839-846.

[8] Ahmed, S. F. (2010). *Preparation and Characterization of Hollow Fiber Nanofiltration Membranes* (Doctoral dissertation, M. Sc. Thesis presented to University of Technology, Baghdad, Iraq).

[9] Udd, E., & Spillman Jr, W. B. (Eds.). (2011). *Fiber optic sensors: an introduction for engineers and scientists*. John Wiley & Sons.

[10] Kersey, A. D. (1996). A review of recent developments in fiber optic sensor technology. *Optical fiber technology*, *2*(3), 291-317.

[11] Zhu, Y., & Wang, A. (2005). Miniature fiber-optic pressure sensor. *IEEE Photonics Technology Letters*, *17*(2), 447-449.

[12] Xu, J., Wang, X., Cooper, K. L., & Wang, A. (2005). Miniature all-silica fiber optic pressure and acoustic sensors. *Optics letters*, *30*(24), 3269-3271.

[13] Murphy, K. A., Gunther, M. F., Vengsarkar, A. M., & Claus, R. O. (1991). Quadrature phase-shifted, extrinsic Fabry–Perot optical fiber sensors. *Optics letters*, *16*(4), 273-275.

[14] Lin, J. (2000). Recent development and applications of optical and fiber-optic pH sensors. *TrAC Trends in Analytical Chemistry*, *19*(9), 541-552.

[15] Bhatia, V. (1999). Applications of long-period gratings to single and multi-parameter sensing. *Optics express*, *4*(11), 457-466.

[16] Vaughan, A. A., & Narayanaswamy, R. (1998). Optical fibre reflectance sensors for the detection of heavy metal ions based on immobilised Br-PADAP. *Sensors and Actuators B: Chemical*, *51*(1-3), 368-376.

[17] Mason, A., Mukhopadhyay, S. C., & Jayasundera, K. P. (Eds.). (2014). *Sensing technology: Current status and future trends III* (Vol. 11). Springer.

[18] Pollock, C. R. (1995). Fundamental of Optoelectronics. Chicago: Richard d. Irwin.

[19] Gloge, D. (1971). Weakly guiding fibers. *Applied optics*, *10*(10), 2252-2258.

[20] Powers, J. P. (1993). *Introduction to fiber optic systems*. McGraw-Hill Professional.

[21] Tai, H., Tanaka, H., Yoshino, T. (1987): Fiber-optic evanescent-wave methane-gas sensor using optical absorption for the 3.392-microm line of a He-Ne laser. Optics Letters 12(6), 437–439

[22] Palais, J. C. (1988). *Fiber optic communications*. Englewood Cliffs: Prentice Hall.

[23] Satija, J., Punjabi, N. S., Sai, V. V. R., & Mukherji, S. (2014). Optimal design for U-bent fiber-optic LSPR sensor probes. *Plasmonics*, *9*(2), 251-260.

[24] Ligler, F. S., & Taitt, C. R. (Eds.). (2011). *Optical biosensors: today and tomorrow*. Elsevier.

[25] Ahmad, M., & Hench, L. L. (2005). Effect of taper geometries and launch angle on evanescent wave penetration depth in optical fibers. *Biosensors and Bioelectronics*, *20*(7), 1312-1319.

[26] Kuswandi, B., Andres, R., & Narayanaswamy, R. (2001). Optical fibre biosensors based on immobilised enzymes. *Analyst*, *126*(8), 1469-1491.

[27] Ruddy, V., MacCraith, B. D., & Murphy, J. A. (1990). Evanescent wave absorption spectroscopy using multimode fibers. *Journal of Applied Physics*, *67*(10), 6070-6074.

[28] Love, J. D., Henry, W. M., Stewart, W. J., Black, R. J., Lacroix, S., & Gonthier, F. (1991). Tapered single-mode fibres and devices. Part 1: Adiabaticity criteria. *IEE Proceedings J (Optoelectronics)*, *138*(5), 343-354.

[29] Black, R. J., Lacroix, S., Gonthier, F., & Love, J. D. (1991). Tapered single-mode fibres and devices. II. Experimental and theoretical quantification. *IEE Proceedings J-Optoelectronics*, *138*(5), 355-364.

[30] Littlejohn, D., Lucas, D., & Han, L. (1999). Bent silica fiber evanescent absorption sensors for near-infrared spectroscopy. *Applied spectroscopy*, *53*(7), 845-849.

[31] DE Grandpre, M. D., & Burgess, L. W. (1988). Long path fiber-optic sensor for evanescent field absorbance measurements. *Analytical Chemistry*, *60*(23), 2582-2586.

[32] Gupta, B. D., Dodeja, H., & Tomar, A. K. (1996). Fibre-optic evanescent field absorption sensor based on a U-shaped probe. *Optical and Quantum Electronics*, *28*(11), 1629-1639.

[33] Gupta, B. D., & Sharma, N. K. (2002). Fabrication and characterization of U-shaped fiber-optic pH probes. *Sensors and Actuators B: Chemical*, *82*(1), 89-93.

[34] Khijwania, S. K., Srinivasan, K. L., & Singh, J. P. (2005). An evanescent-wave optical fiber relative humidity sensor with enhanced sensitivity. *Sensors and Actuators B: Chemical*, *104*(2), 217-222.

[35] Sai, V. V. R., Kundu, T., & Mukherji, S. (2009). Novel U-bent fiber optic probe for localized surface plasmon resonance based biosensor. *Biosensors and Bioelectronics*, *24*(9), 2804-2809.

[36] Thompson, V. S., & Maragos, C. M. (1996). Fiber-optic immunosensor for the detection of fumonisin B1. *Journal of Agricultural and Food Chemistry*, *44*(4), 1041-1046.

[37] Pilevar, S., Davis, C. C., & Portugal, F. (1998). Tapered optical fiber sensor using near-infrared fluorophores to assay hybridization. *Analytical chemistry*, *70*(10), 2031-2037.

[38] Leung, A., Shankar, P. M., & Mutharasan, R. (2008). Label-free detection of DNA hybridization using gold-coated tapered fiber optic biosensors (TFOBS) in a flow cell at 1310 nm and 1550 nm. *Sensors and Actuators B: Chemical*, *131*(2), 640-645.

[39] Rijal, K., Leung, A., Shankar, P. M., & Mutharasan, R. (2005). Detection of pathogen Escherichia coli O157: H7 AT 70 cells/mL using antibody-immobilized biconical tapered fiber sensors. *Biosensors and Bioelectronics*, *21*(6), 871-880.

[40] Zibaii, M. I., Latifi, H., Arabsorkhi, M., Kazemi, A., Gholami, M., Azar, M. K., & Hosseini, S. M. (2010, September). Biconical tapered optical fiber biosensor for real-time monitoring of bovine serum albumin at femtogram/mL levels on antibody-immobilized tapered fibers. In *Fourth European Workshop on Optical Fibre Sensors* (Vol. 7653, p. 765322). International Society for Optics and Photonics.

[41] Hale, Z. M., Payne, F. P., Marks, R. S., Lowe, C. R., & Levine, M. M. (1996). The single mode tapered optical fibre loop immunosensor. *Biosensors and Bioelectronics*, *11*(1-2), 137-148.

[42] John, S. M. (2000). Evanescent wave fibre optic sensors: design, fabrication and characterization.

[43] Radhakrishnan, P., Nampoori, V. P. N., & Vallabhan, C. P. G. (1993). Fiber optic sensor based on evanescent wave absorption. Optical Engineering, 32(4), 692-695.

[44] Gupta, B. D., & Sharma, D. K. (1997). Evanescent wave absorption based fiber optic pH sensor prepared by dye doped sol-gel immobilization technique. Optics communications, 140(1-3), 32-35.

[45] GHATAK, A. A., Ghatak, A., Thyagarajan, K., & Thyagarajan, K. (1998). An introduction to fiber optics. Cambridge university press.

[46] Memon, S. F., Ali, M. M., Pembroke, J. T., Chowdhry, B. S., & Lewis, E. (2017). Measurement of ultralow level bioethanol concentration for production using evanescent wave based optical fiber sensor. IEEE Transactions on Instrumentation and Measurement, 67(4), 780-788.
[47] Azil, K., Ferria, K., & Bouzid, S. (2020). Cladless optical fiber sensor based on evanescent wave absorption for monitoring methylene blue induced water pollution. JOSA B, 37(11), A253-A258.

Chapter III

TURBIDITY MEASUREMENT SYSTEM FOR PARTICLE ANALYSIS

I. Introduction

In this section, we will describe the theoretical and the experimental parts of the second method achieved at photonics research laboratory as follows:

Water turbidity can be analyzed by investigating the optical properties of the water taking distilled water as a reference. Turbidity level is basically scaled by the degree at which the water can lose its transparency. The turbidity leads to change in optical properties of the water by light scattering and absorption effects due to the presence of various inorganic and organic solid particles called as Total Suspended Solids (TSS) in total. American Public Health Association (APHA) has defined turbidity as a significant existence of the TSS in water. TSS are solids in water that can be trapped by a filter (mg/l). TSS can include a wide variety of materials such as silt, clay, decaying plant and animal particles, industrial wastes, and sewage etc. We can define TSS are the particles that are sizeable larger than 2 microns exist in the water. Any other particles smaller than 2 microns are considered a total dissolved solid (TDS) **[1]**. The amount of TSS that cause turbidity in water can be defined using an NTU turbidity meter (NTU-Nephelometric Turbidity Unit) based on the measurement of the 90° scattered light power which is recognized as the most sensitive angle according to the Environmental Protection Agency (EPA) Method 180.1 **[2,3].**

Several experimental studies have reported an empirical relationship between NTU and TSS given by

$$NTU = a\,(TSS)^{b} \qquad \text{(III.1)}$$

Where a and b are the power regression coefficients and more commonly, b is approximately equals to 1 **[2].**

In order to completely analyze the water quality, it is also essential to measure the Total Dissolved Solid (TDS, mg/l) in water, which expresses the total concentration of dissolved substances. This parameter includes the presence of inorganic salts such as potassium**,** sodium**,** chlorides and a small amount of organic materials contributing to the TDS level**.** According to World Health Organization (WHO), the water that has a TDS level more than 1000mg/L is unfit for consumption. Because, high level of TDS in usable water can be hazardous and make health problems **[4]**. The World Health Organization also warns that the presence of toxic ions such as lead, nitrate, cadmium, and arsenic in water can lead to a number of serious health problems. This is specifically important for children since they are more sensitive to contaminants since their defense systems have not fully developed **[5]**. High concentrations of suspended solids can cause many problems for stream health and aquatic life.

II. Turbidity measurement units, calibration methods and standards

Standard turbidity measurement methods presented in literature are mostly based on optical transmitted and scattered light power measurements. The sensitivity of measurement depends on different parameters including incident light wavelength, angle of detection and the number of photodetectors **[6]**.

The following three standards are widely used in the assessment of water quality sub-disciplines. While there are other standards, these three are the most commonly used by researchers on the properties of natural waters. Summaries of these principles are described below in order to illustrate some of the methodological inaccuracies found in their measurement methodologies:

II.1. US EPA method 180.1.

This standard has been in use in numerous revisions since the early 1970s, and specifies that it is applicable to the measurement of turbidity in 'drinking, ground, surface and saline waters, domestic and industrial waste'. The norm uses a comparison between the light scattered by the test sample and the light scattered by the 'standard reference suspension'. This reference suspension consists of a given mixture of two chemicals, hydrazine sulphate and hexamethylenetramine, to create a 'stock standard suspension' known as formazin. The primary standard suspension is then formed by diluting 10 ml of stock standard in 100 ml of reagent water. This concentration is characterized as having a turbidity of 40 nephelometric turbidity units (NTU).

There is also another appropriate widely standard based on styrene divinylbenzene polymer. The instrumentation requirements for the calculation of scattered light by this standard are the use of a tungsten light source with a color temperature of 2200–3000 K and a beam length is not more than 10 cm. The detector response should peak at 400–600 nm and the measurement angle should be at 90°. Note that there is a very wide range of light wavelengths and scattering angles, including forward, side and back-scattering geometries **[7, 8]**.

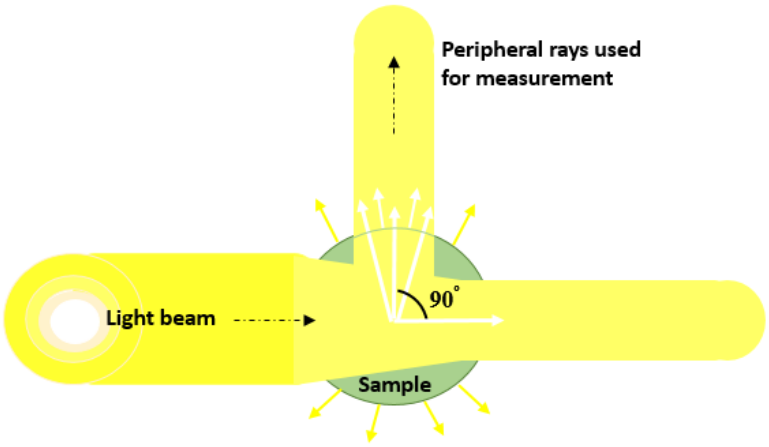

Figure1: EPA method measures the amount of light scattered at a 90-degree angle from the transmitted light.

II.2. ISO 7027

This standard has been in operation in Europe since 1994. It depends, in part, on the use of light dispersion and attenuation with normal suspensions for comparison with the same measurements in the test sample as with EPA System 180.1. An important distinction between the two standards is that ISO 7027 (1999) requires the use of near-infrared light (l 1⁄4 860 nm) for all measurements.

The norm indicates that interference caused by natural water coloring (e.g. dissolved humic substances) can be greatly decreased at wavelengths greater than 800 nm. In addition to the measurement of diffuse radiation (i.e. nephelometry) expressed in the formazin nephelometric units (FNU – in the range 0–40), the standard also specifies a procedure for evaluating attenuation of radiant flux, which is more applicable to extremely turbid waters (e.g. waste or contaminated water). This measurement is expressed in Formazin Attenuation Units (FAU) in the range 40–4000 FAU **[9, 10]**.

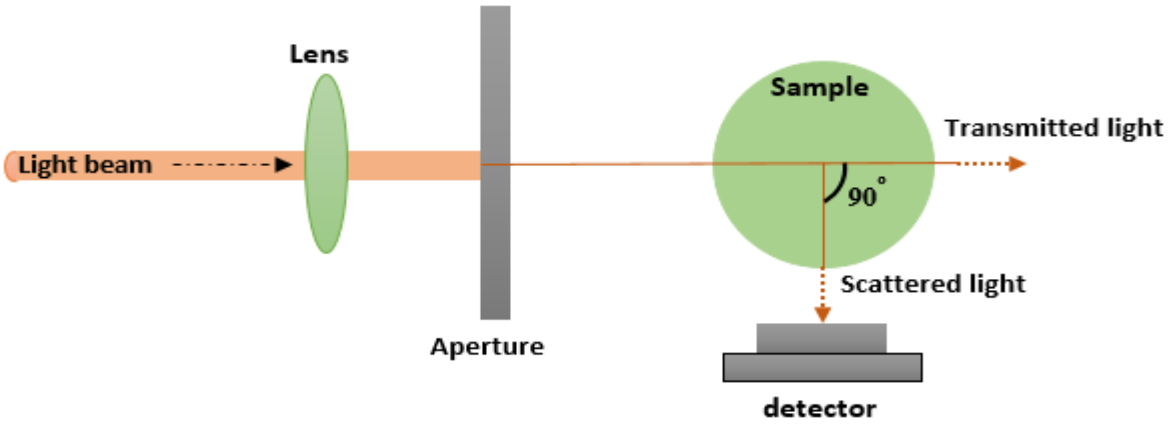

Figure2: ISO 7027 design standards also rely on turbidity technology, within an infrared monochromatic light source.

II.3.GLI method 2.

This method is specifically used for the determination of turbidity of drinking water. It is a nephelometric and attenuation-based ratio metric system based on 860 nm infrared light wavelength, typical with ISO 7027. The use of dual-beam instruments with two light sources and two detectors is specified. Each light source is pulsed sequentially and a 90 active intensity and a 0 reference intensity measurement is taken for each measurement phase (Figure 3).

A ratio-based algorithm is then used to calculate the NTU value on the basis of four data points (i.e. two 0 and two 90 measurements). The recognized explanation for using this method is that it increases the stability of the instrument due to interference induced by the degradation of the light source, the fouling of the sensor windows and the effects of water coloring.

It should be mentioned that the ratio methodology is not defined in the norm, which means that the implementation is left to the instrument designer (the subject of the ratio methods is discussed in more detail later). As in the standards discussed above, the Formazin suspensions are used for calibration purposes. This is an example of a multi-parameter measurement method [9].

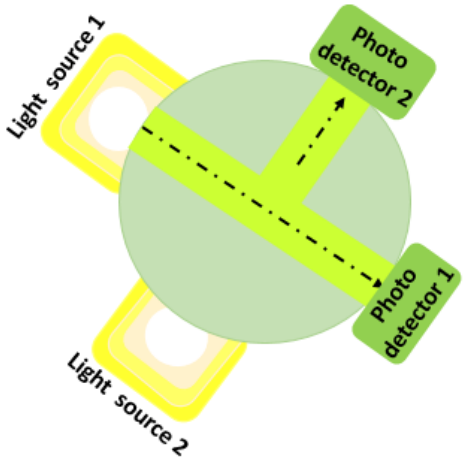

Figure 3: GLI method as a turbidimeter that alternates light pulses from two light sources into two photodetectors.

III. Brief review investigate the relationship between the Turbidity (NTU) and TSS (mg/L):

Various parameters can be associated with water quality. One of the common variables often measured and correlated to water quality is the total suspended solids (TSS) capacity per unit liter of pure water (mg/L). While in the other hand, water quality can also be represented in its appearance, which relates to its clarity and specifically defined as turbidity with the standard unit of measurement in NTU. In some instances, experimental study have been realized to measure TSS in turbid water is based on light absorption measurements using an infrared light

source at 940nm and a phototransistor as a detector [11]. Another measurement method proposed by Mohd. Zubir and Bashah measures TSS in water using a simple multispectral optical system with three LED (950nm, 875nm, 635nm) light sources [2, 12].

In addition to the standard turbidity measurement methods, several different methods have recently been proposed to improve the detection limits of turbidity sensors such as LIDARs [13] and optical fiber sensors based on light reflection measurement from the surface of the water [14]. Kontturi et al [15] have developed a sensor that uses the total internal reflection of a laser beam at a liquid–prism interface and observed a good correlation between the standard deviation of the resultant dynamic laser speckle pattern and the turbidity. In addition, more recent studies have confirmed that the chromaticity coordinates can give a significant indication for the turbidity of the liquids with the spectroscopic analyzing methods [16]. All these studies have shown that the turbidity measurement methods mostly relevant to phenomenon of light absorption and scattering in water. However, it is significantly complicated to realize a precise turbidity sensor [17, 18].

IV. The physics of light absorption and scattering through turbid water

IV.1. a brief review of optical theories:

In order to understand the physics of light dispersion by particles suspended in water, it is important to have some knowledge of the theoretical models used to explain the different absorption and dispersion processes. Fundamental theory and mathematical model construction continue to progress in this field, but the basic points of interest related to the understanding of turbidity in water for the realistic investigator are outlined in this section.

Three primary theories have been discussed: Rayleigh theory, Mie theory and geometric optics. Two hypotheses that can be perceived as approximations to Mie's theory for specific conditions are also explored. There are Fraunhofer Diffraction Theory (FDT) and Van De Hulst's Anomaly Diffraction Theory (ADT) (1957).

The reason that these two theories are considered here is that they both yield computationally fast algorithms that are utilized by laser-based particle-sizing instruments. These instruments are used widely in suspended particle analysis (organic and inorganic) both in situ and off-line in laboratories, and are extensively employed for suspended sediment characterization.

- **Rayleigh and Mie scattering.** The third Baron Rayleigh proposed his scattering hypothesis to account for the blue color of the sky (Strutt, 1871). Rayleigh scattering includes particles that are much smaller than the wavelength of the incident light and are often known as being optically soft – indicating that the particles are restricted to have a refractive index

very close to 1 (air molecules in the Rayleigh model). Rayleigh has demonstrated that the scattering of small particles is highly wavelength dependent on shorter wavelengths and is spatially isometric (i.e. uniformly scattered in all directions), thus the blue color of the sky. He determined that this blue color was prevalent because the scattered light intensity was inversely proportional to the fourth power of the incident light wavelength, i.e. That is, the shorter wavelengths of light (e.g. the blue end of the visible spectrum) are more quickly spread than the longer wavelengths of light (e.g. the red end of the visible spectrum).

- **Gustav Mie.** Originally, his hypothesis was developed to describe the colouration of metals in the colloidal state (Mie, 1908). Mie 's hypothesis successfully demonstrates the dominance of forward scattering where particles are of equal size or greater than the incident wavelength of light, as compared to the isotropic scattering of light by much smaller particles than in Rayleigh scattering.
- **Geometric optics**. Geometric optics, often known as ray optics, describes the light traveling through a medium in terms of a straight path (hence 'ray'). It illustrates the fact that there is a change in the path of a light ray at the interface between two regions with different refractive indices. It also allows reflection and absorption, and is better applicable in conditions where the wavelength of light is much less than the size of the scattering molecule **[19, 20]**.

Thus, Light is absorbed and/or scattered by suspended solid particles and dissolved matters in the water **[9].** The particles in water can partly absorb the transmitted light and can partly scatter the light in all directions with different intensities **[2, 21].** The amount of light interaction with the suspended solid particles depends on the size, shape and composition of the particles in the water and also the wavelength of the incident light **[22, 23].** In this thesis, we have selected sodium chloride (NaCl) particles as the turbid material since it can resemble inorganic and organic particles. In addition, the salinity is one of the main factors affecting the water quality and human health **[24]**. The sodium chloride particles have also influence on the aggregation and settling velocity of other suspended particles. In other words, salt ions collect suspended particles and linked them to form new colloidal particles having higher weights. This leads to a higher level of turbidity in the water or a darker color of the water surface **[25]**.

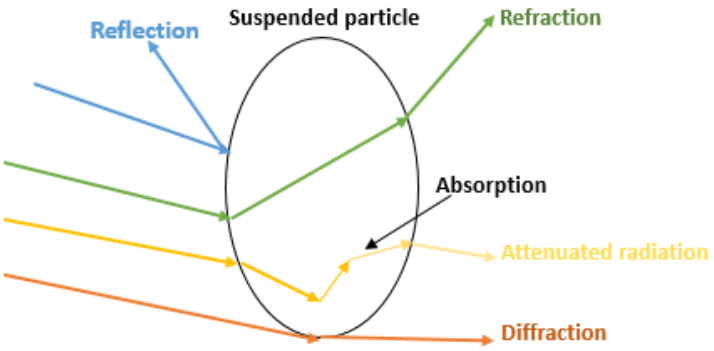

Figure4: Scattering processes of reflection, refraction and diffraction, and the attenuation process of light absorption due to particle suspended in water.

In the next section, we will select sodium chloride (NaCl) particles as the turbid material since it can resemble inorganic and organic particles. In addition, the salinity is one of the main factors affecting the water quality and human health [23]. The sodium chloride particles have influence on the aggregation and settling velocity of other suspended particles. In other words, salt ions collect suspended particles and linked them to form new colloidal particles having higher weights [24, 25]. This leads to a higher level of turbidity in the water or a darker color of the water surface.

V. Measurement Results

V.1. Electrical conductivity measurements in water leading to TSS and TDS

Electrical conductivity is a common water quality parameter used in turbidity measurements. In addition, electrical conductivity is an early indicator used for monitoring the water system variations [1]. Therefore, it is important to measure electrical conductivity as well as total dissolved solids (TDS). For this purpose, we have used a commercial Mettlar Toledo electrical conductivity (E_c) and TDS measurement device shown in Figure 5.

Figure 5: METTLAR TOLEDO conductivity and TDS measurement device.

The TDS and TSS variations for distilled and tap waters as a function of NaCl concentration in Figure 6 clearly show a slight difference in levels, which means that the distilled water mixed with NaCl, has more dissolved particles than the tap water.

On the other hand, it is apparent from that the TSS level of the tap water is slightly higher than the distilled water. This difference can be explained with the reality that the tap water has a higher amount of total suspended solids (TSS) level increasing turbidity. A higher TSS level in tap water can arise from different types of pollutants and environmental minerals such as chemicals used for treating water, runoff from the road salts and chemicals or fertilizers from the farms.

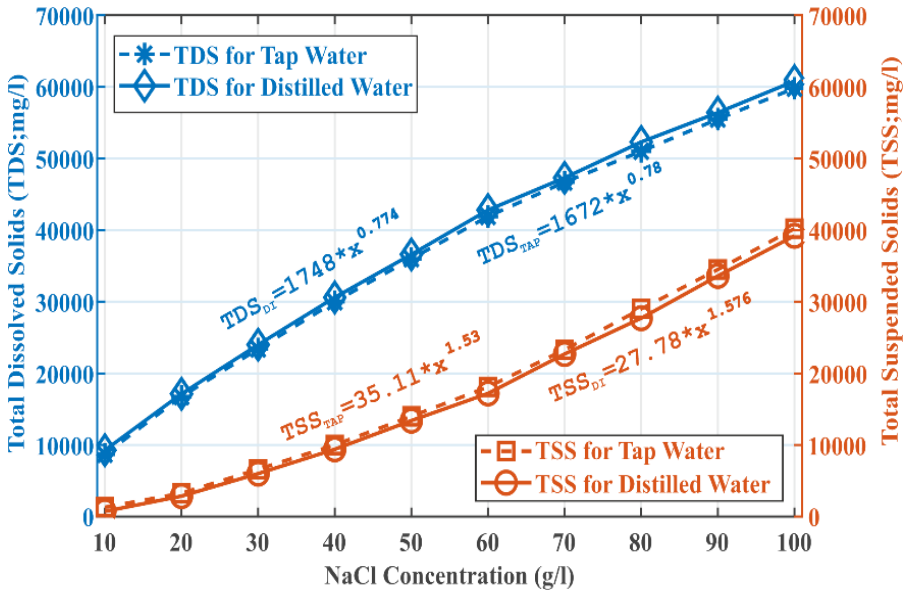

Figure 6: Variation of TDS and TSS as a function of NaCl concentration for distilled and tap waters.

V.2. NTU Turbidity measurements in water using a portable turbidity meter

NTU (Nephelometric Turbidity Unit) is the unit used to measure the turbidity or the level of suspended particles exist in the water. In order to measure NTU level in NaCl solution, we have used a micro TPI portable turbidity meter operating based on the measurement of the scattered light caused by suspended particles in the water (shown in figure7). The device has accurate, direct NTU measurement capability and especially is useful for measuring low turbidities less than 5 NTU.

Figure 7: A micro TPI portable turbidity meter.

In this step, we have measured the turbidity in the tap water for comparison with distilled water. Figure 8 shows the turbidity (NTU) of distilled water with varying NaCl concentrations.

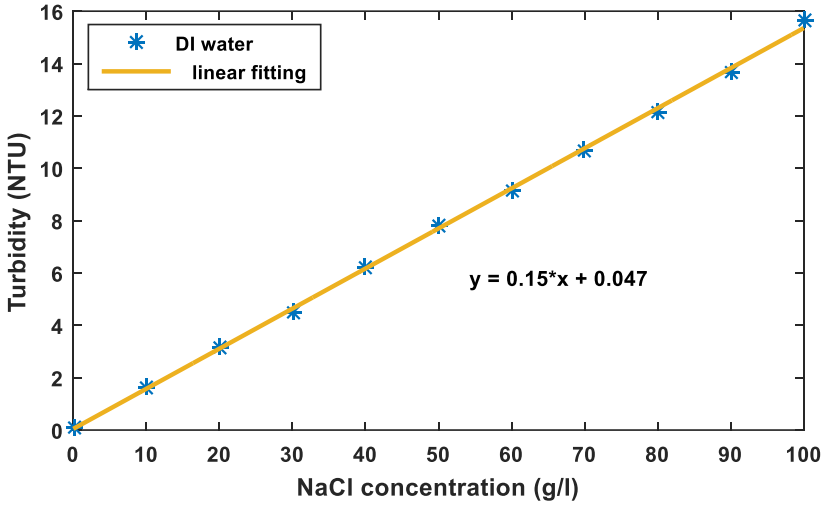

Figure 8: Turbidity (NTU) variation as a function of NaCl concentration in distilled water.

As it is expected NTU increase with NaCl concentration is linear with a fitted line equation of NTU = 0.15·C +0.047.

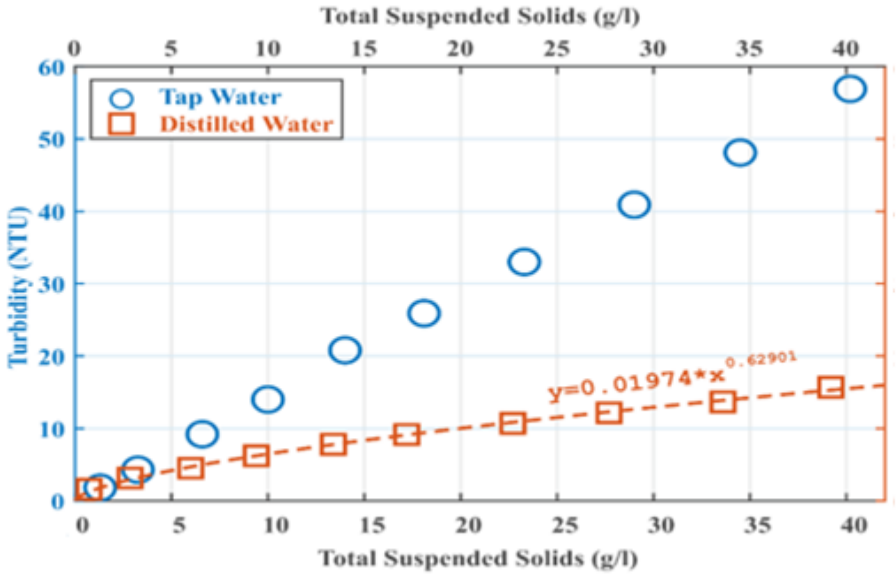

Figure 9: Turbidity (NTU) variations for the tap and distilled waters mixed with total suspended solids (TSS, mg/l).

The results show that the turbidity increase per unit increase in NaCl concentration in tap water is significantly higher comparing with the sample that has distilled water with NaCl concentration. This difference is due to the impurities exist in the tap water solution that can make a high level of turbidity.

In addition, the compositions of the distilled and the tap water are different. Impurities exist in tap water may arise from various environmental pollutants. Partly, it may be a result of our daily pollutants; partly, it may arise due to industrial pollutants. The particles of the pollutants can scatter the light, specifically; the suspended solid particles (TSS) are the main sources of turbidity in water. Commercial tap water may have a small turbidity level (0.11 NTU in our case) comparing with the distilled water with an approximately zero NTU level.

Finally, in this section, we have extracted a relationship between turbidity level (NTU) and NaCl concentration (C) mixed with distilled water using the curve fitting equations obtained from Figures 2:

$$TSS = d \cdot C^{e} \text{ where } d = 27.78; \text{ and } e = 1.576 \quad \text{(III.1)}$$

$$NTU = a\,(TSS)^{b;\ \text{with}}\ a = 0.01974;\ b = 0.629 \quad \text{(III.2)}$$

Consequently a relationship between the turbidity (NTU) and the NaCl concentration in distilled water can be expressed by the following equation with the coefficients a = 0.1597 and b = 0.9913

$$NTU = 0,1597 \cdot C^{0.9913} \cong 0.16\ C \quad \text{(III.3)}$$

This relationship is very close to NTU (C) variation obtained through the measurement realized with micro TPI portable turbidity meter and presented in Fig.8 as

$$NTU = 0,15 \cdot C + 0.047 \cong 0.15 \cdot C \quad \text{(III.4)}$$

The difference between the measurement results obtained with different devices arises from the measurement errors, uncertainties and calibration errors of the devices used.

V.3. Water turbidity based on transmitted and 90°-scattered light measurements using a LD-PD system.

The level of turbidity in water can be determine by transmitted and 90°-scattered light measurements. Fig.10 shows a common used setup for measuring the transmitted and 90°-scattered light to determine the level of turbidity in water and define NTU level. In this setup, input light is generated from a Laser Diode (LD, L650P007) and passed through a rectangular plastic sample bowl, the transmitted and 90°-scattered light levels are detected by a photodetector (PD, SM05PD1A).

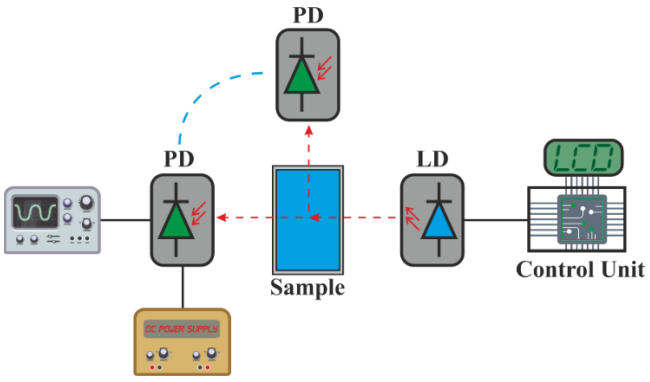

Figure 10: Experimental setup used for water turbidity characterization by transmitted and 90°-scattered light measurements.

Figure 11 shows the transmitted light measurement results for the LD wavelength of 650 nm as a function of NaCl concentration (g/l). The transmitted light measurements were repeated for tap and distilled water-NaCl samples and the distance between LD and PD1 was d=10cm. Fig.12 shows the results of a similar measurement repeated for the LD wavelength of 850nm.

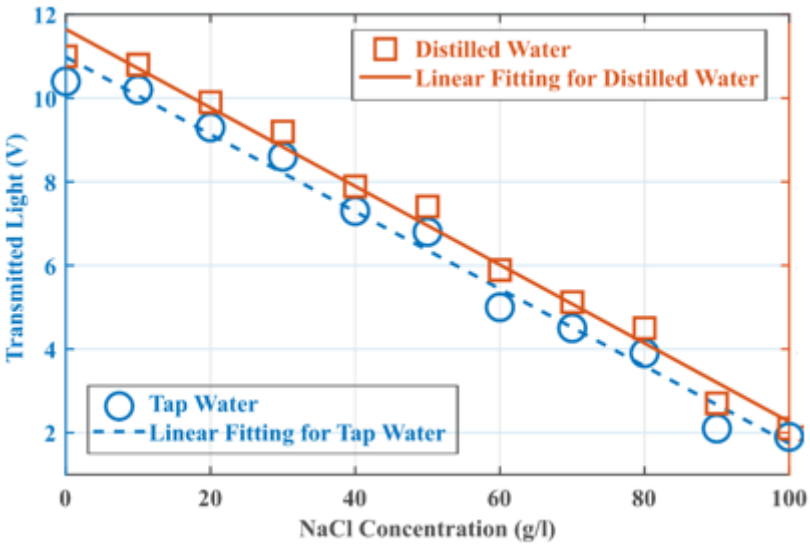

Figure 11: The transmitted light measurement results obtained for a LD wavelength of 650 nm and as a function of NaCl concentration (g/l) in tap and distilled water samples. The distance between LD and PD1 was d=10cm.

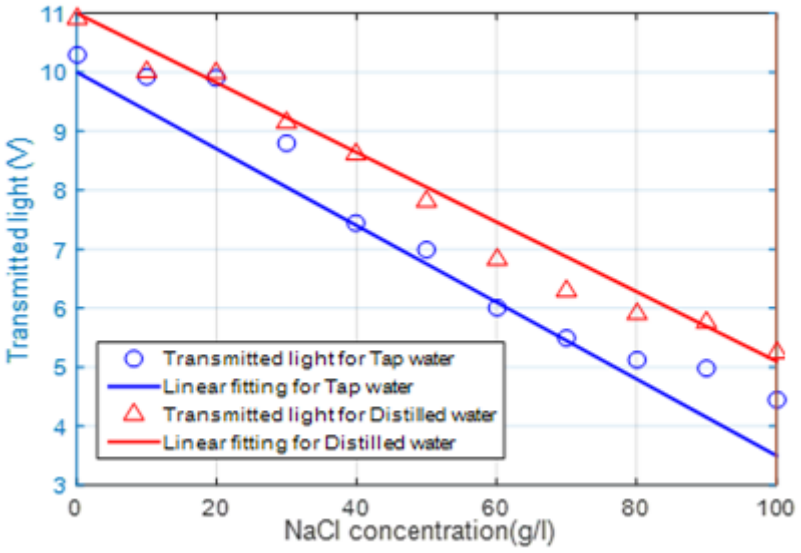

Figure 12: The transmitted light measurement results obtained for a LD wavelength of 850 nm and as a function of NaCl concentration (g/l) in tap and distilled water samples. The distance between LD and PD1 was d=10cm.

From Fig.11 and 12, it can be seen that the light absorption increases in the sample with the increase in NaCl concentration (or TSS increase) and this has resulted in a linear decrease in the transmitted light level for both 650nm and 850nm LD sources. Another important result from the figures is that the level of transmitted light is less for tap water in respect to distilled water due to having different types of impurities **[8]** as it is expected. It should also be noted

that the level of transmitted light is higher at 650nm due to plastic sample bowl used has less absorption loss at this wavelength.

Figure 13 shows the 90°-scattered light measurement results for the LD wavelength of 650 nm as a function of NaCl concentration (g/l). The 90°-scattered light measurements were repeated for tap and distilled water-NaCl samples and the distance between LD and PD1 was d=10cm. Fig.14 shows the results of a similar measurement repeated for the LD wavelength of 850nm.

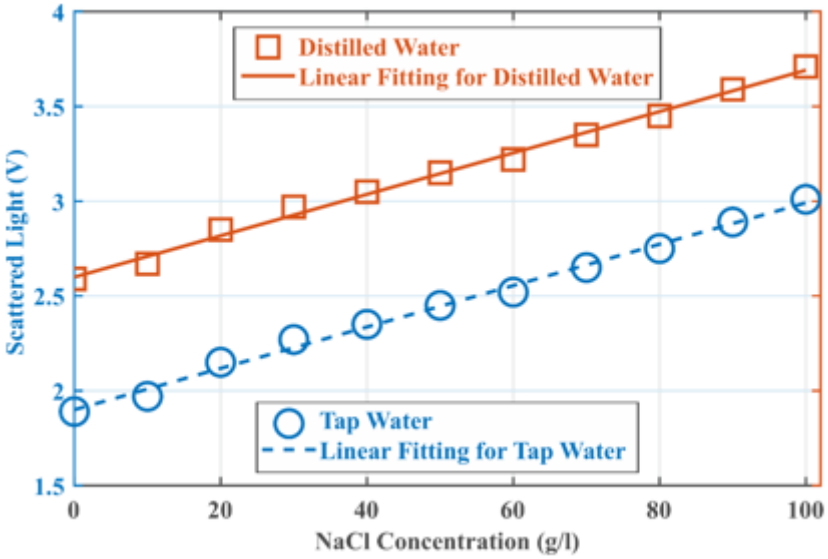

Figure 13: The 90°-scattered light measurement results for the LD wavelength of 650 nm as a function of NaCl concentration (g/l).

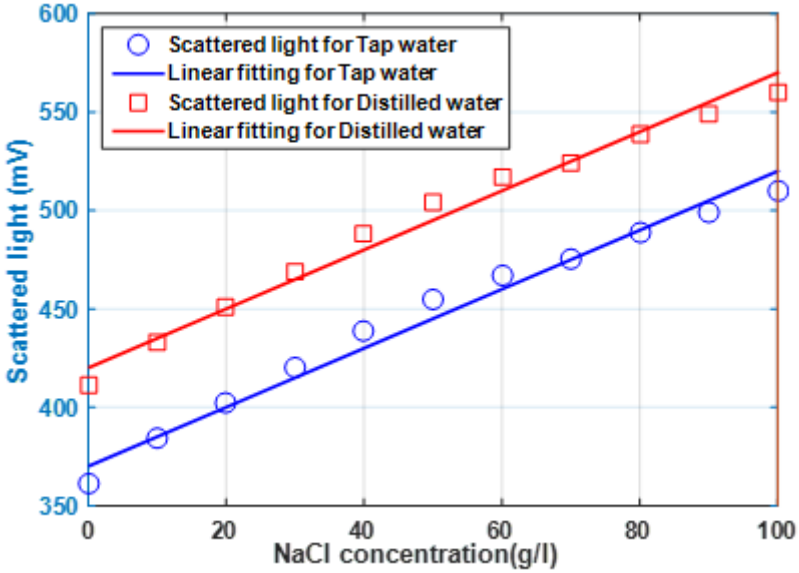

Figure 14: The 90°-scattered light measurement results for the LD wavelength of 850 nm as a function of NaCl concentration (g/l).

From Fig.13 and 14, it can be seen that the light scattering linearly increases in the sample with the increase in NaCl concentration (or TSS increase) for both 650nm and 850nm. Because, as the scattered light strikes more and more particles, multiple scattering occurs and light absorption increases **[10]**.

Another important result from the figures is that the level of 90°-scattered light is less for tap water in respect to distilled water due to having impurities and therefore a higher absorption loss in 90°- scattering direction. It should also be noted that the intensity of the 90°-scattered light is higher at 650nm with respect to 850nm due to higher absorption losses arising from plastic sample bowl used.

For that the afore mentioned results that demonstrates experimentally that the wavelength 650nm is more sensitive to any variation of the tested solutions comparing with 850nm, in the next section we will just focus on the this wavelength.

In order to realize a comprehensive analysis for causes of turbidity in water, it is useful to measure the transmitted and scattered light intensities as functions of TDS and TSS. The results obtained will help to explain the effect of TDS and TSS parameters.

Figure 15 shows the 90° and 10°-scattered light measurement results obtained as a function of TSS (mg/l) for different distilled water-NaCl concentrations at 650nm LD wavelength. The conversion from NaCl concentration to TSS was realized using $TSS = (27.78 \cdot C^{1.576})$ (g/l). The 90°-scattered light variation shown in Fig.15 shows that the light intensity variation is linear and has a higher dynamic range at 650nm for both 90° and 10° scattering angles. A similar result was obtained for a 10°-scattered light measurements (forward scattered light) as a function of TSS except that the scattered light variation (dynamic range) was higher and more linear at 10° scattering angle. These results indicate that the total suspended solids (TSS) is a quantitative expression of turbidity and 10°-scattered light measurements (forward scattered light) can be a better choice to determine turbidity level (NTU) of the water.

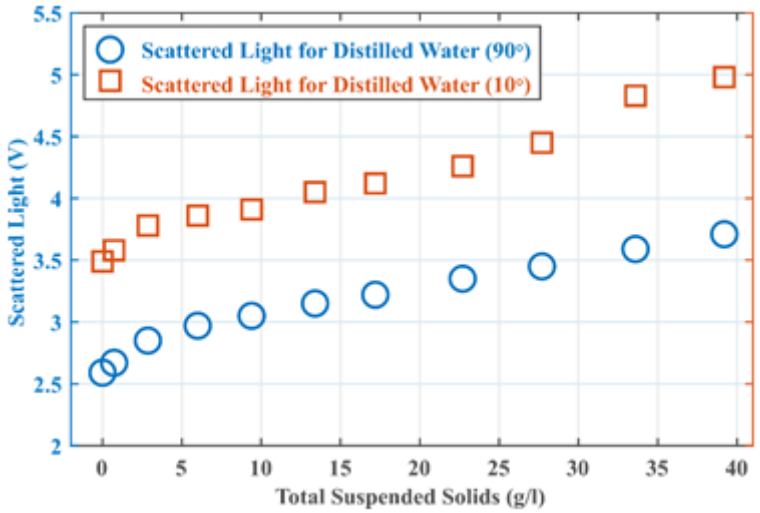

Figure 15: The scattered light as a function of TSS for different distilled water-NaCl concentrations at 650nm LD wavelength. The distance between LD and PD is d=10cm and the scattered light angle is 90° and 10°.

Figure 16 shows the 90° and 10°-scattered light measurement results obtained as a function of TSS (g/l) for tap water-NaCl sample at 650nm LD wavelength. The scattered light measurements done at both angles (90° and 10°) generally indicate that the scattered light intensity increases linearly with increasing TSS parameter. The present results also suggest that the increase in the scattered light intensity is mainly due to the TSS component of commercial NaCl and, with a small percentage, the TSS of the impurities exist in the tap water.

The 90°-scattered light variation shows that the light intensity variation is highly linear and has a higher dynamic range at 650nm, on the contrary, for both 90° and 10° scattering angles. A similar result was obtained for a 10°-scattered light measurements (forward scattered light) as a function of TSS except that the scattered light variation (dynamic range) was higher and more linear at 10°-scattering angle. These results indicate that the total suspended solids (TSS) is a quantitative expression of turbidity and 10°-scattered light measurements (forward scattered light) can be a better choice to determine turbidity level (NTU) of the water.

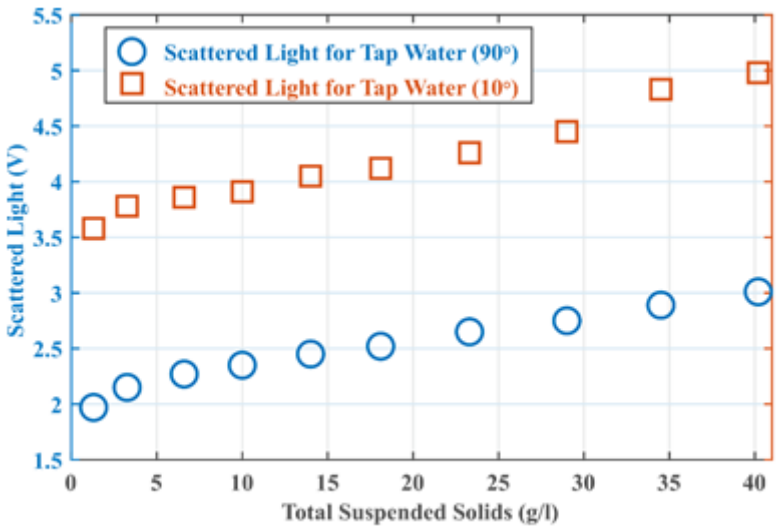

Figure 16: The 90° and 10°-scattered light measured as a function TSS for tap water-NaCl sample at 650 nm wavelength. The distance between LD and PD1 is 10cm.

Figure 17 illustrates the turbidity (NTU1) measurements as a function of the 90° and 10°-scattered light for tap water-NaCl sample at 650 nm LD source as follow:

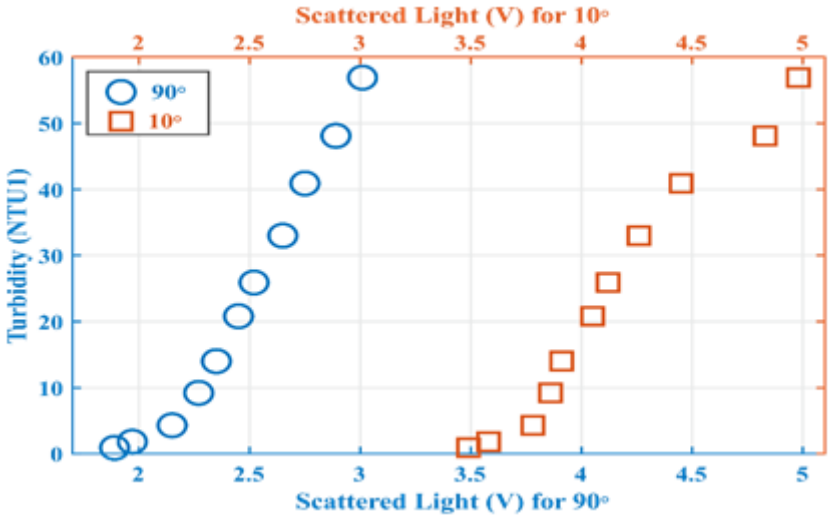

Figure 17: Turbidity (NTU1) measurements as a function of the 90° and 10°-scattered light for tap water-NaCl sample at 650 nm LD source. The distance between LD and PD1 is 10cm.

The following figure (18, 19) present the ratio of 90 and 10°-scattered light/transmitted light according to NTU for 650nm for tap and distilled water:

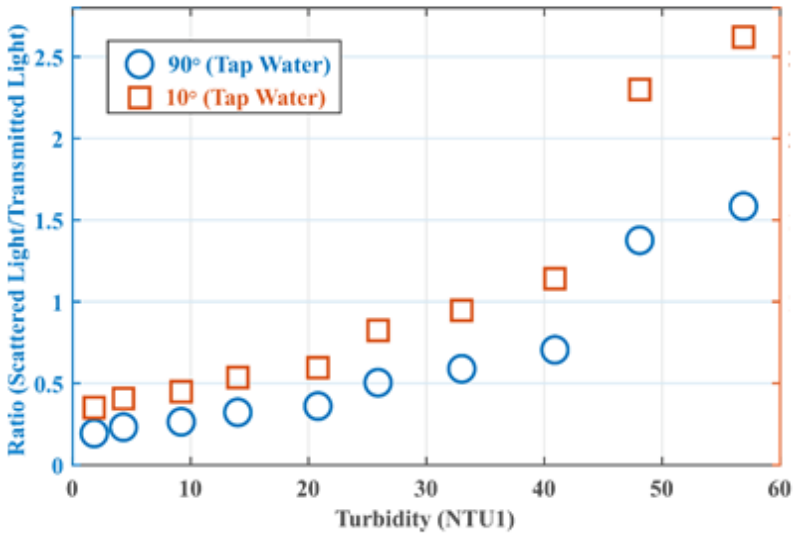

Figure 18: The ratio of 90° and 10°-scattered light/transmitted light = f (NTU) for 650nm for tap water.

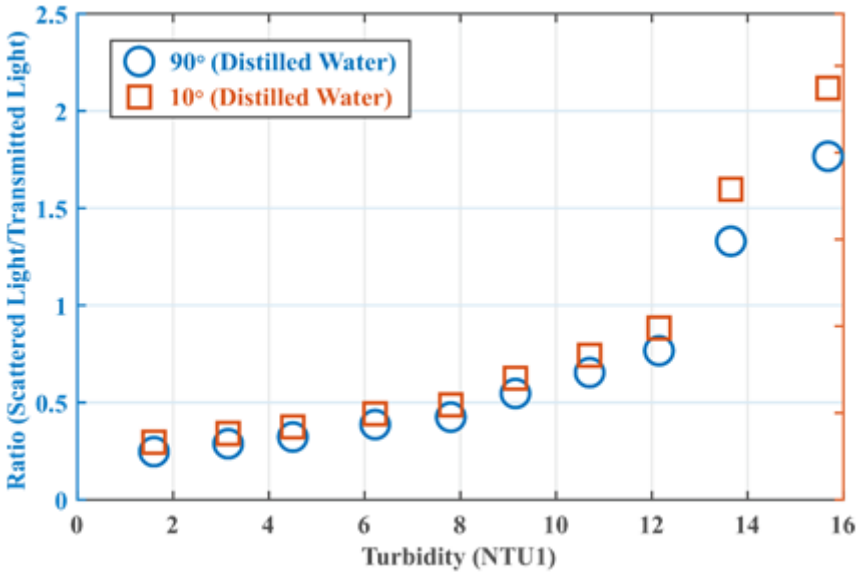

Figure 19: The ratio of 90 and 10°-scattered light/transmitted light = f (NTU) for 650nm for distilled water.

V.4. Water turbidity induced transmitted and forward scattered light measurements using LD-CCD line sensor system.

As a proposed method of turbidity measurement, we have used a CCD line sensor TCD1304DG instead of a photodetector in order to be able to measure transmitted and forward scattered light. Figure 20 shows CCD line sensor evaluation card and schematic diagram of the water turbidity measurement setup with a LD-CCD line sensor system. The CCD line sensor used was an image

sensor with 3648 linear pixel elements having high sensitivity and low dark current. The TCD1304DG has electronic shutter function (ICG) which can keep output voltage stable and varying linearly with the intensity of light. The light source used in the setup is a 650nm laser diode (L650P007 LD). The LD light is passed directly through distilled water-NaCl sample and the transmitted light and the scattered light between 0-10° is detected with the CCD line sensor. The transmitted light intensity is measured at the middle pixel of the CCD sensor and (0-10°) the forward scattered light intensity is measured using the half of the pixels of the line sensor, simultaneously.

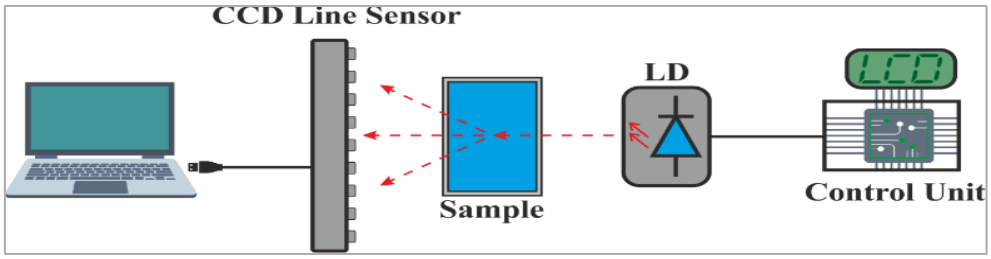

Figure 22: CCD line sensor and (b) Schematic diagram of the water turbidity measurement setup with a LD-CCD line sensor system.

Fig.21 shows (0-10°) the forward scattered light measured as a function of TSS in distilled and tap waters for comparison. As it can be seen in Fig.21, the tap water-TSS sample is a more scattering medium for the light due to additional particles exist in the tap water.

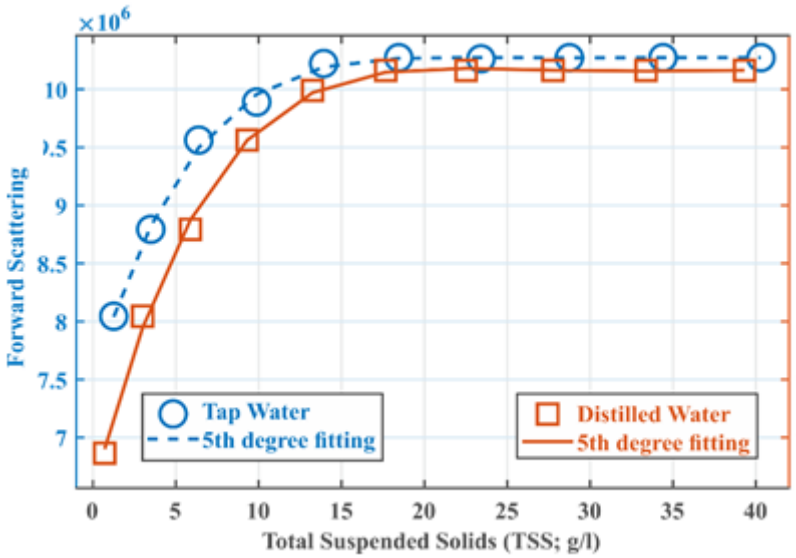

Figure 21: (0-10°) the forward scattered light measured as a function of TSS of tap and distilled water-NaCl sample using a 650nm LD source.

Fig.22 shows the transmitted light measured as a function of TDS concentration (g/l) in distilled and tap waters for comparison. As it can be seen in Fig.22, the transmitted light is decreasing

with increasing NaCl concentration for two types of water. On the other hand, the tap water-NaCl sample is a more absorbing medium for the light due to additional particles exist in the tap water. It has also a more linear variation with NaCl concentration.

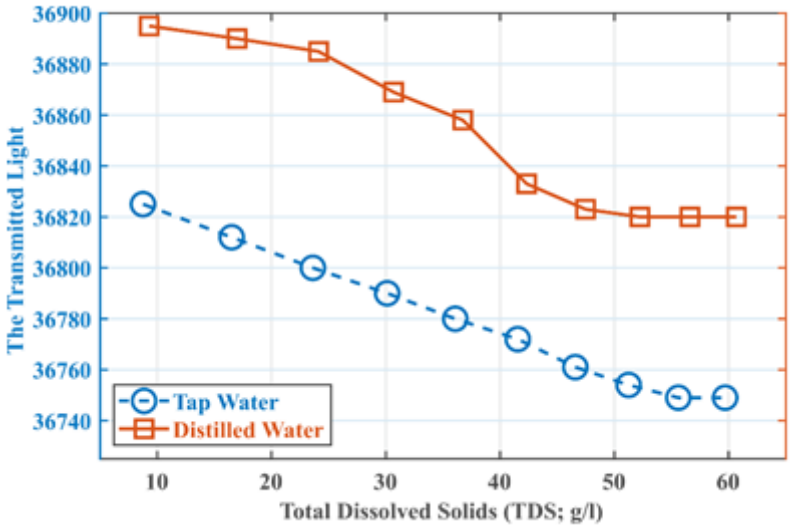

Figure 22: The transmitted light intensity measured as a function of TDS (g/l) in tap and distilled water. The wavelength of LD is 650nm.

Figure 23 shows the comparison between the ratio of 90°-Scattered/transmitted light measured and the ratio of (0-10° degree) forward Scattered /transmitted light measured as a function of turbidity (NTU) of tap and distilled water, the wavelength of LD is 650nm:

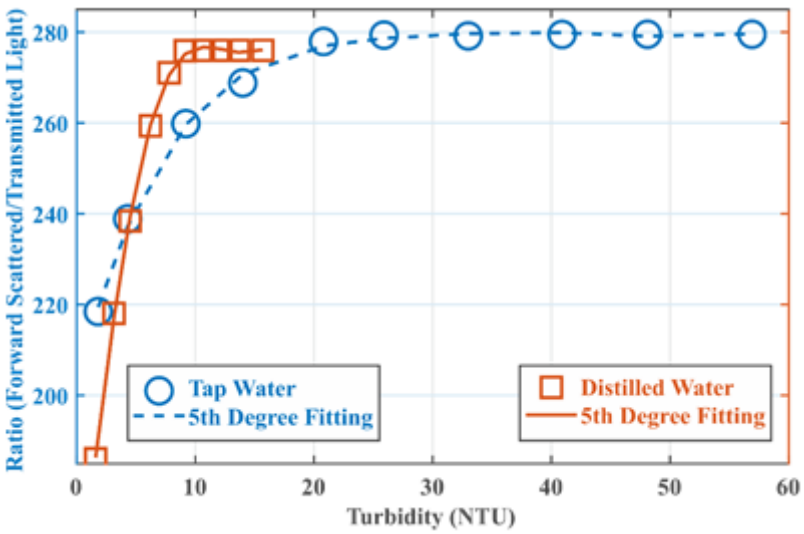

Figure 23: The ratio of (0-10°) forward scattered/transmitted light measured as a function of turbidity (NTU) in tap and distilled water. The wavelength of LD is 650nm.

The aim of this paper is to compare between the classical method by using LD-PD system and a CCD linear sensor systems for water turbidity monitoring, in the next section, we will compare between the ratio of scattering to the transmitted light (Scattered light /Transmitted light) at (90°, 10°) of the LD-PD system and (0-10° degree) forward Scattered /transmitted light measured by CCD line sensor.

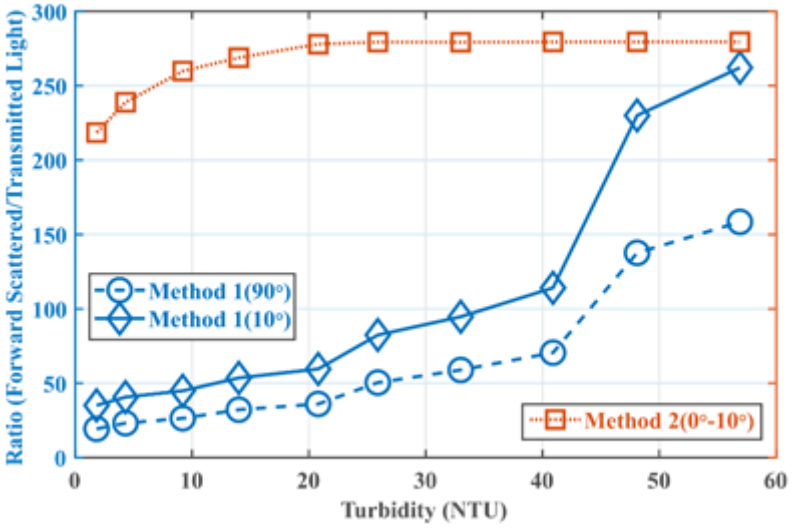

Figure 24: the comparison between the ratio of 90° and 10°-Scattered/transmitted light measured and the ratio of (0-10° degree) forward Scattered /transmitted light measured as a function of turbidity (NTU) of tap water, the wavelength of LD is 650nm.

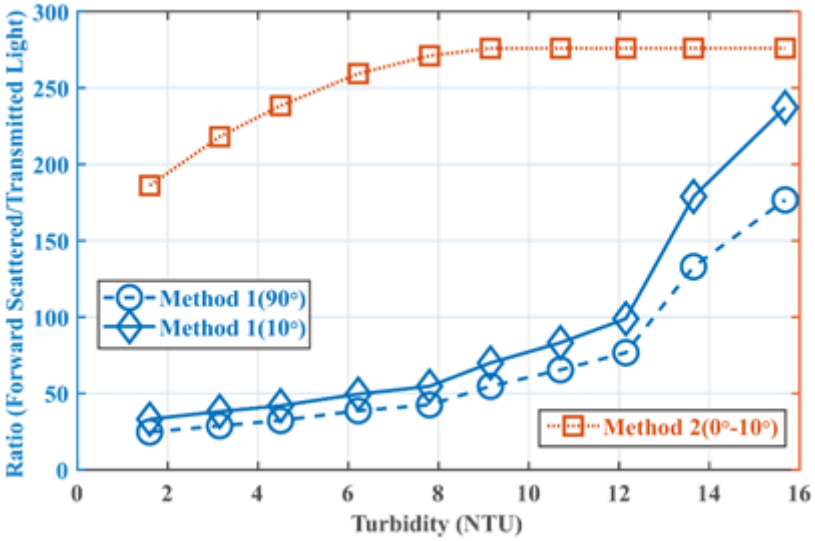

Figure 25: the comparison between the ratio of-90°and 10° Scattered/transmitted light measured and the ratio of (0-10° degree) forward Scattered /transmitted light measured as a function of turbidity (NTU) of distilled water, the wavelength of LD is 650nm.

It can be seen from figure 26 and 27, in the case of using tap and distilled waters; that the CCD linear sensor gave an important results comparing by the ratio of (90° et 10°) scattering/transmitted with the ratio of LD-PD system. This explain the precision, fast detection and the high sensitivity of the CCD line sensor. Moreover, that CCD line sensor is feasible tool for turbidity measurements within simple system, low cost, and remote sensing.

Conclusion

In this last chapter, a turbidity NaCl measurement system intended for water quality monitoring was carried out at the Photonics research laboratory (Turkey). Following to the theoretical investigation about the standard techniques to control the turbidity as well as , we have introduced the experimental results from turbidity system that was employed to control the water quality by using electro-optic components, based on a combined measurement of transmitted and forward scattered light using an optical CCD line sensor array.

In the Turkish laboratory, we focused on an important optical parameter for water quality: turbidity. Briefly, an optical water turbidity measurement methods that are available commercially as portable devices are investigated. Next, two well-known measurement methods given in the literature were employed to assess the water transparency; by measuring the conductivity and NTU (Nephelometric Turbidity Unit) of the water to directly relate to other important water turbidity parameters namely (i) TDS (Total Dissolved Solid) and (ii) TSS (Total Suspended Solid); which are mainly responsible for explaining the turbidity measurement results and connecting to our new measurement method based on an optical CCD line sensor. Accordingly, a novel and proposed water turbidity measurement system based on a combined measurement of transmitted and forward scattered light using an optical CCD line sensor array is demonstrated by introducing its preliminary and comparative measurement results obtained for distilled and tap water with varying amount of NaCl concentrations as a turbid material. The experimental results have shown that trustable measurements of water turbidity in a wide turbidity range can be achieved with the proposed method.

Although, the proof of concept of our system was accomplished but, for the accurate estimation of particle concentration with the proposed sensor, other variables have to be considered and studied, namely particle size.

References

[1] Miller, R. L., Bradford, W. L., & Peters, N. E. (1988). Specific conductance: theoretical considerations and application to analytical quality control (Vol. 142). US Government Printing Office.
[2] Bin Omar, A. F., & Bin MatJafri, M. Z. (2009). Turbidimeter design and analysis: a review on optical fiber sensors for the measurement of water turbidity. *Sensors*, *9*(10), 8311-8335.
[3] Instrumentation, A. B. B. "Turbidity Measurement." *Technical Note* (1999). Available Online: http://www.tbi-bailey.com/faq/pdf/1_turbty.pdf (accessed on September 15, 2007).
[4] Branigan, J. (2013). Development of a Field Test for Total Suspended Solids Analysis.
[5] Islam, M. R., Sarkar, M. I., Afrin, T., Rahman, S. S., Talukder, R. I., Howlader, B. K., & Khaleque, M. A. (2016). A study on total dissolved solids and hardness level of drinking mineral water in Bangladesh. *Am J Appl Chem*, *4*(5), 164-169.
[6] Zhu, Y., Cao, P., Liu, S., Zheng, Y., & Huang, C. (2020). Development of a New Method for Turbidity Measurement Using Two NIR Digital Cameras. *ACS omega*, *5*(10), 5421-5428.
[7] Kitchener, B. G., Wainwright, J., & Parsons, A. J. (2017). A review of the principles of turbidity measurement. *Progress in Physical Geography*, *41*(5), 620-642.
[8] US EPA (1993) Method 180.1: determination of turbidity by nephelometry. Available at https://www.epa.gov/sites/production/files/2015-08/documents/method_ 180-1_1993.pdf (accessed 4 September 2016).
[9] ISO 7027:1999 (1999) Water quality – determination of turbidity. Available at: www.iso.org/iso/catalogue_detail.htm?csnumber¼30123 (accessed 18 September 2016).
[10] Mohd Zubir, M; Bashah, N.M. (2004). *A Simple Sensor for the Detection of Water Pollution, Design and Application;* Project Report, Al-Mashoor School: Penang, Malaysia,
[11] Daraigan, S. G. S. (2006). *The development of multispectral algorithms and sensors setup for total suspended solids measurement* (Doctoral dissertation, PhD Thesis, University Science Malaysia: Penang, Malaysia).
[12] Richter, K., Maas, H. G., Westfeld, P., & Weiß, R. (2017). An approach to determining turbidity and correcting for signal attenuation in airborne lidar bathymetry. *PFG–Journal of Photogrammetry, Remote Sensing and Geoinformation Science*, *85*(1), 31-40.
[13] Yeoh, S., Matjafri, M. Z., Mutter, K. N., & Oglat, A. A. (2019). Plastic fiber evanescent sensor in measurement of turbidity. *Sensors and Actuators A: Physical*, *285*, 1-7.
[14] Kontturi, V., Turunen, P., Uozumi, J., & Peiponen, K. E. (2009). Robust sensor for turbidity measurement from light scattering and absorbing liquids. *Optics letters*, *34*(23), 3743-3745.
[15] Wen, Y., Mao, Y., & Wang, X. (2018). Application of chromaticity coordinates for solution turbidity measurement. *Measurement*, *130*, 39-43.
[16] Chiang, C. T., Huang, S. M., & Wu, C. N. (2016). Development of a calibrated transducer CMOS circuit for water turbidity monitoring. *IEEE Sensors Journal*, *16*(11), 4478-4483.
[17] Liu, Y., Chen, Y., & Fang, X. (2018). A review of turbidity detection based on computer vision. *IEEE Access*, *6*, 60586-60604.
[18] Strutt JW (1871) on the light from the sky, its polarization and colour. Philosophical Magazine XLI: 107–120, 274–279.
[19] Mie G (1908) Contributions to the optics of turbid media, particularly of colloidal metal solutions. Annalen der Physik (Leipzig) 25: 377–445. Available at: http://doi. wiley.com/10.1002/andp.19083300302 (accessed 22 April 2017).
[20] Jonasz, M., & Fournier, G. (2011). *Light scattering by particles in water: theoretical and experimental foundations*. Elsevier.
[21] Sadar, M. J. (1998). *Turbidity science*. Hach Company.

[22] Martelli, F., & Zaccanti, G. (2007). Calibration of scattering and absorption properties of a liquid diffusive medium at NIR wavelengths. CW method. *Optics express*, *15*(2), 486-500.
[23] Cañedo-Argüelles, M., Kefford, B., & Schäfer, R. (2019). Salt in freshwaters: causes, effects and prospects-introduction to the theme issue.
[24] Van Leussen, W. (1988). Aggregation of particles, settling velocity of mud flocs a review. In *Physical processes in estuaries* (pp. 347-403). Springer, Berlin, Heidelberg.
[25] Azil, K., Altuncu, A., Ferria, K., Bouzid, S., Sadık, Ş. A., & Durak, F. E. (2021). A faster and accurate optical water turbidity measurement system using a CCD line sensor. *Optik*, 166412.

Water quality is defined as a measure of the physical, chemical, biological, and microbiological characteristics of water. Monitoring water quality in the 21st century is a growing challenge because of the large number of pollutants used in our everyday lives and in commerce that can make their way into our waters. General Methods of water analysis and knowledge of contaminants toxicity were reviewed in the background of this thesis. Therefore, development of simple and sensitive, low cost, portable sensors capable of direct measurement of environmental pollution are of considerable interest in this context.

In the framework of this thesis, we were interested about the optical methods; accurately in the laboratory of applied optics, we selected the field of fiber optic sensor based on evanescent wave absorption, due to; that field of optical fiber technology offers several advantages for chemical sensing over conventional methods and hence, it is worthwhile to investigate the feasibility of this method to the above problem of pollution monitoring. The present thesis gives a detailed account on the design, fabrication and characterizations; likewise, the implementation of various sensitive and low cost fiber optic sensors for the detection of certain environmental pollutants such as dissolved methylene blue (MB). The designed sensor represents a significant advancement to accurately monitor MB concentration changes in distilled water. This investigation was in good agreement with previously reported studies, on other pollutants by different authors.

Accordingly, we achieved the expected objectives; a simple low-cost real-time response optical fiber sensor system was theoretically and experimentally carried out; to monitor various concentrations of water-MB solutions. The basic idea involved using a polymer optical fiber without cladding immersed in a polluted solution. The sensing operation depends primarily on the evanescent wave penetration depth in the surrounding medium. A high penetration depth results a higher evanescent wave absorption, and the sensor becomes more effective. Any variation in the liquid refractive index and thus, the MB concentration, can be effectively monitored by detecting the fiber output intensity. The proposed sensor is sensitive to a wide range of MB concentrations (for a light wavelength of =664 nm and different sensitive regions lengths (18, 28, and 38) cm). Further, we observed that the sensitivity of the proposed sensor is fundamentally modulated by the emission spectrum of the LED source.

Whereas, in the photonics research laboratory in Turkey, we were focused on an important optical parameter for water quality: turbidity. Briefly, an optical water turbidity measurement methods that are available commercially as portable devices are investigated. Next, two well-known measurement methods given in the literature were employed to assess

the water transparency; by measuring the conductivity and NTU (Nephelometric Turbidity Unit) of the water to directly relate to other important water turbidity parameters namely (i) TDS (Total Dissolved Solid) and (ii) TSS (Total Suspended Solid); which are mainly responsible for explaining the turbidity measurement results and connecting to our new measurement method based on an optical CCD line sensor. Accordingly, a novel and proposed water turbidity measurement system based on a combined measurement of transmitted and forward scattered light using an optical CCD line sensor array is demonstrated by introducing its preliminary and comparative measurement results obtained for distilled and tap water with varying amount of NaCl concentrations as a turbid material. The experimental results have shown that trustable measurements of water turbidity in a wide turbidity range can be achieved with the proposed method.

Although, the proof of concept of our system was accomplished but, for the accurate estimation of particle concentration with the proposed sensor, other variables have to be considered and studied, namely particle size. As perspectives, further investigation will also be focused in the study of the effect on the system performance of several sediment properties, such as reflectivity, sediment colour and optical properties of the medium, in different field conditions.

❖ FUTURE PROSPECTS

During the advancement in the technology of optical fiber, sensor and their application accurately water pollution, further theoretical and experimental investigations would be applied under some considerations such as:

- ✓ Continuing the same domain of research, we predict to combine the advantages of polymer fiber optic sensor with the performance of the photo-catalysis process for the degradation of organic pollutants such as Congo red (CR). The main principle in this section is involving a UV light and a good adsorbent, which is TiO_2 due to its inherent advantages. It would be chosen for our experiment; as semiconductor photo catalysts for the degradation of Congo Red (CR). During the photo degradation process, a decrease in the absorbance under UV light accurately at λ=498 nm as a maximum absorption peak would be expected for different concentration of CR. These predicted findings can give an insight about the toxicity of the tested pollutant i.e. the POF sensor can be intended as a tool for monitor the toxicity of the pollutant based on the periodic analysis of the absorbance.

- ✓ Likewise, in order to attempt more experiments in this field, in this case, an external optical system will be carried out; it offers a major benefit that allows the ability to reach places; here, the fiber only serves as a way of carrying the light to the position of the sensor. The present section would be directed for design a low-cost turbidity sensor for making progress comparing with the previous realized investigations in this research project. An extrinsic fiber optic sensor based on a simultaneously transmitted-scattered measurement was made with three configurations by varying the distance between the emitting and the receiver fibers; the main advantage here is to combine two concepts for turbidity assessment i.e. transmittance and nephelometry, that allows a real-time responsivity, as well; it leads to a wide range control of suspended particles.
- ✓ The analysis of various pollutants including pharmaceutical products and heavy metals.
- ✓ As we discovered from the theory that the geometry of the sensor plays an important role in the sensitivity and response of the polymer optical fiber sensor, a wished further configurations would be fabricated.
- ✓ The high sensitivity of SPR sensor will be investigated experimentally and theoretically with different analysis of pollutants.
- ✓ As perspectives in the simulation part as well, a study about these kinds of sensors remain not impossible.

Albert Einstein said:

In the matter of physics, the first lessons should contain nothing but what is experimental and interesting to see!. A pretty experiment is in itself often more valuable than twenty formulae extracted from our minds.

Appendix 1

I-Fiber's characterization:

1. Fiber's diameter measurement:

In order to measure the fiber diameter, we have achieved the following experimental set up (figure 1)

The method operation is to focus the laser beam into the input of fiber core, with a microscope objective ON=0.25. In the other end of the fiber core, we added an optical condenser to produce the focused image projected on the screen.

The constituents of this set up are:

.Laser He-Ne (632nm) with puissance =30mW

.Microscope objective (10X/0.25),

.Sensor cell,

.Optical condenser and screen.

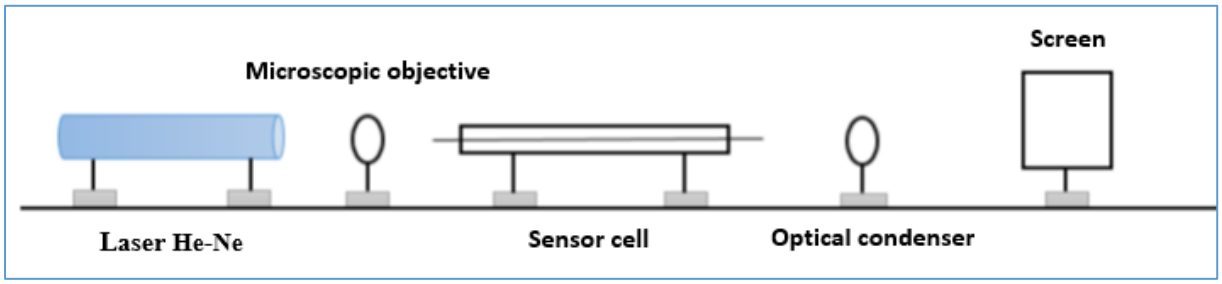

Figure1: Experimental set up for the measurement of fiber core diameter.

This method principle (figure 2) consists of projecting the final net image with distance « à » from the optical condenser. After that, we measured the object distances « a », albeit the image size « y' » for coming finally to the object size, which is, referred as a core diameter.

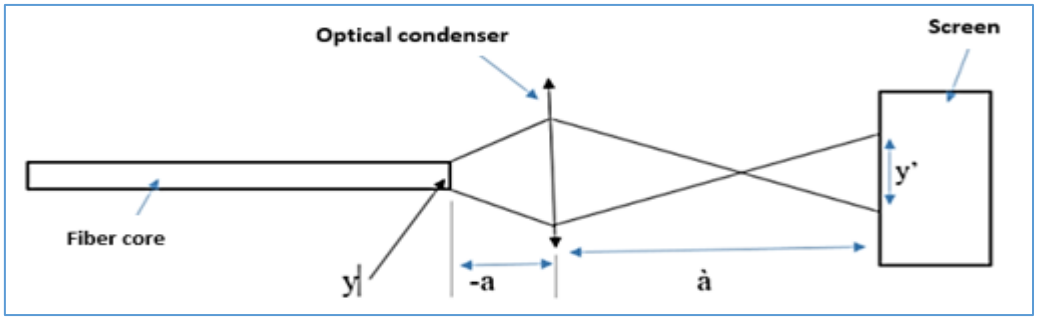

Figure 2. Principle measure of core fiber diameter.

The calculated values are defined in the following table (table1):

Y' (mm)	7	6	5	4	3
à (cm)	22	20	7	6	4
a (cm)	1.1	1	0.3	0.4	0.2
Y (mm)	0.350	0.300	0.200	0.266	0.180

Table1: obtained values from the afore-defined set up.

Therefore, we applied the enlargement law:

$y = y' \frac{a}{a'}$

By using these calculations, we have found that the fiber core is with a diameter approaches y'=0.2592 mm= 259.2 μm.

2. Determination of refractive index profile:

The measurement of refractive index profile of optical fiber is quite important especially in the optimization during fabrication, thus; In order to be more informed about the nature of light propagation through our de-cladded fiber, it is mandatory to know if that de-cladded fiber is step index or graded index fiber. Although, there are many techniques for measurement of refractive index profile, here we discuss a typical optical setup used for assessment the light propagation through the de-cladded fiber (figure 3):

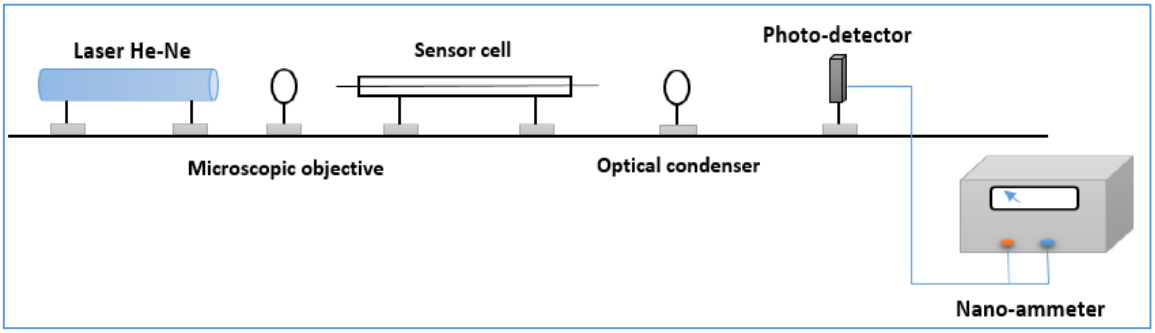

Figure 3: Experimental set up used for measurement of refractive index profile.

The experimental set up used monochromatic light source (λ=632.8nm) employed for exciting the input of the de-cladded fiber. From the other side, the output intensity (I) from the fiber core is focused by a condenser into the scanning photodetector that measures I (X) (where X: is the displacement with 0.05 as a step).

The plotted results are presented below in figure 4:

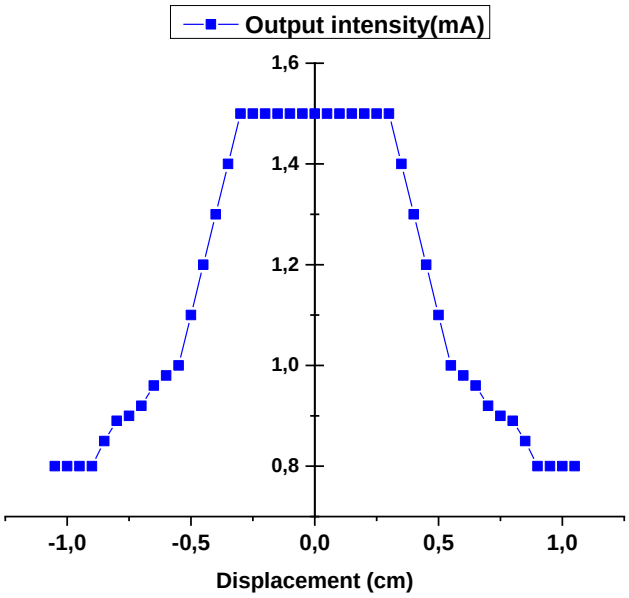

Figure 4: Typical obtained measurement of refractive index profile as step index fiber

Effectively, we noticed from the figure above that it presents a constant part of refractive index in the range of [-0.5-0.5] cm. greater than this range, the transmitted intensity decreases according to displacement X. Thus, we can conclude that our used de-cladded fiber is kind of step index fiber. Besides this is similar with the theory aspect.

3. Measurement of Numerical Aperture (NA):

The Numerical Aperture (NA) is one of the most essential quantities of an optical fiber. It indicates the light accepting efficiency of an optical fiber. Where the maximum of guided rays are excited and launching into the fiber. More the value of NA. Better is the fiber. In this case, we have used the distilled water as a cladding for our designed sensor:

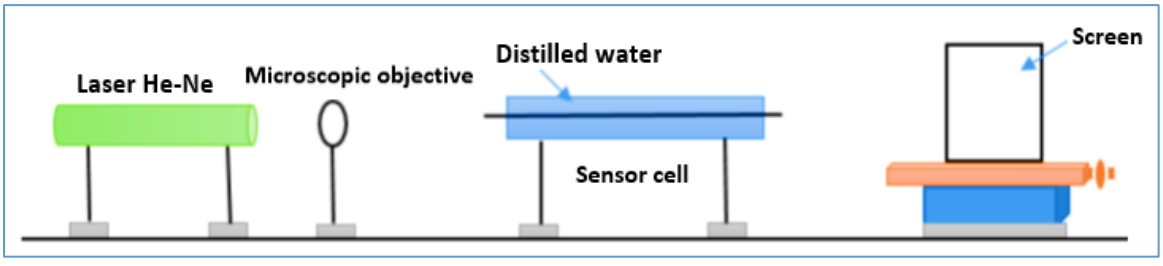

Figure 5: Typical set up for numerical aperture measurement.

A direct measurement of NA can also be performed by a laser source that illuminates the input of 38 cm long fiber core besides, measuring the far field of this used fiber core (see figure 6) at different distances (d) due to displacement micrometric table will be in use.

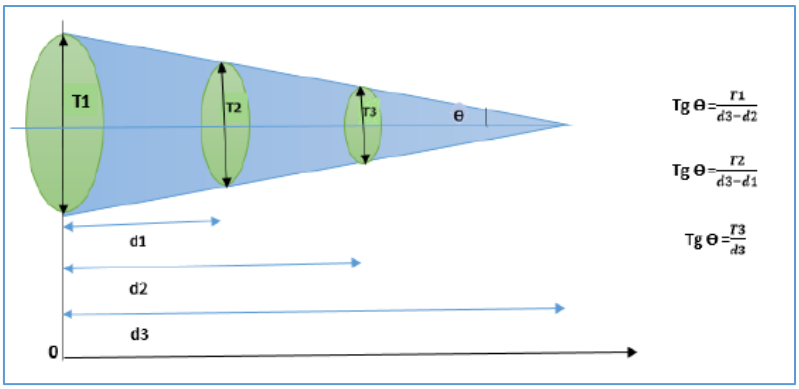

Figure 6: Schematic representation principle measure of obtained spots from far field.

Where **Θ:** represents the acceptance angle, **d** displacement axis (d1, d2, d3) and the spot diameters **T** (T1, T2, and T3).

-Equation below shows the relation of the **NA** with the refraction index contrast:

$$\mathbf{NA = n_0 \sin \theta = \sqrt{n_{core}^2 - n_{clading}^2}}$$

Where $\mathbf{n_0}$, $\mathbf{n_{core}}$ and $\mathbf{n_{cladding}}$ are the refraction index of the air, core and cladding respectively. We have obtained the value of numerical aperture: **NA=0.529** for $\mathbf{n_{cladding}}$ **=1.333**

As a result, we can get $\mathbf{n_{core}}$ **=1.425**.

-The calculated results are introduced in the following table 3:

Displacement d(cm)	0.29	0.55	0.8	1.1
Spot diameter T(cm)	0.35	0.7	1.05	1.4
acceptance angle **θ**	31.10	32	32.31	32.47
Numerical Aperture **(NA)**	0.51	0.52	0.53	0.53
Refractive index of the fiber core **(n_{co})**	1.42	1.42	1.43	1.43

Table3: The obtained values of displacement(d); diameter (T); acceptance angle (θ); Numerical Aperture (NA); refractive index of the fiber core (n_{co}).

The V-number or the normalized frequency of an optical fiber is a very essential parameter in this part, which is proportional to the frequency (or wavelength) of the light source. We can distinguish between, fibers whose V-number lower than 2.4, can allow only one mode, i.e. no other mode can propagate in this fiber. Therefore, such a fiber is called a single mode fiber. In

other side, if the V-number of the fiber higher than 2.4 in such case, we can call it a multimode or over-mode fiber.

The V-number (normalized frequency) of a fiber does not depend on the individual characteristics of the core or the cladding but depends on the characteristics of the core-cladding combination, as it is evident from the expression below:

V= $k \cdot a \cdot NA$ = 1362.05 >2.405 (for λ=632.2nm)

Where: a of the fiber core radius and k= $\frac{2\pi}{\lambda}$: free space wave number.

The profile height parameter: of the waveguide is an important physical parameter, which can describe the dispersion between modes. Higher the profile height parameter the more will be the dispersion phenomena, it is given by $\Delta=\frac{n_{core}^2-n_{cladding}^2}{2n_{core}^2}$

By applying numerical results: thus Δ=1.59 (for n_{core}=1.425 and $n_{cladding}$=1.3333).

-The following deduction emerged from the present investigation is that our unclad used fiber behaves as a step multimode fiber.

II- Choice of the appropriate microscope objective

The aim from this study is the determination of the microscopic objective (the appropriate numerical aperture) which is employed as a convergence tool for emerging light beam. It is shown in the following figure 7:

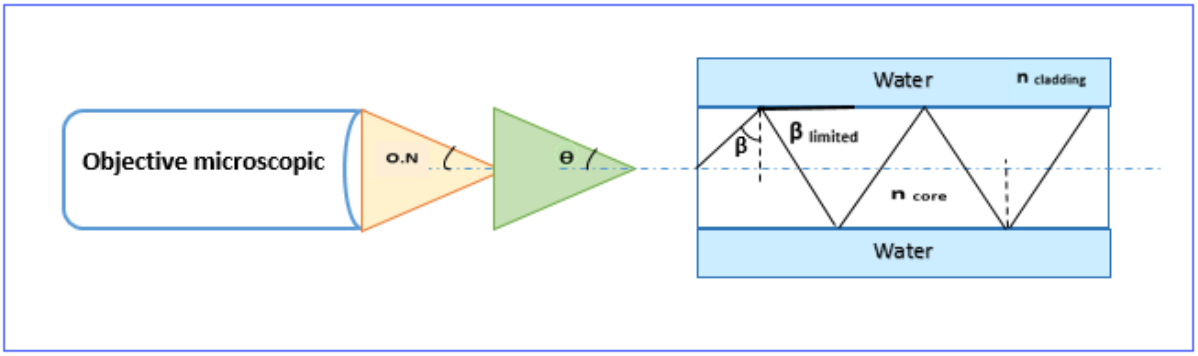

Figure 7: Schematic represents the selection of the microscopic objective's numerical aperture.

In this part, the ideal case is having the same numerical aperture of the microscopic objective as the fiber (in the case of making the distilled water as a cladding). If we pollute the distilled water with the methylene blue, this solution will get a refractive index greater than the one of distilled water. Therefore, the numerical aperture decreases, in addition the acceptance angle

smaller than for the distilled water. Absolutely, the transmitted intensity from the fiber is reduced.

The following figures 8, 9 illustrate this explication:

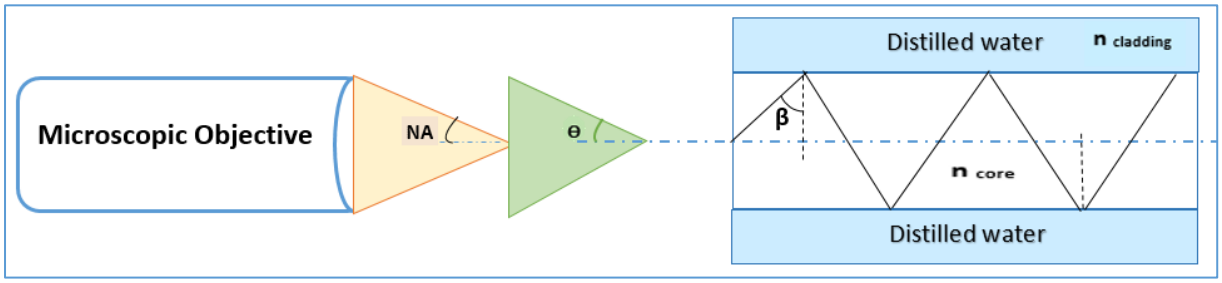

Figure 8: Numerical aperture is similar to the fiber's numerical aperture (distilled water).

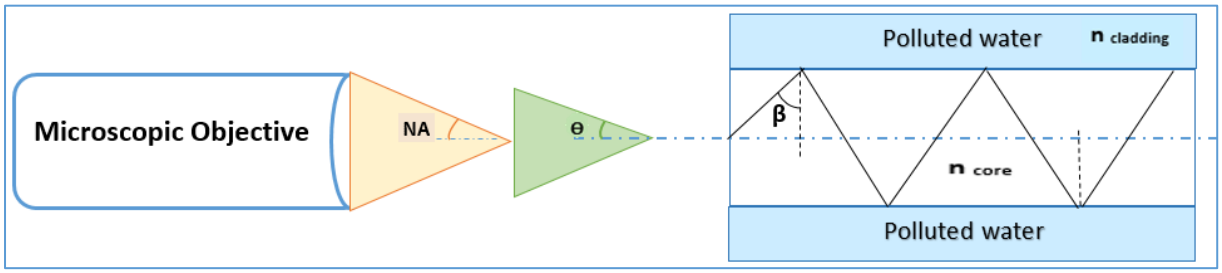

Figure 9: Numerical aperture is greater than fiber's numerical aperture (polluted water).

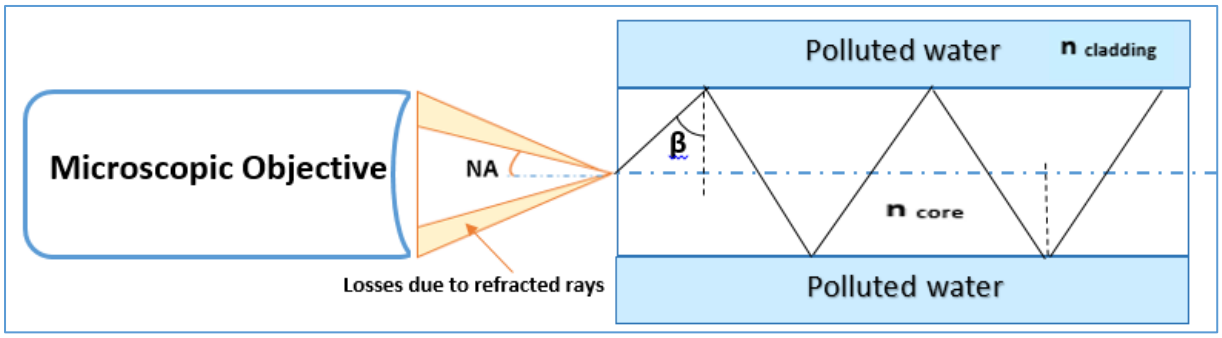

Figure 10: Losses induced by refracted rays during the variation of acceptance angle.

-In order to define the suitable numerical aperture of the microscopic objective, we have created this program, which was affected by Mat lab software:

-We have fixed the refractive index of the cladding as the distilled water $n_{cladding}=1.33$ and $n_{core}=1.425$.

Besides we have put the acceptance angle from [5-60] °, in every point of this range, we verify the difference $\Delta\beta=\beta-\beta_{lim}$. The angle Θ which takes the value $\Delta\beta = 0$ correspond the maximal numerical aperture of the appropriate microscope objective [Appendix 3].

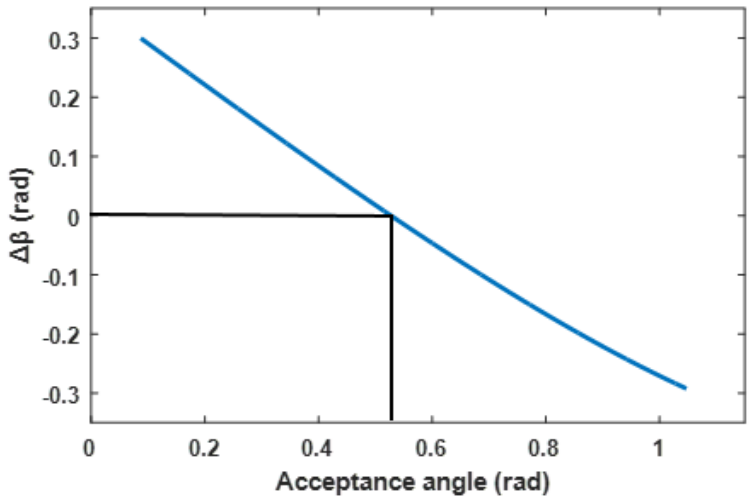

Figure 11: the variation of **Δβ** according to acceptance angle

From this figure, it can be seen that **Δβ** takes the value 0 when the maximal acceptance angle is close to 32°.For that reason, we have to choose the appropriate numerical aperture of the microscopic objective equal to 0.52 (NA=0.52).

Appendix 2

```
ncoeur=1.425;
nair=1;
neau=1.3333:0.001:1.3372;
X=asin(neau/ncoeur);
theta= asin((ncoeur/nair).*cos(X));
Gama=theta.*180/pi;
plot (neau,Gama);
```

Appendix 3

```
neau=1.3333 ;
ncoeur=1.425 ;
nair=1;
X=asin(neau/ncoeur);
T=5:0.1:60;
F=T.*pi/180;
```

```
B= (pi/2)-asin((nair/ncoeur).*sin(F));
DB= B-X;
plot(F,DB);
```

SCIENTIFIC PRODUCTION LIST

International and national contributions was achieved such as:

- **The international conference on Advanced Engineering in Petrochemical industry in Skikda, 2017.**
- **Optic & and photonic Algerian society in Oran, 2018.**
- **Ecole thématique Nano-optique et Plasmonique in Tizi Ouzou, 2018.**
- **International day of light in Setif, 2018.**
- **International conference on industrial metrology & maintenance in Setif, 2018.**
- **Le 12éme Congrès National de fa Physique et de ses Applications in Algiers, 2018.**
- **7ème Séminaire National sur tes Matériaux, Procédés et Environnement ; Boumerdès, Algérie in 2018.**
- **Journée des doctorants in Setif, 2018.**
- **First international workshop on environmental engineering in Setif, 2019.**
- **International article published in the Optical society of America journal, 2020.**
- **Online conference on physics education optics and photonics technology in Malaysia, 2020.**
- **International article published in Optik journal- Elsevier, 2021.**

ABSTRACT

Water pollution has become a huge problem in many countries all over the world. This small portion of freshwater is now under serious stress due to various reasons such as fast developed population, This dominant trouble needs an innovative technology to control continuously and in situ the water quality These optic methods are the only response possible for our need, they open a developed manner of diagnosis. In this thesis the theory, design, fabrication and characterization was reported; to delve into the optical fiber sensor based on evanescent wave absorption, for testing methylene blue (MB) at the laboratory of applied optics (Algeria). The designed sensor represents a significant advancement to accurately monitor MB concentration changes in distilled water. This investigation was in good agreement with previously reported studies. In addition, a turbidity NaCl measurement system intended for water quality monitoring was carried out at the Photonics research laboratory (Turkey). Following to the theoretical investigation about the standard techniques to control the turbidity as well as, experimental results from turbidity system that was employed to control the water quality by using electro- optic components, based on a combined measurement of transmitted and forward scattered light using an optical CCD line sensor array was introduced. The experimental results have shown that trustable measurements of water turbidity in a wide turbidity range can be achieved with the proposed method.

Résumé

La pollution de l'eau est devenue un problème majeur dans de nombreux pays du monde entier. Cette petite portion d'eau douce est maintenant soumise à de sérieux stress en raison de diverses raisons telles que le développement rapide de la population, Ce problème dominant nécessite une technologie innovante pour contrôler en continu et in situ la qualité de l'eau Ces méthodes optiques sont la seule réponse possible à notre besoin, elles ouvrent un mode de diagnostic développé. Dans cette thèse, la théorie, la conception, la fabrication et la caractérisation ont été rapportées ; pour se plonger dans le capteur à fibre optique basé sur l'absorption d'ondes évanescentes, pour tester le bleu de méthylène (MB) au laboratoire d'optique appliquée (Algérie). Le capteur conçu représente une avancée significative pour surveiller avec précision les changements de concentration de MB dans l'eau distillée. Cette enquête était en bon accord avec les études précédemment rapportées. Par ailleurs, un système de mesure de la turbidité NaCl destiné au suivi de la qualité de l'eau a été réalisé au laboratoire de recherche Photoniques (Turquie). Suite à l'enquête théorique sur les techniques standard pour contrôler la turbidité ainsi que, les résultats expérimentaux du système de turbidité qui a été utilisé pour contrôler la qualité de l'eau en utilisant des composants électro-optiques, basé sur une mesure combinée de la lumière diffusée transmise et vers l'avant à l'aide d'un un réseau de capteurs optiques de ligne CCD a été introduit. Les résultats expérimentaux ont montré que des mesures fiables de la turbidité de l'eau dans une large plage de turbidité peuvent être obtenues avec la méthode proposée.

الملخص

أصبح تلوث المياه مشكلة كبيرة في العديد من البلدان في جميع أنحاء العالم. يتعرض هذا الجزء الصغير من المياه العذبة الآن لضغط خطير لأسباب مختلفة مثل التطور السريع للسكان، وتحتاج هذه المشكلة المهيمنة إلى تقنية مبتكرة للتحكم في جودة المياه بشكل مستمر وفي الموقع. هذه الطرق البصرية هي الاستجابة الوحيدة الممكنة لحاجتنا، فهي طريقة مفتوحة متطورة للتشخيص. في هذه الأطروحة تم البحث في النظرية والتصميم. للتعمق في مستشعر الألياف الضوئية على في مختبر البصريات التطبيقية (الجزائر). يمثل المستشعر المصمم تقدمًا كبيرًا لمراقبة تغيرات تركيز بدقة امتصاص الموجة الزائلة لاختبار الميثيلين الأزرق المخصص لمراقبة في الماء المقطر. كان هذا التحقيق في اتفاق جيد مع الدراسات التي تم الإبلاغ عنها مسبقًا. بالإضافة إلى ذلك، تم إجراء نظام قياس تعكر جودة المياه في مختبر أبحاث الضوئيات (تركيا). بعد البحث النظري حول التقنيات القياسية للتحكم في التعكر وكذلك النتائج التجريبية لنظام التعكر الذي تم استخدامه للتحكم في جودة المياه باستخدام المكونات الكهروضوئية، بناءً على القياس المشترك للضوء المنتشر والأمامي باستخدام تم تقديم مجموعة المستشعر البصري. أظهرت النتائج التجريبية أنه يمكن تحقيق قياسات موثوقة لعكارة المياه في نطاق عكارة واسع باستخدام الطريقة المقترحة.